Protozoan predation drives the adaptive evolution of *Vibrio cholerae*

by

Md Mozammel Hoque

The thesis submitted in fulfilment of the requirements for
the degree of

Doctor of Philosophy

Under the supervision of A/Prof. Diane McDougald

University of Technology Sydney
Faculty of Science
The iThree Institute

January 2022

Certificate of original authorship

I, Md Mozammel Hoque declare that this thesis, is submitted in fulfilment of the requirements for the award of Doctor of Philosophy, in the Faculty of Science at the University of Technology Sydney.

This thesis is wholly my own work unless otherwise reference or acknowledged. In addition, I certify that all information sources and literature used are indicated in the thesis.

This document has not been submitted for qualifications at any other academic institution.

This research is supported by the Australian Government Research Training Program.

Signature:

Production Note:
Signature removed prior to publication.

Date: 15th January 2022

Table of contents

Acknowledgements vi

Publications and conference presentations associated with this thesis vii

List of Figures..... viii

List of Tables..... ix

Abbreviations..... x

Abstract..... 1

Chapter One: General Introduction and Literature Review..... 3

1.1 General Introduction 4

1.2 *Vibrio cholerae*: the causative agent of cholera 5

1.3 Factors contributing to pathogenesis 7

1.4 Regulatory network of virulence 8

1.5 Environmental persistence and adaptation 11

1.6 Genomics and genetic diversity 13

1.7 Protozoa: major grazers of bacteria in the environment 14

1.8 Mechanisms of bacterial resistance to protozoan grazing 16

1.9 Protists as a reservoir and vehicle for transmission of pathogenic bacteria 18

1.10 Evolution of bacterial virulence in response to protozoan predation 19

1.11 Adaptive evolution of *Vibrio cholerae* in response to protozoan predation 21

1.12 Chapter synopsis and project aims 22

Chapter Two: Adaptation of *Vibrio cholerae* in an amoeba host drives trade-offs of virulence traits and enhanced colonisation in zebrafish..... 25

2.1 Introduction 26

2.2 Materials and methods 28

2.2.1 Organisms and growth conditions 28

2.2.2 Experimental co-adaptation of *V. cholerae* with *A. castellanii* 29

2.2.3 Intracellular survival assays 29

2.2.4 Competition assays 30

2.2.5 Motility assays 30

2.2.6 Quantification of biofilm biomass 30

2.2.7 Protease assay 31

2.2.8 Haemolysin assay …… 31
2.2.9 Generation and complementation of *flrA* mutant …… 32
2.2.10 Scanning electron microscopy ……... 32
2.2.11 Fluorescent tagging ……... 33
2.2.12 Adult zebrafish infection and histology …… 33
2.2.13 Statistical analysis ……. 34
2.3 Results ...…… 34
2.3.1 Increased intracellular survival of amoeba-adapted isolates ……... 35
2.3.2 Increased competitive fitness of amoeba-adapted isolates ……. 35
2.3.3 Virulence related phenotypes of amoeba-adapted isolates ……. 38
2.3.4 Amoeba-adapted isolates with A213V and V261G mutations in *flrA* ……... 40
2.3.5 Changes in virulence-associated phenotypes…….....……. 41
2.3.6 Adaptation leads to enhanced colonisation of an aquatic host …… 45
2.3 Discussion.…… 47
Chapter Three: Increased iron acquisition and oxidative stress tolerance in a *Vibrio cholerae flrA* mutant confers resistance to amoeba predation ……. 50
3.1 Introduction ...……..... 51
3.2 Materials and methods ...……... 53
3.2.1 Organisms and growth conditions …… 53
3.2.2 Intracellular survival assay ……... 53
3.2.3 Generation of mutants ……. 53
3.2.4 RNA extraction and sequencing ……... 53
3.2.5 Transcriptomics analysis ……. 54
3.2.6 Oxidative stress sensitivity assay ……. 55
3.2.7 Catalase activity assay ……. 55
3.2.8 Quantitative real-time PCR (qRT-PCR) assay …… 55
3.2.9 Statistical analysis …… 56
3.3 Results ...…… 56
3.3.1 The flagellar transcriptional regulator *flrA* mutant……... 56
3.3.2 It is the loss of motility that is responsible for reduced uptake by amoeba ……. 57
3.3.3 Transcriptome of the Δ*flrA* mutant during predation by amoeba …….…….. 58
3.3.4 Differential expression of type VI secretion genes …… 61
3.3.5 KEGG pathway analysis of up- and down-regulated genes …….. 62

3.3.6 The Δ*flrA* mutant showed increased oxidative stress resistance …… 64
3.3.7 The Δ*flrA* mutant exhibits increased growth in iron-limited condition……... 66
3.4 Discussion …… 66
Chapter Four: Adaptation of *Vibrio cholerae* in an amoeba host leads to mutations in the flagellar transcriptional regulator, *flrA* ……..... 70
4.1 Introduction ...……..... 71
4.2 Materials and methods ...…… 73
4.2.1 Organisms and growth conditions ……... 73
4.2.2 Experimental co-evolution of *V. cholerae* in *A. castellanii* …… 73
4.2.3 Extraction of genomic DNA ……... 73
4.2.4 Sequencing and genomic analysis ……... 74
4.2.5 Amplification refractory mutation system (ARMS)-PCR ……... 74
4.2.6 Functional classification of the mutated genes …… 75
4.2.7 Data availability ……... 75
4.3 Results ...……... 75
4.3.1 Dynamics of mutations arising in *V. cholerae* during co-incubation ……... 75
4.3.2 Long-term predation by amoeba drives mutations in conserved regions.……... 80
4.3.3 Temporal mutation of flrA during co-adaptation ……...…… 82
4.3.4 Functional classification of mutated genes …… 83
4.3.5 Analysis of the genes under selection ……...…… 85
4.4 Discussion ...…… 86
Chapter Five: General Discussion and Future perspective……. 89
5.1 Prelude...……..... 90
5.2 Adaptation strategies during long-term co-evolution ……. 91
5.3 Fitness trade-off and evolution of virulence ……... 93
5.4 Shift from antagonistic to neutral interaction ……. 95
5.5 Potential impact of global warming on the evolution of virulence ……. 96
5.6 Conclusion ……...……... 97
Supplementary Information…… 99
References …… 118

Acknowledgments

First of all, I like to thanks to Almighty Allah (The Most Gracious, The Most Merciful) for everything I achieved and to enable me to work on my thesis to the best of my abilities.

It is a great pleasure to express my best regards, profound gratitude, and sincere appreciation to my supervisor Associate Professor Diane McDougald. Thank you very much for allowing me to work in this excellent project and to support me in every step involved in my Ph.D. candidature. I am very much fortunate that I got such an excellent supervisor like you. Also, afraid at the same time that, perhaps I will never find a supervisor like you. You are simply awesome.

Next, I would like to thanks my co-supervisor Associate Professor Maurizio Labbate and Professor Scott Rice for their guidance and valuable advice throughout the entire period of time study. I wish to convey my indebtedness to Dr. Stefan Ohelers and his team facilitating collaboration on zebra fish model. He always had the time to give prompt and generous support throughout the course of this study. I am deeply grateful to my lab mates Dr. Parisa Noorian and Dr. Gustavo Espinoza-Vergara who were always beside me with their sincere help and continuous support.

I am thankful to Professor Gary Meyers and Associate Professor Iain Duggin for many stimulating discussions and their valuable suggestion during my candidature assessment. I am greatly thankful to Dr. Shuyang Sun for his initiative advice on conducting my work. I would like to convey my heightened appreciation to all of my former teacher particularly my childhood tutor Late. Mr. Animesh Kumar Saha and Ms. Suchona.

Finally, I wish to offer heartfelt thanks to my family particularly my wife Sima, my kid Arshi, my parents, my brother Sohag and all friends and colleagues for their invaluable affection, inspiration, encouragement, best wishes, sacrifice and all sorts of support for completion of this study.

Author
The iThree institute, Faculty of Science
University of Technology Sydney
January, 2022

Publications and conference presentations associated with this thesis

Publications

Hoque MM, Noorian P, Espinoza-Vergara G, Manuneedhi Cholan P, Kim M, Rahman MH, *et al*. (2021) Adaptation to an amoeba host drives selection of virulence-associated traits in *Vibrio cholerae*. **The ISME Journal**. https://doi.org/10.1038/s41396-021-01134-2

Hoque MM, Noorian P, Espinoza-Vergara G, Ismail MH, Rice SA, McDougald D. Increased iron acquisition and oxidative stress tolerance in a *Vibrio cholerae flrA* mutant confers resistance to amoeba predation. (Manuscript under preparation)

Other Publications

Espinoza-Vergara G, Noorian P, Silva-Valenzuela CA, Raymond BBA, Allen C, **Hoque MM**, *et al*. (2019) *Vibrio cholerae* residing in food vacuoles expelled by protozoa are more infectious in vivo. Nature Microbiology. https://doi.org/10.1038/s41564-019-0563-x

Espinoza-Vergara G, **Hoque MM**, McDougald D and Noorian P. (2020) The Impact of Protozoan Predation on the Pathogenicity of *Vibrio cholerae*. Frontiers Microbiology. 11:17. https://doi.org/10.3389/fmicb.2020.00017

Leong W, Poh WH, Williams J, Lutz C, **Hoque MM,** Poh YH *et al*. (2022) Adaptation to an amoeba host leads to *Pseudomonas aeruginosa* isolates with attenuated virulence. Applied and Environmental Microbiology. aem0232221. https://doi.org/10.1128/aem.02322-21

Conference presentations

M. Mozammel Hoque, Parisa Noorian, Gustavo Espinoza-Vergara, Pradeep Manuneedhi Cholan, Mikael Kim, Maurizio Labbate, Scott A. Rice, Mathieu Pernice, Stefan H. Oehlers, Diane McDougald. Presentation title: Protozoan predation drives trade-off of virulence traits in *Vibrio cholerae* leads to enhance colonization in zebrafish. Conference: Australian Society for Microbiology Annual Scientific Meeting 2021, Virtual Meeting, Held on 31st May to 3rd June 2021.

M. Mozammel Hoque, Parisa Noorian, Gustavo Espinoza-Vergara, Diane McDougald. Presentation title: Protozoan predation drives the adaptive evolution of *Vibrio cholerae.* Conference: 54th US-Japan Joint Panel Conference on Cholera and Other Bacterial Enteric lnfections, Osaka, Japan. Held on 10th to 13th December 2019.

List of Figures

Figure 1.1 *Vibrio cholerae* quorum sensing circuits……... 10
Figure 2.1. Intracellular survival and competitive fitness of adapted and non-adapted isolates. 37
Figure 2.2. Virulence phenotypes of adapted and non-adapted isolates……. 39
Figure 2.3. Scanning electron micrograph showing presence or absence of flagellum on *V. cholerae*……... 41
Figure 2.4. Altered phenotypes in adapted isolates are due to mutations in *flrA* ……... 43
Figure 2.5. Principal component analysis of the four virulence phenotypes ……. 44
Figure 2.6. Enhanced colonisation of adapted isolates in a zebrafish infection model ……. 46
Figure 3.1. Intracellular growth kinetics, survival and uptake of ΔflrA mutant and wild type in amoeba ……... 57
Figure 3.2. Transcriptional analysis of Δ*flrA* mutant compared to the wild type strain during amoeba predation, reveals up-regulation of iron acquisition genes ……... 60
Figure 3.3. Expression of type VI secretion genes in the Δ*flrA* relative to wild type ……. 61
Figure 3.4. KEGG pathway analysis of the differentially expressed genes in Δ*flrA* mutant compared to the wild type.…… 63
Figure 3.5. Oxidative stress resistance is due to increased catalase activity and KatB expression ……... 65
Figure 3.6. Growth of wild type and ΔflrA under iron-limited conditions…….. 66
Figure 4.1. Mutations in adapted and non-adapted populations and isolates …… 78
Figure 4.2. Unique mutations in coding regions of adapted populations ……... 79
Figure 4.3. Schematic representation of the non-synonymous mutations affecting the conserved region of the FlrA protein ……. 81
Figure 4.4. Temporal appearance of the A213V (C638T) mutation in *flrA* gene during adaptation ……... 83
Figure 4.5. Functional annotation of mutated genes in adapted and non-adapted populations.. 84
Figure 4.6. The genes with nsSNP and sSNP in adapted and non-adapted populations ……... 86
Supplementary Figure 1. Non-synonymous mutations in coding regions of adapted and non-adapted isolates ……. 99
Supplementary Figure 2. Amino acid sequence alignment of the FlrA protein …… 101

List of Tables

Supplementary Table 1. List of strains, plasmids, and primers 104

Supplementary Table 2. **Unique** genes mutated in adapted and non-adapted **populations** at three different time points 106

Supplementary Table 3. **Common** genes mutated in adapted and non-adapted **populations** sequenced at three different time points 107

Supplementary Table 4. **Unique** genes mutated in adapted and non-adapted **isolates** sequenced at three different time points 108

Supplementary Table 5. **Common** genes mutated in adapted and non-adapted **isolates** sequenced at three different time points 109

Abbreviations

AI	Autoinducer
ANOVA	Analysis of variance
ARMS	Amplification refractory mutation system
ATCC	American type culture collection
BLAST	Basic Local Alignment Search Tool
C	Celsius
cAMP	Cyclic adenosine monophosphate
CI	Competition index
COGs	Cluster of orthologous groups
c-di-GMP	Cyclic di-guanosine monophosphate
CFU	Colony forming unit
CLSM	Confocal laser scanning microscopy
cm	Centimetre
CT	Cholera toxin
DNA	Deoxyribonucleic acid
g	Gravitational force
GFP	Green fluorescent protein
h	Hour
HAP	Hemagglutinin protease
HMDS	Hexamethyldisilazane
HTH	Helix turn helix
INDELS	Insertion and Deletions
KEGG	Kyoto Encyclopedia of Genes and Genomes
LB	Lysogeny Broth
min	Minute
ml	Millilitre
µl	Microlitres
mm	Millimetre
mM	Millimolar
µM	Micromolar
MOI	Multiplicity of infection

NCBI	National Center for Biotechnology Information
nM	Nanomolar
NO	Nitric oxide
NSS	Nine salts solution
nsSNPs	Non-synonymous single nucleotide polymorphisms
OD	Optical density
PAMP	Pathogen-associated molecular pattern
PBS	Phosphate buffer saline
PCA	Principal Component Analysis
PCR	Polymerase chain reaction
PYG	Proteose yeast extract
QS	Quorum sensing
qRT-PCR	Quantitative real-time polymerase chain reaction
rpm	Revolutions per minute
ROS	Reactive oxygen species
RNS	Reactive nitrogen species
RNA	Ribonucleic acid
RT	Room temperature
SD	Standard deviation
SEM	Scanning Electron Microscopy
SNP	Single nucleotide polymorphisms
sSNPs	Synonymous single nucleotide polymorphisms
T6SS	Type VI secretion system
TCP	Toxin-coregulated pili
VPS	Vibrio polysaccharide
WHO	World Health Organization
WT	Wild type

Abstract

Protozoa are unicellular eukaryotic organisms that play an important role in controlling bacterial population structure and composition in the environment. Heterotrophic protozoa survive by feeding on bacteria. Many pathogenic bacteria are capable of resisting predation and some are able to multiply inside of these hosts. To resist predation, bacteria have evolved many mechanisms or defensive traits and often these traits contribute to the persistence of the pathogen in the environment and give rise to virulence upon encounter with human and animal hosts.

The waterbourne bacterium, *Vibrio cholerae,* is the etiological agent of the disease cholera and shares an ecological niche with the free-living amoeba, *Acanthamoeba castellanii*. Here, the experimental evolution of the model pathogen *V. cholerae* with *A. castellanii* was performed for three months with the aim to increase our understanding of the effects of long-term protozoan predation on the evolution of virulence-related traits and how that impacts environmental persistence.

Long-term adaptation with the amoeba host leads to phenotypic and genetic variability in *V. cholerae*. Late-stage amoeba adapted *V. cholerae* showed trade-offs among multiple phenotypic traits that contribute to their enhanced intracellular survival and fitness in amoeba. Whole genome sequencing and mutational analysis revealed that these altered phenotypes and improved fitness were linked to non-synonymous mutations in conserved regions of the flagellar transcriptional regulator, *flrA.* Transcriptomic analysis of the Δ*flrA* mutant revealed that increased iron acquisition, oxidative stress resistance and metabolic co-ordination are also associated with improved intracellular survival and fitness. Additionally, adaptation with the amoeba host result in *V. cholerae* isolates that exhibited an increased capacity to colonise

zebrafish, establishing a connection between protozoan predation and enhanced environmental persistence.

The results presented here highlight multiple adaptation strategies acquired by the pathogen when under intense grazing pressure. Predation pressure drives the accumulation of beneficial mutations that serve as key drivers of the adaptation process and enhance commensalism with the host protozoa. Further, this study provides an important contribution to the understanding of the adaptive traits that evolve in pathogens under predatory pressure, and how these adaptive traits impact colonisation of eukaryotic hosts.

Chapter One

General Introduction and Literature Review

Chapter One

General Introduction and Literature Review

1.1 General Introduction

The environment acts as a reservoir for many opportunistic bacterial pathogens. These pathogens are transmitted through water, soil or air, where they interact with a large number of organisms, including protists, bacteriophage, algae, other bacteria, nematodes, insects, and plants [1]. Among these organisms, heterotrophic protists or protozoa are the major grazers of bacteria in the environment [2]. Protozoan predation on bacteria plays a crucial role in nutrient recycling and in controlling bacterial communities [3]. The constant threat from predatory protists is a major challenge for bacteria and their ability to adapt to this challenge is important for survival and persistence. To counter this threat, bacteria have evolved many sophisticated survival strategies, including changing cell shape and surface properties, increasing motility, forming biofilms and releasing toxins or secondary metabolites. [4, 5]. Survival strategies of bacteria in the environment are not limited to avoiding digestion but also include establishing mutualistic or endosymbiotic relationships with protozoal hosts [6, 7].

The long history of co-evolution of bacteria and protozoa led to the rise of many anti-protozoal traits [8]. It is now widely believed that the adaptive traits that are gained by pathogenic bacteria to defend against protist predation result in increased virulence potential in human and animal hosts, where these hosts are the outcome of accidental infections [8, 9]. Due to the close association and long history of interactions with bacteria, protozoa have been utilised as model organisms for interactions with bacteria, including for ecology and evolutionary biology [10]. A better understanding of bacterial evolution in response to protozoan predation has the potential to increase our ability to predict the emergence of pathogens. Moreover, investigations on bacterial evolution and mechanisms of persistence in the environment and

virulence potential in human hosts is vital for development of preventive strategies against outbreaks of emergent pathogens.

To understand how protozoal-bacterial interactions potentially lead to the emergence of bacterial traits related to persistence and virulence, this project aims to test the hypothesis that protozoan predation and the associated expression of defensive traits by bacteria are responsible for the evolution of pathogens in the environment. To test this hypothesis, this project aimed to determine the effects of long-term exposure to amoeba predation on the phenotype and genotype of the human pathogen, *V. cholerae,* the causative agent of the deadly disease cholera. The disease cholera has afflicted mankind since ancient times and is currently the cause of a resurgence of cholera epidemics. Cholera has distinctive epidemiological features as it follows a regular seasonal pattern in endemic areas, suggesting that environmental factors play a role in modulating epidemics [11]. As protozoa and *V. cholerae* co-occur in their natural habitat, it is highly likely that protozoa play a vital role in the environmental persistence of *V. cholerae.* A number of reports have described mechanisms of grazing resistance of *V. cholerae* [12-15]. Nonetheless, many aspects of the molecular mechanisms of the interactions between protozoa and *V. cholerae* are yet to be explored, particularly how the pathogen adapts under long-term predation pressure. This project is, therefore, one of the first to directly test the hypothesis that predation by protozoa affects colonisation and virulence potential of opportunistic pathogens. This chapter reviews the features of *V. cholerae* including virulence properties and mechanisms of environmental persistence. It further explores the potential role of protozoa in the evolution of bacterial virulence, particularly in *V. cholerae*.

1.2 *Vibrio cholerae*: the causative agent of cholera

Cholera is an acute diarrhoeal disease resulting from intestinal infection by toxigenic strains of *V. cholerae*. The consumption of contaminated water or food containing *V. cholerae* is the

primary source of cholera infections. Cholera leads to severe dehydration and death in the absence of treatment. Administration of oral rehydration solution (ORS) is the primary means of intervention, which restores the balance of body fluids of cholera patients [16]. The global cholera incidence is estimated to be between 1.3 and 4 million with death tolls between 21,000 and 143,000 annually [17] in both epidemics and pandemics. To date, the world has experienced seven pandemics since 1817 [18]. The last and ongoing pandemic originated in 1961 in Indonesia and has spread to different continents around the world [19]. The British physician, John Snow, first discovered the link between contaminated water from London well pumps and cholera cases in 1854 [20]. In the same year in Italy, Filippo Pacini observed bacteria-like objects under the microscope in samples from the intestines of corpses of deceased cholera patients, but his work was not widely recognised [21]. In 1883, Robert Koch proposed that pure cultures of bacteria from the intestines of cholera patients were the causative agent of cholera infection [22].

V. cholerae is a Gram-negative motile bacterium which naturally inhabits many freshwater, estuary and brackish water ecosystems [23]. *V. cholerae* strains are classified into different serogroups based on their lipopolysaccharide (LPS) moieties. [24]. Of the over 200 serogroups, only O1 and O139 serogroups can cause cholera infections, as they harbour the cholera toxin (CT) genes, *ctxAB*. The O1 serogroups are further divided into two biotypes, classical and El Tor [25]. The El Tor biotype of *V. cholerae* is responsible for the ongoing seventh pandemic, while the classical biotype was presumably responsible for the first six pandemics. Global phylogeny of seventh pandemic isolates reveals that they are genetically homogeneous and also identifies the Bay of Bengal as a source of origin [26]. The disease also has a seasonal pattern in the endemic region of the Ganges River Delta of Bangladesh and India [27]. A variety of environmental factors ranging from temperature, salinity, rainfall, plankton blooms and

interactions with other organisms like protozoa and phage are thought to be responsible for the seasonality of cholera [28].

1.3 Factors contributing to pathogenesis

Pathogenic strains of *V. cholerae* are ingested through contaminated water or food. Once ingested, the cells pass through the highly acidic stomach into the small intestine where the expression of many different virulence factors contribute to cholera infection. CT is the primary virulence factor of *V. cholerae* secreted in the intestine and is responsible for the characteristic symptoms of watery diarrhoea [29]. Virulent strains of *V. cholerae* acquired the genes encoding CT from the CTXφ bacteriophage by a horizontal gene transfer (HGT) event [30]. CT consists of one copy of subunit A and five copies of subunit B (AB5) [31] and is secreted via the type II secretion system [32].

The infection process starts by the binding of the five-membered ring of the B-subunits of the CT with the GM1 gangliosides on intestinal epithelial cell surface receptors [33]. CT enters intestinal epithelial cells by receptor-mediated endocytosis, where the A subunit is cleaved into A1 (approximately195 amino acid residues) and A2 (approximately 45 amino acid residues) fragments [34]. A1 catalyses ADP ribosylation of the Gαs subunit of the G protein which in turn results in constitutive cAMP production and over-activation of the cytosolic protein kinase A (PKA). Active PKA phosphorylates cystic fibrosis transmembrane conductance regulator (CFTR) chloride channel proteins and causes an imbalance in the movement of electrolytes, leading to secretion of water and important electrolytes (Na^+, K^+, Cl^-, HCO_3^-) into the intestinal lumen. Excessive electrolyte secretion coupled with decreased sodium uptake into enterocytes results in rapid fluid loss leading to severe dehydration and manifestation of characteristics symptoms of cholera, including rice-water stools [35, 36].

While CT is the critical virulence factor responsible for the manifestation of the major symptoms of cholera, the synergistic action of many other factors are necessary for cholera infection [37]. For example, a colonisation factor, the toxin co-regulated pilus (TCP), and the regulatory protein, ToxR, are also involved in cholera pathogenesis and are found in all strains capable of causing cholera [38]. TCP is crucial for colonisation of the intestinal epithelial cell surface. The TCP pilus belongs to the type IV family of pili usually involved in surface attachment. The genes for the biogenesis of TCP are present in the TCP operon found in a 39.4 kb genomic element known as Vibrio pathogenicity island (VPI). TCP facilitates microcolony formation on the intestinal epithelial cells and *in vitro* expression leads to auto-agglutination of bacteria [39, 40]. The CTXφ phage that harbours the genes encoding CT uses TCP as a high-affinity receptor that allows successful delivery of the genes into the bacterium [41].

Along with CT and TCP, several other factors are associated with virulence of *V. cholerae*. Among them are the accessory cholera toxin (Ace) that forms pores in eukaryotic cell membranes and the zonal occludens toxin (Zot) that affects the permeability and structural integrity of the intestinal mucosa [42, 43]. Another secreted toxin, RTX, which causes depolymerisation of actin, leads to the rounding of epithelial cells [44]. *V. cholerae* also secretes a haemolysin, HlyA, which is cytotoxic for epithelial cells [45]. Finally, the haemagglutinin-protease (HAP) which is regulated by the quorum sensing (QS) cascade facilitates *V. cholerae* penetration of the mucus lining of the gut [46].

1.4 Regulatory networks controlling virulence of *V. cholerae*

The regulation of virulence gene expression is tightly coordinated in *V. cholerae* which allows the bacterium to adapt to different environmental conditions as well as to conditions in the eukaryotic host [47]. ToxR is the master regulator that coordinates expression of genes in the ToxR regulon. The cascade of gene expression begins with proteins encoded by *aphA* and *aphB*

synergistically activating membrane-bound TcpP and TcpH [48]. These two proteins along with two other transmembrane proteins, ToxR and ToxS, control the expression of *toxT*, encoding the protein that acts as a direct transcriptional activator [49]. ToxT directly regulates genes in the ToxR regulon, such as the *ctxAB* genes which encode CT, the TCP operon, accessory colonisation factors, outer membrane proteins and various lipoproteins [47, 50-52].

Quorum sensing (QS) signalling also plays a vital role in *V. cholerae* virulence gene expression. QS is a social behaviour, which in bacteria regulates physiological processes like bioluminescence, virulence, biofilm formation, production of secondary metabolites and induction of competence [53]. Bacterial cells elicit social behaviour through communication by small chemical molecules called autoinducers (AI). Several sensory inputs modulate QS responses in *V. cholerae* (Figure 1.1) [54, 55]. Two well characterised inputs known as autoinducers CAI-1 and AI-2 are synthesised by CqsS and LuxS, respectively, and are detected by trans-membrane histidine sensor kinase receptors CqsS and LuxPQ, respectively [56]. Two other newly identified QS inputs are CqsR and VpsS and it has been recently shown that ethanolamine acts as a ligand for CqsR while ligand for VpsS remains unknown [54, 57]. Another AI, DPO (3,5-dimethylpyrazin-2-ol) synthesised by Tdh, binds to a cytoplasmic receptor, VqmA, that also modulates QS, but this system is independent of LuxO regulation [55].

QS systems coordinate virulence gene expression in a cell density-dependent manner. At low cell density and minimal levels of autoinducers, the receptors act as kinases that phosphorylate and activate the response regulator LuxO through LuxU [58]. The active form of LuxO induces the expression of four small regulatory RNAs (Qrr1-4) [59]. These Qrr sRNAs ultimately activate the expression of the low cell density (LCD) master regulator, *aphA,* while repressing the high cell density (HCD) master regulator, *hapR* [60]. Coordinated expression of proteins

encoded by *aphA* and *hapR* modulates virulence factor production and biofilm formation. At HCD, autoinducers bind with their cognate receptors and induce dephosphorylation of LuxO. Thus, no Qrr sRNAs are transcribed and AphA production ceases while repression of HapR is relieved, which in turn represses the production of virulence factors and biofilm formation [61, 62]. At HCD, the VqmA-DPO complex also inhibits expression of AphA through VqmR sRNA, hence inhibiting biofilm formation by repressing VpsT [55]. HapR also activates HAP protease production which degrades the mucin layer of the small intestine facilitating detachment and movement of *V. cholerae* along the gastrointestinal tract, thereby releasing the bacterium to the environment [63].

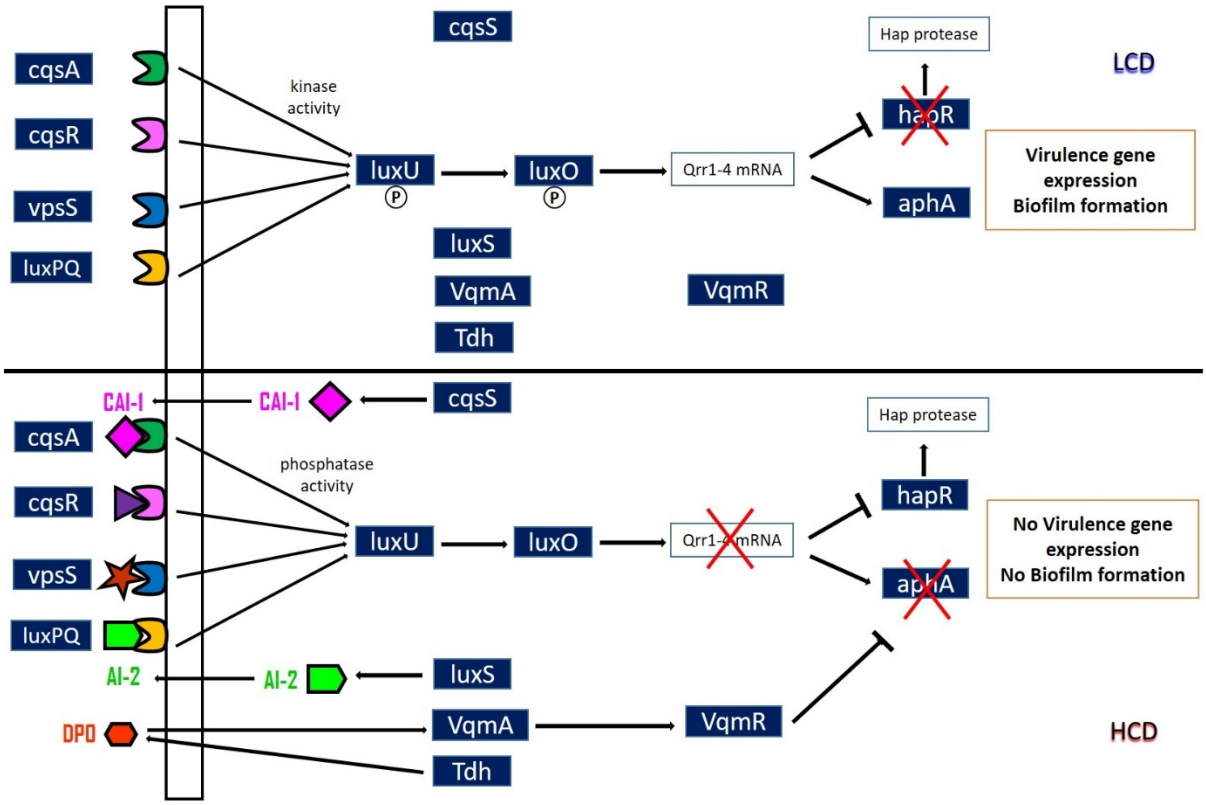

Figure 1.1 *Vibrio cholerae* quorum sensing circuits. The figure adapted from Watve *et al.* [57] and Herzog *et al* [55]. Described in detail in text.

Cyclic di-guanosine monophosphate (c-di-GMP) is an important signalling molecule that regulates the behavioural switch between biofilm and free-living life styles in many bacteria

[64]. C-di-GMP is produced by diguanylate cyclases (DGC) and is degraded by phosphodiesterases (PDEs), enzymes carrying GGDEF and EAL or HD-GYP domains, respectively [65, 66]. The intracellular level of c-di-GMP is modulated by multiple proteins harbouring these domains [67]. C-di-GMP signalling in *V. cholerae* is a critical factor in biofilm formation and motility. Elevated c-di-GMP levels activate VpsT, a transcriptional regulator which increases biofilm formation by binding to the promoter of the VPS-II cluster of genes that control the production of Vibrio polysaccharide (VPS). Furthermore, c-di-GMP represses *V. cholerae* motility by induction of VPS expression [68-70].

1.5 Environmental persistence and adaptation of *V. cholerae*

V. cholerae transits from the host to the environment where it encounters changes in environmental parameters, including temperature, salinity, pH and nutrient levels. In addition to these physicochemical parameters, *V. cholerae* also faces predation pressure by protozoa and bacteriophage [71]. This bacterium adapts to the dynamic environment encountered in the eukaryotic host and the aquatic environment using sophisticated mechanisms. Biofilm formation plays a key role in environmental persistence and survival of *V. cholerae* [72]. Biofilms are surface-attached communities of microorganisms surrounded by extracellular polymeric substances (EPS) secreted by those cells [73]. Biofilm formation initiates with the attachment of cells to a surface followed by the formation of a monolayer of cells. *V. cholerae* employs three different type IV pili to adhere to surfaces. TCP is required for colonisation of intestinal epithelia, the mannose-sensitive haemagglutinin pilus (MSHA) facilitates attachment to abiotic surfaces and the chitin-regulated pilus (ChiRP) is used for colonisation of chitinous surfaces of plankton [39, 74, 75].

After initial attachment, the biofilm undergoes a maturation process, forming a three-dimensional biofilm architecture aided by the accumulation of the EPS, extracellular DNA

(eDNA) and VPS. VPS is the major component of the biofilm matrix and is encoded by VPS-I and VPS-II genomic islands present on chromosome I [76-78]. Several distinct signalling systems are known to regulate biofilm production in *V. cholerae*. Among them, the QS master regulator, HapR, increases VPS synthesis and biofilm formation by modulating c-di-GMP levels and repressing *vpsT* [62, 79]. Absence of a flagellum is also known to induces the expression of VPS synthesis [80]. In addition, conversion of smooth to rugose (wrinkled) variants is also associated with an increased capacity to produce VPS and hence biofilm formation [81].

In aquatic systems, *V. cholerae* occurs as both free-living planktonic cells and in surface-associated biofilms. *V. cholerae* also forms biofilms on algae and the chitinous surfaces of zooplankton [82, 83]. Chitin induces natural competency in *V. cholerae*, allowing for acquisition of exogenous genetic material leading to increased genomic diversity [84]. In cholera endemic regions, the disease cholera follows a seasonal pattern with two peaks of cases during the warmer periods of the year just before and after monsoon season [11]. Temperature has a significant impact on seasonality and hence on outbreaks of cholera. The warm environmental conditions promote algal growth and copepod and phytoplankton blooms, facilitating increased *V. cholerae* numbers and thus cases during warm periods [85].

In response to low nutrient availability or adverse temperatures, *V. cholerae* can enter into a dormant state which is referred as the viable but non-culturable (VBNC) state [86]. Entering into this dormant state is another key strategy for *V. cholerae* survival under adverse environmental conditions and presumably during inter-epidemic periods. VBNC cells are not culturable by conventional techniques but can recover as fully virulent forms of *V. cholerae* when passaged through rabbit intestines [72]. The surface water from cholera endemic regions, as well as stool samples of cholera patients, contain biofilm-like clumps of dormant cells of

pathogenic *V. cholerae*. Virulent forms of *V. cholerae* can resuscitate into planktonic cells from these biofilm/dormant cells in the mammalian intestine, and QS autoinducer molecules act as a vital resuscitation factor [72, 87].

V. cholerae biofilms are more infective than planktonic cells, which was supported by a study in Bangladeshi villages when it was demonstrated that drinking of water that had been filtered through traditional Sari cloth reduced the number of cholera cases by 48% [88, 89]. Formation of biofilms is a very effective strategy for avoidance of protozoan grazing as the grazers cannot ingest large clumps of cells [12]. In addition, biofilms protect *V. cholerae* from a variety of physiochemical stresses, including bactericidal agents such as chlorine and antimicrobial agents [81, 90]. Biofilms represent an efficient mode of delivery of an infectious dose of *V. cholerae* cells to the gut of cholera victims as these cells can better survive the highly acidic environment of the stomach [91]. Biofilms are, therefore, an essential mode of lifestyle for *V. cholerae* which allows for increased survival and dissemination inside and outside of the host.

1.6 Genomics and genetic diversity

The *V. cholerae* genome is comprised of two circular chromosomes (chromosome I and II) containing approximately 2.96 and 1.07 megabase pairs, respectively. The first sequenced genome of *V. cholerae* was N16961, an El Tor O1 strain with 3,885 predicted open reading frames [92]. Accumulating evidence from advances in modern sequencing and molecular tools suggests remarkable genetic diversity among *V. cholerae* isolates. Sequence data from multiple *V. cholerae* isolates suggests that most of the virulence genes are found in clusters, such as the CT, RTX, *rfb*, *pil* clusters, VPI, integrons and SXT elements. Non-toxigenic *V. cholerae* strains can become toxigenic through the acquisition of CTX phage by HGT. The genes for the major virulence determinant, CT, is incorporated into the genome by the single-stranded filamentous DNA phage, CTXΦ, with the aid of a satellite phage, TLCΦ [41, 93]. The genes for the CT

receptor, TCP, and the accessory colonisation factor (ACF) also located in VPI, are likely acquired by the integration of a mobile element [94]. The SXT element which is a conjugative transposon, confers resistance to multiple antibiotics [95]. The seventh pandemic El Tor strains harbour two gene clusters, the Vibrio seventh pandemic islands VSP-I and VSP-II [96]. The *rfb* gene cluster, also known as the *wbe* cluster, encodes genes expressing the LPS O-antigen. This O-antigen is the major determinant of over 200 identified serogroups of *V. cholerae* which suggests great variation in the encoded enzymes responsible for the synthesis of O-antigens. Several non-O1 stains share a common LPS backbone with O1 strains. The variation in the O-antigen moiety is thought to be mediated by homologous recombination events facilitating the exchange of O-antigen biosynthetic genes among the *rfb* cluster [97]. All these gene clusters in the *V. cholerae* genome are thought to mediate fitness advantages to the bacterium resulting in greater pathogenic potential and diversity.

1.7 Protozoa: major predators of bacteria in the environment

Protozoa are free-living unicellular eukaryotic microorganisms ranging from 2 to 2000 µm in size [98]. Rapid generation times make them the most abundant eukaryotic organisms in the oceans [99]. They are the primary consumers of bacterioplankton and phytoplankton and are thus responsible for constraining the planktonic populations of microorganisms as well as driving nutrient flux in water ecosystems [3]. Protozoa feed on detritus, bacteria, and other protozoa by engulfing cells using pseudopodia, cilia or flagella, or absorb dissolved organic particles by pinocytosis [100]. Based on their morphology and feeding behaviour, they are classified into three major groups, amoebae, ciliates and flagellates [98].

Amoeba are typically 20 – 2000 µm in size and use pseudopodia for locomotion on solid surfaces and for capturing prey [98]. They inhabit both biotic and abiotic surfaces in water and soil environments as well as in the human host [101]. They are most efficient at feeding on

surface-associated bacteria and can consume between 0.2 and 1465 bacteria per hour, but are not very efficient at feeding on suspended bacteria [102]. Amoeba engulf and package prey in phagosomes that ultimately fuse with lysosomes allowing for digestion of the ingested prey, and possess a contractile vacuole for maintaining homeostasis [98]. *Acanthamoeba castellanii* is an amoeba widely studied as a model organism for bacterial protozoal interactions due to their close association with various pathogenic bacteria in diverse habitats [103].

Ciliates have characteristic rows of cilia on their cell surface that are used for locomotion and feeding purposes [100]. Ciliates vary in shape (e.g., spheres, ovals or cylindrical) with sizes ranging from 20 to 1000 µm. Ciliates such as *Tetrahymena* spp. draw water containing food particles towards their oral cavity and into a food vacuole. Their ingestion rates are relatively high, and according to one study, they can consume 1254 bacteria per hour [98].

Heterotrophic nanoflagellates such as *Cafeteria roenbergensis* and *Rhynchomonas nasuta* are the smallest protozoa ranging from 2 to 20 µm and thus are only capable of ingesting smaller sized prey [104]. Generally, they have one to four flagella which help them to perform activities like swimming, attachment to surfaces and capturing prey [98]. A single flagellate can ingest 2 to 300 bacteria per hour, and are considered to be the dominant consumers of bacterioplankton in water ecosystems [105].

Protozoan predation controls the phenotypic and genotypic composition of bacterial communities and also alters bacterial community structure [2, 106]. Both the feeding habits of protozoa and bacterial defence mechanisms contribute to the shaping of the bacterial community composition. Bacteria may develop grazing resistance against some protozoan grazers while at the same time being susceptible to others [106]. Microbial food webs are intricately related networks of species like protozoa, bacteria, virus, and organic materials, etc. Protozoan grazing plays a crucial role in the microbial food web as they recycle nutrients and

transfer carbon, nitrogen and phosphorus and hence energy through different trophic levels [107]. The occurrence of grazing resistance among bacteria plays a significant role in reducing carbon transfer and recycling of nutrients between different trophic levels [108]. Mechanistic models predict that the availability of nutrients controls the final abundance of the bacterial population, while grazing by protozoa determines the specific growth rates [109, 110]. Thus, more nutrient availability reflects more production of biomass while more predators reflect less biomass and activity. Predation of bacterial prey by protozoa follows Lotka-Volterra-like oscillations dynamics where both the predator and prey population changes throughout the time in a harmonic fashion [111].

Temperature is an important environmental factor regulating metabolism and feedings rates of protozoa. Increased temperature has stimulating effects on feeding rates, respiration, growth, and cell density of protozoa [112, 113]. Higher temperatures modulate the intensity of top-down effects by increasing predator metabolic processes and through the increased numbers of predators [114]. The increased grazing pressure exerted by protozoa on bacteria at higher temperatures is highly likely to increase the selective pressure for the expression of defensive traits by the bacterial prey, potentially impacting the virulence of these bacteria.

1.8 Mechanisms of bacterial resistance to protozoan grazing

Bacteria use wide varieties of defence strategies to avoid and/or survive protozoan predation. They can deploy those strategies at different stages of interaction, both prior to ingestion and after internalisation [4, 115]. Protozoa feed on bacterial prey in a size dependent-manner, and therefore, different sized prey are not ingested with equal efficiency. Protozoa preferentially consume microbial cells in the size range of 1 to 3 μm, whereas cells outside of this range benefit from reduced of consumption rates [116]. Some bacterial species show morphological plasticity in response to protozoan encounter which helps them to survive protozoan grazing.

For example, *Comamonas* sp. and *Flectobacillus* sp. can form filamentous cells increasing their size from 2 to 40 µm under grazing pressure [117, 118]. Thus, filamentous bacteria escape grazing because they exceed the feeding size range of most bacterivorous protists [119]. Increased swimming speed also protects bacteria as it affects the capture efficiency of protozoa resulting in decreased ingestion rates. Grazing experiments with mixed bacterial communities and bacterivorous flagellates revealed that bacteria with high swimming speeds become more prevalent in the community while bacteria with low swimming speeds are rapidly consumed [120]. Bacterial cell surface properties like O-antigen, LPS and outer membrane proteins (OMP) also greatly contribute to grazing resistance. O-antigen diversity in *Salmonella* sp. has been shown to affect grazing by amoeba [121]. LPS and OMP protect *Klebsiella pneumoniae* from grazing by *Dictyostelium discoideum* and macrophage. The inability to produce LPS and certain OMPs makes *K. pneumoniae* susceptible to phagocytosis [122]. Production of EPS such as lipids, polysaccharides, proteins, and nucleic acids significantly enhances bacterial survival during grazing. EPS-producing bacteria develop microcolonies embedded in the EPS matrix which are protected from grazing [123]. A combination of EPS production and QS-regulated toxigenic compounds regulates the grazing resistance of *V. cholerae* [12].

Bacteria also use several mechanisms to avoid digestion once inside the protozoa. Bacterial efflux systems protect bacteria from the toxicity of micronutrients (Fe, Cu, Mn, and Zn) inside of protozoan phagosomes. Mutations in the efflux system genes reduced the grazing resistance of *Escherichia coli* and *Pseudomonas aeruginosa* [124]. The type III secretion system of *Vibrio parahaemolyticus* and *P. aeruginosa* is an important factor for survival in the presence of the amoeba, where the latter was capable of killing biofilm-associated amoeba using the type III secretion system (T3SS) [125, 126]. *V. cholerae* uses type six secretion system (T6SS) as a virulence factor to kill *D. discoideum* [127]. Production of secreted toxins and secondary metabolites plays a critical role in killing predatory protozoa. Violacein, an alkaloid purple

pigmented secondary metabolite produced by *Chromobacterium violaceum* and *Janthinobacterium lividum* causes apoptosis of flagellates [128]. Another secondary metabolite, pyomelanin, which is produced by the biofilm cells of *V. cholerae,* provides grazing resistance against amoeba [14]. This was shown to be due at least in part to the production of reactive oxygen species (ROS) during auto-oxidation of the pigment. Shiga toxin producing enterohemorrhagic *E. coli* (EHEC) strains that carry Shiga toxin containing prophage is capable of killing *Tetrahymena thermophila* [129].

1.9 Protists as a reservoir and vehicle for transmission of pathogenic bacteria

Not all the bacteria that are ingested are digested in the protozoan host, rather some species can survive and replicate. Phagocytosed bacteria have a number of potential outcomes. Firstly, phagocytosed bacteria can multiply to high numbers, eventually lysing the host cell [130]. Secondly, they may be released in food vacuoles without rupturing the host cell [131]. Thirdly, they may survive inside of the encysted form of protist hosts and finally, phagocytosed bacteria may be able multiply inside of the host but do not escape by host cell lysis [132, 133]. There is growing evidence suggesting that many pathogenic bacteria can establish a symbiotic relationship with diverse protist hosts like amoeba (*Acanthamoeba* sp., *Hartmanella* sp., and *Naegleria* sp.) and ciliates (*Tetrahymena* sp.) [134]. *Legionella pneumophila* is the facultative intracellular bacterium responsible for legionellosis and is found associated with free-living amoebae, including *Acanthamoeba* sp. and *Naegleria* sp. [135, 136]. They can survive and multiply intracellularly by preventing phagosome-lysosome fusion and are released from amoeba in excreted food vesicles [137]. These bacteria-containing vesicles can be inhaled and thus act as a vector for direct dissemination of *L. pneumophilia* to humans [135]. *P. aeruginosa,* the causative agent of pneumonia and other nosocomial infections are widely distributed in the environment. *Acanthamoeba* sp. infected with *P. aeruginosa* was found in hospital-associated contaminated drinking water [138]. The obligate intracellular bacterial parasite, *Chlamydia*

spp, was found in amoeba isolated from human nasal mucosa suggesting that amoeba could act as potential transmission vectors [139]. Various strains of *E. coli* (K1, K12 and pathogenic strains O157: H7) widely studied for their interaction with protozoa can also survive intracellularly within *Acanthamoeba* sp. and *Tetrahymena* sp. [7]. *Listeria monocytogenes* responsible for listeriosis uses a virulence factor called listeriolysin O to grow and survive in the ciliate, *Tetrahymena pyriformis* [140]. *V. cholerae* O1 and O139 strains can also survive inside of various amoeba hosts like *A. castellanii, Acanthamoeba polyphaga* and *Naegleria gruberi* [13, 141, 142]. *V. cholerae* and *Acanthamoeba* sp. were also isolated from water in a cholera endemic region in Sudan [143]. In addition, *Mycobacterium* sp., *Burkholderia cepacia*, *Helicobacter pylori*, and *Campylobacter jejuni* can survive and multiply inside of protozoan hosts [144-147]. Protist hosts can provide physical protection from various environmental stressors like UV light and chlorination. For example, *Salmonella typhimurium* and *Shigella sonnei* are resistant to chlorine treatment when in *A. castellanii* and *T. pyriformis*, which facilitates their survival in chlorine-treated water supplies [148]. Therefore, protozoa are regarded as Trojan horses of the microbial world due to the fact that some pathogenic bacterial species are well protected inside the host and can be transmitted to a new environment and are therefore, vectors for transmission of bacteria to human [149].

1.10 Evolution of bacterial virulence in response to protozoan predation

The interactions of bacteria with protozoa are regarded as one of the most primitive interactions between prokaryotes and eukaryotes [150]. Due to their long history of interaction, it is speculated that the virulence properties of human bacterial pathogens arise from the evolution of traits as defences against protozoan predation or for parasitism of the protozoan host [151]. The coincidental evolution hypothesis suggests that virulence of many pathogens arises as a result of selection acting on those pathogens in a different environment where human hosts are an evolutionary dead-end [152]. In support of this, it has been shown that *L. pneumophilia* can

survive and multiply inside an amoeba host and that this significantly enhances its virulence to human hosts [136, 153]. Such interactions also increase the resistance of *L. pneumophilia* to antimicrobial agents. After adaptation in *Acanthamoeba*, the obligate anaerobic bacterium, *Mobiluncus curtisii* can survive aerobically [154]. In grazing experiments with different strains of *E. coli* and *D. discoideum,* virulence factors were developed primarily to resist protozoa predation in the environment [155]. The interaction of *Bordetellae* sp. with predatory amoeba increases their fitness and allows for colonisation of mammalian lungs at the cost of losing adaptation to environmental reservoirs [156]. In another example, amoeba-adapted *Mycobacterium avium* showed increased virulence in a mouse model of infection [157]. Predation of the carp pathogen, *Aeromonas hydrophila,* by *T. thermophila* results in enhanced adaptation against multiple environmental stressors [158].

Thus, the bacterial defensive traits that are used for resisting protozoan predation as described in earlier sections of this review, play critical roles in improving fitness and pathogenicity in human and animal hosts [8]. Predation pressure could also lead to the opposite outcome where bacteria may lose pathogenic potential if the predation defensive traits are different from traits needed for human infection. In this case, bacteria have a fitness trade-off at the cost of predator defence resulting in decreased pathogenicity. The growth of *Serratia marcescens* for an extended period with *Tetrahymena* sp. resulted in attenuation of virulence due to the loss of pigment production which is a virulence factor in humans [159].

Protozoan hosts like amoeba are very similar to macrophages as both are unicellular, capture bacteria by phagocytosis and share various physiological and structural features. Owing to these remarkable similarities, macrophages and amoeba are considered to be evolutionarily related [160]. It is now believed that mechanisms that evolved in bacteria during their association with protozoa also allow for survival in macrophage. This led to the hypothesis that

protozoa serve as a training ground or biological gym for bacterial pathogens which enables survival in human and animal hosts [161]. The capability of *L. pneumophila* to parasitise human macrophages is thought to be the outcome of prior adaptation with diverse protozoan hosts [162]. It is highly likely that bacteria gain these adaptive advantages during co-evolution with protozoa at least in part through the acquisition of eukaryotic genes [163, 164].

1.11 Adaptive evolution of *V. cholerae* in response to protozoan predation

The bacterial pathogen, *V. cholerae,* persists in the water column and interacts with a wide range of organisms, including heterotrophic protists [8]. Long-term persistence and blooms of *V. cholerae* depend on the ability to resist grazing pressure by diverse protists in the aquatic system [165]. As *V. cholerae* lives in a biofilm community in the environment, they are protected from the grazing of most flagellates whereas their planktonic counterparts are grazed [12]. In contrast, biofilm cells are susceptible to grazing by biofilm/surface-feeding amoeba and nanoflagellates. *V. cholerae* must have developed defensive mechanisms to survive predation against these protists [10]. Biofilm cells of *V. cholerae* confer ROS-mediated resistance to predation by *A. castellanii* by the production of the secondary metabolite, pyomelanin [14]. Biofilm cells of *V. cholerae* are also protected from grazing by the surface-feeding nanoflagellate, *R. nasuta* and the amoeba *A. castellanii* by the production of VPS. The rugose variants of *V. cholerae* are more grazing resistant compared to the smooth variants [12].

Both clinical and environmental *V. cholerae* strains use QS to regulate the expression of anti-protozoal factors [13]. Experiments with the null mutant of the QS master regulator, *hapR,* revealed that it is more susceptible to grazing than the wild-type *V. cholerae* but not completely sensitive, which indicates that *V. cholerae* co-ordinates the production of anti-protozoal factors through QS and other unknown environmental sensing systems [166]. PrtV which is an extracellular protease secreted by *V. cholerae* provides grazing resistance against *T. pyriformis*

and *C. roenbergensis* [167]. The absence of QS-regulated haemagglutinin protease (HAP) hampers the encystation process in amoeba through the intoxication of amoeba trophozoites by the haemolysin, HlyA [15]. Thus *V. cholerae* uses the HapA protease to cleave haemolysin to prevent premature lysis of the amoeba host, ensuring successful replication inside of the protist vacuole. *V. cholerae* delivers cytotoxic effector proteins through the T6SS to kill *D. discoideum* [168]. The above examples indicate that *V. cholerae* uses wide varieties of mechanisms and strategies to prevent and survive protozoan predation.

1.12 Chapter synopsis and project aims

This work elucidated how the cholera pathogen, *V. cholerae,* adapts in the natural environment under predatory pressure. The effects of long-term amoeba predation on virulence-associated traits of *V. cholerae* were investigated to identify mechanisms of adaptation under predation stress. The work further investigated how these traits might contribute to the enhanced persistence and fitness of the bacterium in the environment.

Chapter Two investigated the phenotypic diversity in *V. cholerae* that arose during long-term co-incubation with an amoeba predator and characterised the underlying mechanisms of the phenotypic diversity and their role in maintaining bacterial fitness. The chapter also assessed the colonisation potential of the amoeba-adapted strains using an animal model.

Chapter Three elucidated potential mechanisms of anti-predator defences that were acquired by *V. cholerae* during adaptation with an amoeba host and highlighted their role in enhanced fitness of the bacterium during predation stress. Transcriptomic analysis was conducted to identify the bacterial traits associated with the enhanced fitness and survival of *V. cholerae* in amoeba.

Using genome sequencing and mutational analysis, Chapter Four investigated the genetic diversity in *V. cholerae* that arose during long-term co-incubation with amoeba predator. The

chapter also compared the mutations between amoeba-adapted and non-adapted *V. cholerae* to characterise the effect of amoeba predation on driving genomic changes.

Finally, Chapter Five provided a general summary and discussion on the results presented in this work. Future perspective and implications of this research are also highlighted.

Declaration

I declare that the below manuscript meets the following requirements for inclusion as chapters in this thesis.

- I have contributed more than 50 % for the below manuscript.
- The below publication has been peer reviewed
- The below manuscript has been formally published and is formatted to adhere to the specific formatting requirements of ISME J.
- The publication is open access and no approval from the publisher is necessary.

Hoque MM, Noorian P, Espinoza-Vergara G, Manuneedhi Cholan P, Kim M, Rahman MH, Labbate M, Rice SA, Pernice M, Oehlers SH, McDougald D. 2021. Adaptation to an amoeba host drives selection of diverse traits in *Vibrio cholerae.* **The ISME Journal**. https://doi.org/10.1038/s41396-021-01134-2

Publication status: Published

Candidate's signature:

Production Note:
Signature removed prior to publication.

Date: 15th January 2022

Chapter Two

Adaptation of *Vibrio cholerae* in an amoeba host drives trade-offs of virulence traits and enhanced colonisation in zebrafish

Chapter Two

Adaptation of *Vibrio cholerae* in an amoeba host drives trade-offs of virulence traits and enhanced colonisation in zebrafish

2.1 Introduction

Predation by heterotrophic protists and bacteriophages represents a major driving force shaping bacterial population structure and composition [2, 169]. In response to predation pressure, bacteria have evolved adaptive traits which enhance their survival and persistence in the environment [4, 115]. Antipredator strategies are hypothesised to have evolved from predation pressure and play crucial roles in predation resistance and virulence which supports the "coincidental evolution" hypothesis [131, 170-172].The hypothesis states that, virulence arises as an accidental consequence of those antipredator mechanisms in distinct niches rather than for virulence *per se*. In contrast, predation driven attenuation of virulence has also been observed and this results in increased commensalism between bacteria and hosts/predators [173-175]. Such commensal relationships enhance pathogen persistence and transmission in the environment.

Patho-adaptation to protist hosts is now widely recognised to be training grounds for bacterial pathogens including *Vibrio cholerae,* the waterbourne bacterium that causes the acute diarrhoeal disease, cholera [176]. Cholera follows a distinct pattern with recurring episodes of seasonal epidemics suggesting potential involvement of environmental factors in the survival of the organism in the environment [177], including interactions with heterotrophic protists [8]. It has been reported that the free-living amoeba, *Acanthamoeba castellanii,* and the ciliate, *Tetrahymena pyriformis,* serve as environmental hosts for *V. cholerae* [13, 178]. In fact, *T. pyriformis* and other ciliates expel a hyper-infectious form of *V. cholerae* packaged in released

food vacuoles [131], suggesting that protists play an important role in the infection cycle of *V. cholerae*.

A growing number of reports have described the roles of different phenotypic traits in grazing resistance in *V. cholerae*. For example, changes in biofilm formation, secondary metabolite production (e.g. pyomelanin), extracellular proteases (e.g. HapA, PrtV) and quorum-sensing mediated production of anti-protozoal factors are involved in grazing resistance and association with diverse protist hosts [15, 179-181]. Swimming motility is a crucial trait in bacteria that controls the rate of contact and engulfment of prey, depending on the type of protist host. Increased swimming speed help bacteria to avoid grazing by some protists [182], while enhancing the rate of contact with raptorial feeding protists [183, 184]. Grazing resistance of biofilms largely depends on the types of protozoan grazers. The surface-feeding protozoa like amoeba preferentially graze biofilm cells, whereas suspension-feeding protozoa, such as ciliates and flagellates mostly feed on planktonic cells [185].

V. cholerae biofilms produce anti-protozoal factors shown to be involved in grazing resistance against different protozoan hosts [181]. Extracellular proteases also confer grazing resistance against flagellated and ciliated protozoa [167]. Other secreted factors such as the haemolysin also play an important role in the intracellular survival of *V. cholerae* in protozoa [15]. However, many aspects of the interactions between protozoa and *V. cholerae* are yet to be explored, in particular, the selective pressure exerted by long-term exposure to predation and the emergence of adaptive traits which allow the pathogen to persist in the environment.

This chapter illustrates the adaptive traits that arise as a result of long-term co-adaptation of *V. cholerae* with *A. castellanii*. Differences in phenotypic characteristics of *V. cholerae* in the presence and absence of amoeba was investigated in isolates for 90 days. The late-stage amoeba-adapted isolates showed increased survival and competitive fitness in amoeba. There

was a decrease in motility, biofilm formation and haemolytic activity and an increase in protease activity in amoeba-adapted isolates compared to non-adapted isolates. These altered phenotypic behaviours and improved fitness in late-stage amoeba-adapted *V. cholerae* were associated with mutations in the flagellar transcriptional master regulator, *flrA*. Furthermore, the phenotypes observed in the late-stage amoeba-adapted isolates are an indication of increased HapR activity, the quorum-sensing master regulator in *V. cholerae* which positively regulates production of proteases while negatively regulating biofilm formation. Finally, the mutations in *flrA* resulted in increased competitive fitness and enhanced colonisation of *V. cholerae* in the zebrafish model of infection. Taken together, these results show how adaptation of *V. cholerae* in a natural host can also drive the evolution of host-pathogen interactions.

2.2 Materials and methods

2.2.1 Organisms and growth conditions

V. cholerae O1 El Tor strain A1552 and its derivatives were routinely grown on Luria Bertani (LB) agar plates or in liquid LB medium with shaking. *A. castellanii* was routinely maintained axenically in peptone yeast glucose (PYG) medium supplemented with salts (ATCC medium 712) at room temperature in 25 cm^2 tissue culture flasks with ventilated caps (Sarstedt Inc., Nümbrecht, Germany). *A. castellanii* was passaged 3 days prior to harvesting for experiments and enumerated microscopically using a haemocytometer. The long-term co-incubation was performed in (2M) marine minimal medium (1 M MOPS, pH 8.2; 132 mM K_2HPO_4; 952 mM NH_4Cl; 0.4 M Tricine and 1mM $FeSO_4.7H_2O$, pH 7.8 in artificial seawater) supplemented with 0.08% glucose [186]. The artificial seawater, or nine salts solution (0.5 × NSS) was composed of 17.6 g NaCl, 1.47 g Na_2SO_4, 0.08 g $NaHCO_3$, 0.25 g KCl, 0.04 g KBr, 1.87 g $MgCl_2•6H_2O$, 0.45 g $CaCl_2•2H_2O$, 0.01 g $SrCl_2•6H_2O$ and 0.01 g H_3BO_3 in one litre of distilled water [187]. All organisms, oligonucleotide primers and plasmids used in this study are listed in Supplementary Table 1.

2.2.2 Experimental co-adaptation of *V. cholerae* with *A. castellanii*

Three biological replicates of *V. cholerae* A1552 were grown overnight and washed with 2M medium [186], adjusted to 10^9 cells ml^{-1} (OD_{600} = 1.0) and 100 µL of diluted cells (approximately 10^7 cells ml^{-1}) were used to inoculate three independent cultures (P1, P2 and P3) of *A. castellanii* (1×10^5 cells ml^{-1}) in 1 mL of 2M medium in 24-well plates. The plates were incubated at room temperature with shaking at 60 rpm. Every three days, the amoeba in three replicate wells were lysed with 1% Triton X-100 and the released *V. cholerae* passaged to a fresh plate of amoeba. One half of the remainder of the *V. cholerae* cells were placed at -80°C for selection of individual isolates while the remainder was used for isolation of genomic DNA from the population for sequencing. In parallel, three biological replicates of *V. cholerae* were maintained in 2M medium in triplicate in the absence of amoeba and were sub-cultured every three days in fresh 2M medium after treating with 1% Triton X-100 as non-predator controls. The *V. cholerae* grown in the presence or absence of *A. castellanii* were defined as adapted and non-adapted populations, respectively. The individual isolates derived from the populations were defined as adapted and non-adapted isolates, respectively.

2.2.3 Intracellular survival assays

A. castellanii was seeded at a concentration of 1×10^5 cells ml^{-1} in 2M medium in 24-well plates one hour prior to the addition of bacterial cells to allow them to adhere. Overnight amoeba-adapted and non-adapted isolates of *V. cholerae* were washed and diluted to OD_{600} 1.0 in 2M medium. Diluted cells (10^7 cells) were used to inoculate triplicate wells of previously seeded *A. castellanii* at a final amoeba:bacteria ratio of 1:100. The plates were incubated statically at room temperature and intracellular bacteria were recovered at different time points by lysis of the amoeba with 1% Triton-X. Thirty min before lysis, 300 µg ml^{-1} of gentamicin (Sigma-Aldrich, United States) was added to kill extracellular bacteria followed by washing with 2M media to remove antibiotics. Intracellular bacteria were collected and resuspended in

2M medium before plating for enumeration. The percentage of intracellular survival was calculated for each of the isolates using the formula number of surviving bacteria at 4 hours / number of surviving bacteria at 2 hours.

2.2.4 Competition assays

In vitro and *in vivo* competition assays were conducted by mixing a Δ*lacZ* strain of A1552 with the amoeba-adapted isolates at a ratio of 1:1 (v/v). For *in vitro* competition assays, 100 µL of the mixed bacterial cells (approximately 10^7 CFU ml^{-1}) were inoculated into LB and grown 24 hours. Serial dilutions of the cultures were plated on LB agar plates supplemented with 50 µg ml^{-1} X-gal (5-bromo-4-chloro-3-indolyl-D-galactopyranoside) which allowed enumeration of β-galactosidase-positive and negative *V. cholerae* colonies. For competition assays in amoeba, 100 µL (approximately 10^7 CFU ml^{-1}) of the mixed bacterial cells were incubated with amoeba (approximately 10^5 cells ml^{-1}) to a final amoeba:bacteria ratio 1:100 for 24 hours. Amoeba cells were lysed, and intracellular bacteria were recovered as previously described. The competition index (CI) for each of the isolates were calculated by dividing the output ratio (adapted/Δ*lacZ*) after incubation corrected by the input ratio.

2.2.5 Motility assays

The swimming motility assay was performed on LB medium with 0.3 % (w/v) agar. An overnight colony of the *V. cholerae* isolates was inoculated by stab and the plates were incubated at 30 °C for 24 hours and imaged (Bio-Rad, USA). The diameters of the migration zone were measured using ImageJ.

2.2.6 Quantification of biofilm biomass

Biofilms were formed in microtitre plates and biomass was quantified by the crystal violet (CV) staining assay as described previously [188]. Briefly, *V. cholerae* isolates were grown in LB to an OD_{600} of 0.6 (approximately 10^6 cells ml^{-1}). The normalised suspensions were diluted

100-fold and inoculated into fresh LB and grown for 36 hours at room temperature. The aqueous phase was removed and attached biomass washed with 50 % NSS. The CV solution (0.1 %) was added and incubated for 10 minutes at room temperature. The plate was washed to remove unbound CV and biofilm-associated CV was solubilised with 95 % ethanol, and the OD_{600} was measured using a micro-plate reader (Tecan Spark, Switzerland). Values were corrected by deducting the baseline defined as LB medium. The experiment was performed in triplicate and run in three independent experiments.

2.2.7 Protease assay

Protease activity was determined by the azocasein assay as described previously [189]. Briefly, *V. cholerae* isolates were grown overnight in LB at 37 °C with shaking at 200 rpm and adjusted to 10^9 cells ml^{-1} (OD_{600} =1.0). The suspension was filtered and 100 µL of cell-free supernatant was mixed with 900 µL of azocasein solution (1 % in 0.1 M Tris pH 8.0) for 4 hours at 37°C and the reaction stopped with the addition of equal volumes of 10 % trichloroacetic acid. Precipitated, undegraded protein was removed by centrifugation, the supernatant collected, and the absorbance determined by spectrophotometry (450 nm). The enzymatic activity unit was determined by the following formula U = Abs at 450 nm / conc. of substrate (g) / time (hour) and the activity unit standardised by OD_{600} of the culture prior to centrifugation.

2.2.8 Haemolysin assay

Haemolysin assays were performed using previously described methods with some modifications [190]. *V. cholerae* isolates grown in LB were centrifuged, washed and cell numbers adjusted to 10^9 cells ml^{-1} (OD_{600} = 1.0) in PBS (pH 7.4). Equal volumes of cells were mixed with 1% sheep erythrocyte suspensions and incubated at 37 °C for 2 hours followed by incubation at 4°C for 1 hour. Unlysed RBCs were removed by centrifugation and haemolytic activity measured by spectrophotometry at 540 nm. Percentage of haemolysis was calculated

using the formula (sample absorbance – blank absorbance) / (control absorbance – blank absorbance) ×100. As a positive control, cells were lysed with 1% Triton X-100.

2.2.9 Generation and complementation of *flrA* mutant

The *V. cholerae* Δ*flrA* mutant was constructed by splicing overlap extension PCR (SOE PCR) and natural transformation [191]. Briefly, primers were used to amplify two flanking regions of the *flrA* gene (VC2137) and fused with the chloramphenicol acetyltransferase (*cat*) gene amplified from pKD3 using SOE PCR. The construct was transformed into *V. cholerae* using chitin-mediated natural transformation [192]. The transformants were selected on LB agar plates supplemented with 5 µg ml^{-1} of chloramphenicol. The *cat* gene was removed from the resultant transformants using the TransFLP method to get an in-frame deletion mutant [193]. The absence of the gene was confirmed by PCR.

For complementation, *flrA* from wild type A1552 as well as the mutants (A213V and V261G) from amoeba-adapted isolates were amplified by PCR and cloned into pBAD24 using Gibson assembly [194]. The recombinant plasmids were transformed into *E. coli* using chemical transformation and recombinant transformants selected on LB agar plates containing 100 µg ml^{-1} of ampicillin. Recombinant plasmids were extracted from *E. coli* using a GeneJET plasmid miniprep kit (Thermo Fisher Scientific). The recombinant plasmids were transformed into *V. cholerae* Δ*flrA* mutant using chitin-mediated transformation. The transformants were selected on LB agar plates supplemented with 100 µg ml^{-1} of ampicillin. Sequences of all genes were verified using PCR for the WT copy and ARMS-PCR for the mutated copy with primers in Supplementary Table 1.

2.2.10 Scanning electron microscopy

Bacterial cultures were fixed with 2 % glutaraldehyde in PBS and then stored in PBS at 4 °C until processing. Twenty µL of undiluted bacteria samples were vacuum filtered onto

polycarbonate filters (diameter 47 mm, pore size 0.4 μm). The preparation was subjected to a dehydration series with ethanol and milli-Q water (35, 50, 75, and 100% ethanol for 10 min each) followed by hexamethyldisilazane (HMDS) drying (50 and 100% for 10 min each). Filters were mounted onto scanning electron microscopy (SEM) mounts with carbon tape and air dried for 24 h before sputter coating with 10 nm of gold/palladium. Samples were imaged via an SEM (Zeiss supra 55).

2.2.11 Fluorescent tagging

Green fluorescent protein (GFP) and red fluorescent protein (DsRedExpress)-tagged strains were generated using mini-Tn7 delivery plasmids and helper plasmid pUX-BF13 containing the Tn*7* transposase gene as described previously [195]. Plasmids were transformed using chitin-mediated natural transformation into bacterial strains. Transconjugants were selected on LB agar medium containing 50 μg ml^{-1} gentamicin at 30°C. Fluorescent strains were verified by PCR analysis and fluorescence microscopy.

2.2.12 Adult zebrafish infection and histology

Adult zebrafish (*Danio rerio*) infection experiments were carried out with ethical approval from the Sydney Local Health District Animal Welfare Committee approval 19-031. Zebrafish were raised to 6-12 months of age in a recirculating aquarium system. Animals were transferred to a 28°C incubator with a 14:10 hour light:dark cycle in 1 L beakers for overnight acclimatisation. Zebrafish were exposed to 5×10^9 CFU of *V. cholerae* test and parent *lacZ* negative strains for 6 hours in 200 ml of aquarium system water yielding a final concentration of 2.5×10^7 CFU ml^{-1} [196]. Zebrafish were washed in a clean water system and housed until 24 h post infection. Zebrafish were euthanised by tricaine (MS-222, Sigma) overdose and intestines were dissected. Dissected intestines were homogenised in PBS using a bead beater at 4°C and homogenates plated on LB agar containing rifampicin (50 μg ml^{-1}) and X-gal (80

μg ml^{-1}) for enumeration. The CI was calculated by dividing the output ratio (test strain/Δ*lacZ*) after infection corrected by the input ratio.

For the histology, dissected intestines were fixed in 10 % neutral buffered formalin overnight at 4°C, rinsed in PBS, and then incubated in 30 % (w/v) sucrose, 50:50 30 % sucrose:OCT (4583, Tissue-Tek), and OCT for approximately 4 hours each [197]. Tissue was frozen in OCT and cryosectioned in 20 μm sections. Slides were rinsed in PBS, coverslips were mounted with DAPI fluoromount G (ProSciTech), and imaging was carried out on a Leica DM6000B microscope [197]. Fluorescent bacteria were quantified by fluorescent pixel count of sections in ImageJ [198]. Data are pooled from two animals per group.

2.2.13 Statistical analysis

GraphPad Prism software version 9 La Jolla California USA, (www.graphpad.com) was used for statistical analyses. Two-tailed student's t-tests (non-parametric Mann–Whitney tests) were used to compare means between WT and mutant bacteria. Statistical analysis for experiments with multiple samples were performed using either two-way ANOVA and Sidak's multiple comparisons test or one-way ANOVA and Kruskal-Wallis test. Principal component analysis (PCA) was conducted in rstudio using the 'ggfortify' package (https://cran.r-project.org/web/packages/ggfortify/index.html).

2.3 Results

Here we tested the effects of long-term co-adaptation of *V. cholerae* with the amoeba predator, *A. castellanii*. There are indications that long-term predation can result in genotypic and phenotypic changes in the bacterial prey and that these changes can affect persistence and colonisation of host organisms. Here, we co-incubated *V. cholerae* with amoeba for 90 days in triplicate. After co-incubation, we collected intracellular samples from each replicate every 3 days. Samples of *V. cholerae* incubated in 2M media only were also taken every 3 days as

controls. To identify phenotypic changes, we first obtained individual isolates from both the co-incubation and control samples on days 3, 45 and 90. To identify the underlying mechanisms of phenotypic changes, both the population samples and the individual isolates from both the co-incubation and control populations obtained at the 3 times points were sequenced.

2.3.1 Increased intracellular survival of amoeba-adapted isolates

Three biological replicates (P1, P2, and P3) of *V. cholerae* were grown in the presence and absence of amoeba for 90 days in marine minimal (2M) medium. In addition, individual *V. cholerae* isolates were collected every 3 days; adapted isolates were recovered from the co-cultures while non-adapted isolates were collected from 2M without amoeba. In total, 90 adapted and 90 non-adapted isolates were recovered, 30 of which were isolated on days 3, 45 and 90 from each treatment. In order to assess differences in bacterial fitness, the intracellular survival of the adapted isolates in amoeba were assessed and compared to the non-adapted isolates using a standard gentamicin protection assay [199]. The intracellular survival of day 3 adapted and non-adapted isolates was not significantly different, while 45 and 90 day adapted isolates showed a 5-fold increased survival compared to the non-adapted isolates ($p < 0.001$) (Figure 2.1A).

2.3.2 Increased competitive fitness of amoeba-adapted isolates

To further confirm the increased intracellular survival of the adapted isolates, an amoeba intracellular competition assay was performed using a Δ*lacZ* isogenic strain. After 24 h of incubation, day 3 adapted isolates showed a competitive index (CI) of approximately 1.0, while the CI of 45 and 90 day adapted isolates were 100.8 and 102.8 respectively, indicating an approximately 100-fold increased fitness compared to the day 3 adapted isolates ($p < 0.001$) (Figure 1B). In addition to the intracellular competitive fitness, the *in vitro* competitive fitness

in LB medium was investigated using the Δ*lacZ* isogenic strain to further understand if the increased fitness of the adapted isolates was due to a growth advantage. In this condition, the CI for the day 3 adapted isolates was approximately 1.0, while the day 45 and 90 adapted isolates showed a 10-fold increase in fitness (Figure 1C) ($p < 0.001$). The CI of the adapted isolates is significantly higher for intracellular survival compared to *in vitro* growth in LB suggesting that the increased intracellular survival is due to factors beyond a growth advantage. Taken together, these results show that long-term adaptation with amoeba results in *V. cholerae* isolates with increased fitness when cultured in LB and when incubated intracellularly in amoeba.

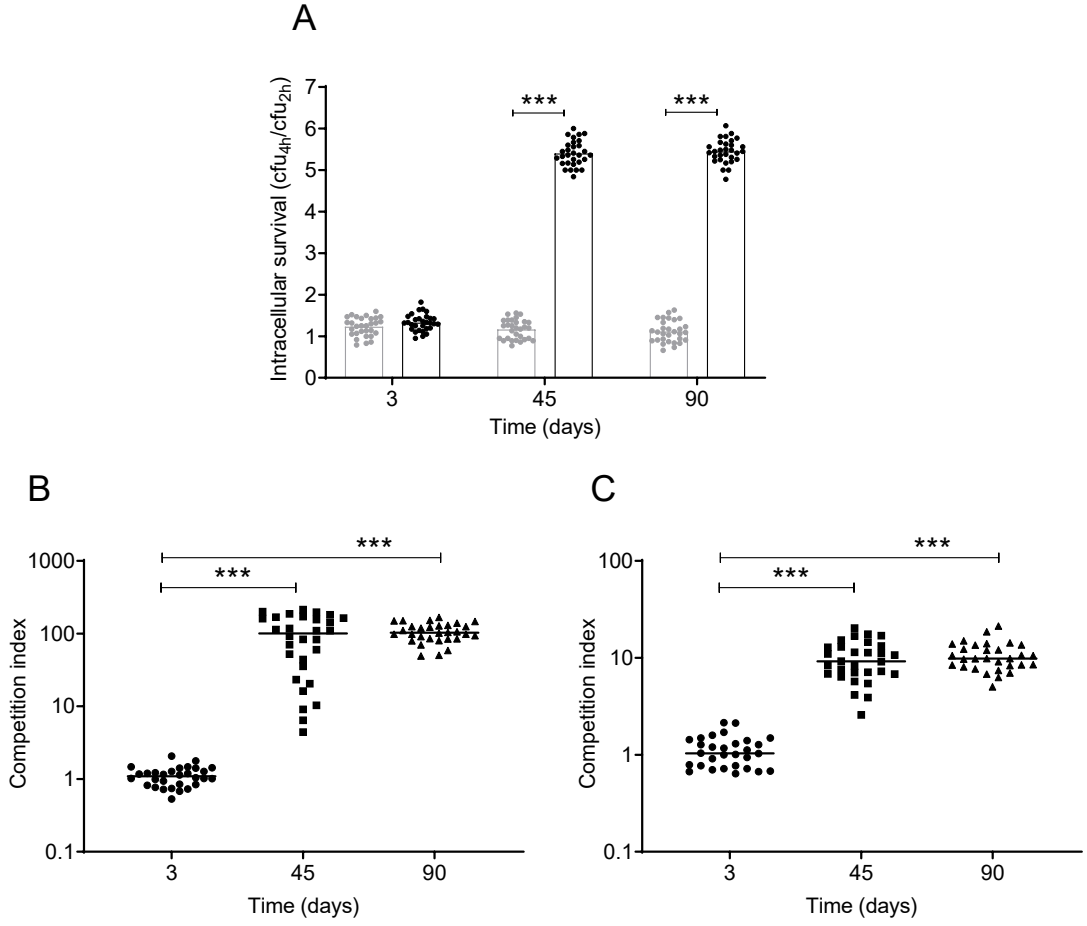

Figure 2.1. Intracellular survival and competitive fitness of adapted and non-adapted isolates. (A) Intracellular survival in *A. castellanii* of adapted (black) and non-adapted (grey) isolates calculated by dividing the CFU at 4 h by the CFU at 2 h of the assay. (B) Intracellular competitive fitness of adapted isolates in *A. castellanii*. (C) *In vitro* competition assay of adapted isolates grown in LB for 24 hours. CI in amoeba (B) and in LB medium (C) was calculated by dividing the output ratio (adapted/Δ*lacZ*) after incubation, corrected by the input ratio. Statistical analysis was performed to determine the significance of the CI of days 45 and 90 isolates compared to day 3 isolates. Data are obtained from 30 individual adapted and non-adapted isolates from 3 time points (days 3, 45 and 90). Data are shown as the median. Statistical analyses for A, was performed using two-way ANOVA and Sidak's multiple

comparisons test. For B and C statistical analyses were performed using one-way ANOVA and Kruskal-Wallis test. Statistical significance is indicated by ∗∗∗, $p < 0.001$.

2.3.3 Virulence-related phenotypes of amoeba-adapted isolates

To elucidate the factors contributing to the increased fitness of the adapted isolates, virulence-associated phenotypes such as motility, biofilm formation, haemolysin and protease production were evaluated. Results showed that the motility of the adapted and non-adapted isolates decreased over time. The motility of the day 3 adapted and non-adapted isolates did not differ significantly ($p = 0.67$; mean diameter approximately 14 mm), while the motility of 45 and 90 day adapted isolates were significantly decreased compared to the respective non-adapted isolates ($p < 0.001$; mean 2.4 and 2.7 mm, respectively) (Figure 2.2A). There was no significant difference in biofilm formation for the day 3 adapted and non-adapted isolates ($p = 0.37$) (Figure 2.2B). However, the biofilm biomass of adapted isolates from days 45 and 90 was significantly reduced to 40.8 % ($p < 0.001$) and 54.9 % ($p < 0.001$) respectively, compared to the non-adapted isolates.

Long-term adaptation also led to significant decreases in haemolytic activity of amoeba-adapted *V. cholerae* (Figure 2.2C). The haemolytic activity of the day 3 adapted and non-adapted isolates did not differ significantly ($p = 0.31$), however, the haemolytic activity of adapted isolates from days 45 and 90 decreased to 30.4% ($p < 0.001$) and 43.1% ($p < 0.001$), respectively, compared to non-adapted isolates. In contrast to the results observed for haemolytic activity, long-term co-adaptation of *V. cholerae* with amoeba resulted in increased proteolytic activity (Figure 2.2D). The protease activity of adapted and non-adapted isolates of *V. cholerae* from day 3 did not differ significantly ($p = 0.33$), while it increased significantly for adapted isolates from days 45 and 90 to 37.1 % ($p < 0.001$) and 59.4 % ($p < 0.001$), respectively. Thus, the amoeba-adapted isolates exhibit a temporal change in these virulence

phenotypes with decreases in motility, biofilm formation and haemolysin activity while exhibiting increased protease activity.

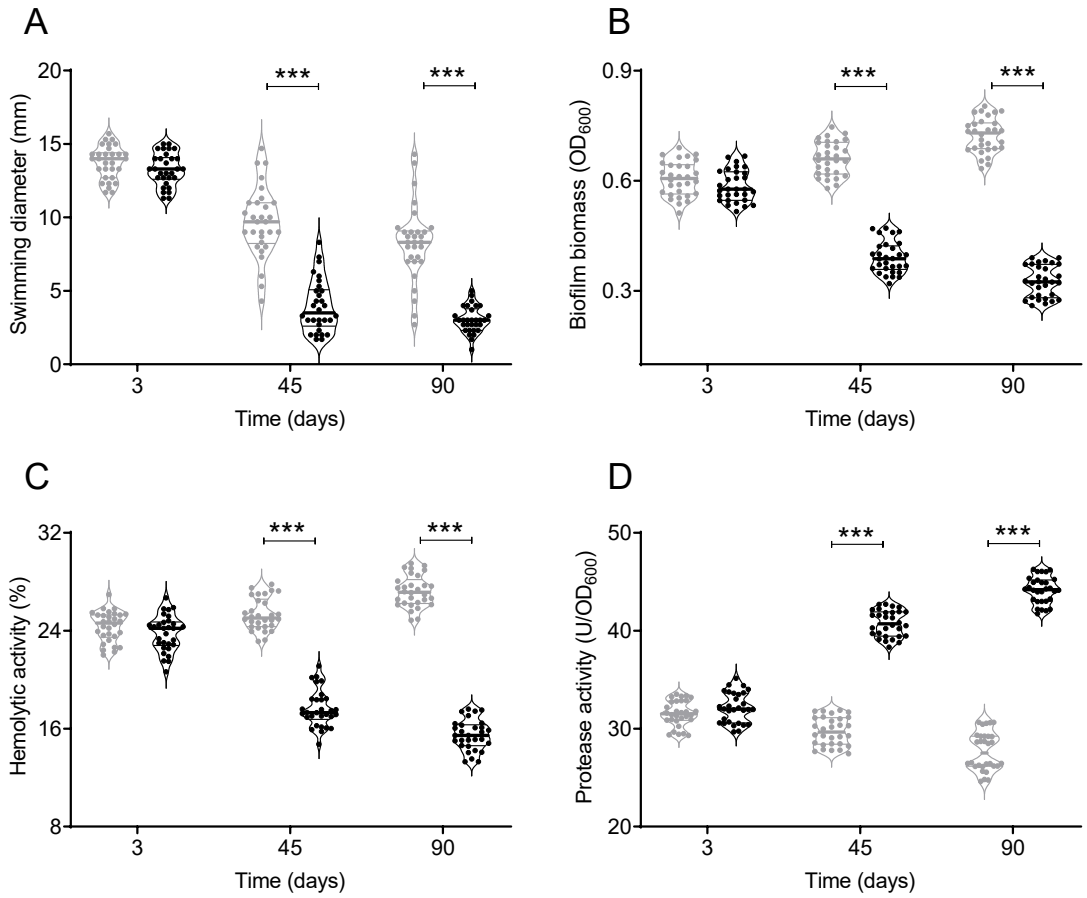

Figure 2.2. Virulence-related phenotypes of adapted and non-adapted isolates. (A) Swimming motility of the adapted (black) and non-adapted (grey) isolates expressed as diameter (mm) of the zone travelled from point of inoculation by bacteria grown overnight on semi-solid LB agar plates. (B) Biofilm biomass of adapted (black) and non-adapted (grey) isolates as quantified by crystal violet staining. (C) Haemolytic activity of adapted (black) and non-adapted (grey) isolates expressed as percent haemolysis of 1% sheep erythrocyte suspension. (D) Protease activity of cell free supernatants of adapted (black) and non-adapted (grey) isolates measured by azocasein hydrolysis. Data are obtained from 30 individual adapted and non-adapted isolates from 3 time points (days 3, 45 and 90). Data are shown as the median.

Statistical analyses were performed using two-way ANOVA and Sidak's multiple comparisons test. Statistical significance is indicated by ∗∗∗, $p < 0.001$.

2.3.4 Amoeba-adapted isolates with A213V and V261G mutations in *flrA* are aflagellar

To identify the underlying genetic causes for phenotypic diversity, whole genomes of amoeba adapted and non-adapted *V. cholerae* isolates were sequenced and analysed for presence of mutations. The result of the mutational analysis presented in Chapter Four revealed that adapted *V. cholerae* isolates from day 45 and 90 harbour non-synonymous mutations in the *flrA* gene. It is important to note that the *flrA* gene was the only gene mutated in the adapted isolates and was not mutated in non-adapted *V. cholerae* isolates. The *flrA* gene is the flagellar transcriptional master regulator which regulates flagellar synthesis by initiating transcription of its downstream genes [200, 201]. *V. cholerae* fails to synthesise a flagellum in the absence of the *flrA* gene. To determine the effect of point mutations detected in *flrA* in the adapted isolates on flagellum formation, adapted isolates harbouring A213V and V261G mutations in *flrA* gene were analysed using SEM, which confirmed no flagellum in *flrA* mutants (Figure 2.3). Hence, the two amino acids, alanine at 213 and valine at 261 are important for *flrA* controlled flagellar synthesis.

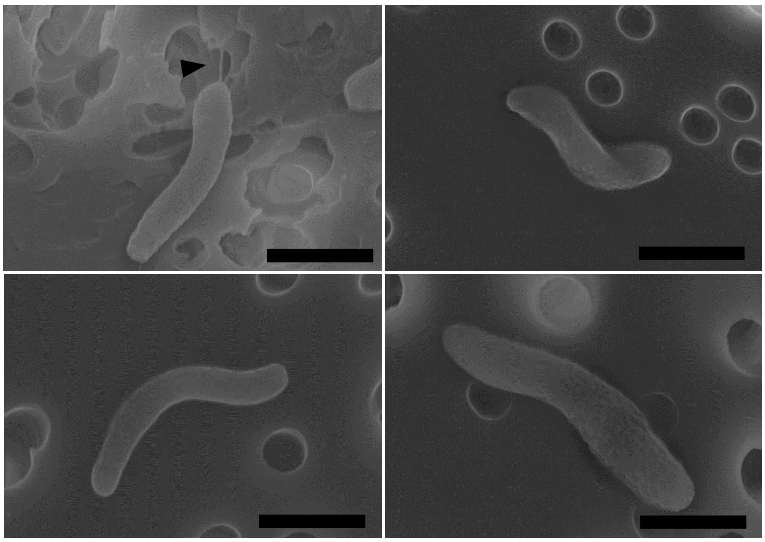

Figure 2.3. Scanning electron micrograph showing presence or absence of flagellum. Wild type A1552 (top left), A1552 Δ*flrA* (top right), A1552 *flrA* A213V (bottom left), A1552 *flrA* V261G (bottom right). The presence of flagella in the wild type is indicated with the black arrow. Scale bars: 1µm.

2.3.5 Changes in virulence-associated phenotypes, increased intracellular survival and fitness are due to *flrA* mutations

To examine whether genetic mutations in *flrA* explain the observed changes in virulence factor production, increased intracellular survival and improved fitness of the 45 and 90 day adapted isolates, a *flrA* deletion mutant (Δ*flrA*) was generated. Interestingly, all the phenotypic features that were observed in the adapted isolates were observed in the Δ*flrA* mutant. The intracellular survival of Δ*flrA* was approximately seven times greater than the WT and the mean survival of the non-adapted isolates (Figure 2.4A). The CI of Δ*flrA* was 100-fold greater compared to the WT in amoeba (Figure 2.4B) and 10-fold greater in LB (Figure 2.4C). The Δ*flrA* mutant showed a 7.5-fold reduction in swimming motility (diameter of 2 mm) (Figure 2.4D), a 55% reduction in biofilm biomass (Figure 2.4E) and a 30% reduction in haemolysin activity

compared to the WT (Figure 2.4F). In contrast, the average protease activity for Δ*flrA* was 70% higher when compared to the WT (Figure 2.4G). Principal component analysis (PCA) of the changes in the four phenotypes (motility, biofilm, haemolysin and protease) revealed divergent patterns of the adapted isolates (Figure 2.5). The PCA also shows that the observed phenotypic changes in late-stage adapted isolates correlated with those of Δ*flrA*.

To further confirm the mutations that arose during amoeba predation in *flrA* leads to all the observed phenotypes, we targeted two nsSNPs in the *flrA* gene, A213V and V261G (Chapter Four). These two mutations appeared in single isolates from the adapted populations. The WT copy of *flrA* as well as the mutated copies (A213V and V261G) were expressed in a Δ*flrA* background under the control of the arabinose inducible promoter of the expression vector pBAD24. To compare the motility of the complemented clones of Δ*flrA*, an empty vector control was also tested. As expected, *flrA* complementation by induction with arabinose restores motility of Δ*flrA* to WT levels while the expression of the mutated *flrA* alleles does not (Figure 2.4H).

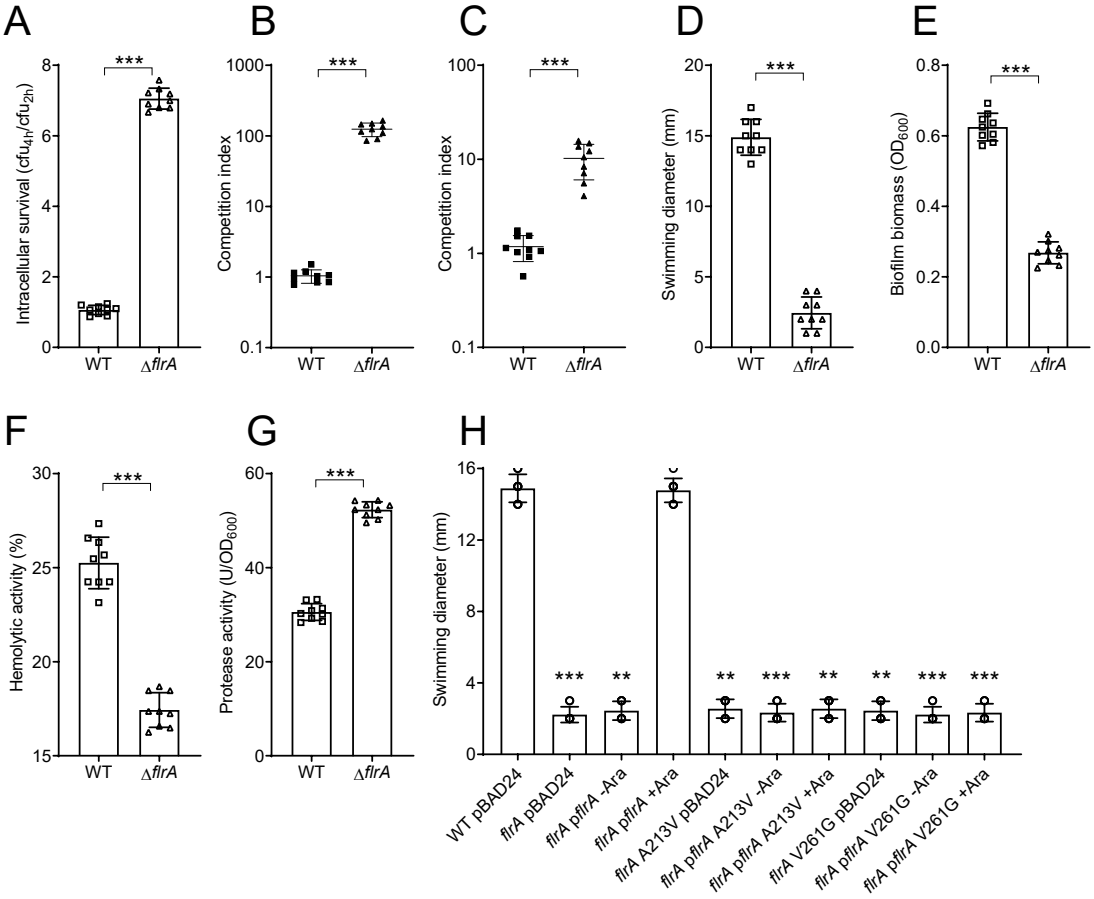

Figure 2.4. Altered phenotypes in adapted isolates are due to mutations in *flrA* (A) Intracellular survival of the wild type and Δ*flrA* in *A. castellanii* calculated by dividing the number of bacteria that were detected at 4 h by the 2 h samples. (B) CI of the wild type and Δ*flrA* in *A. castellanii* and LB (C) calculated by dividing the output ratio (WT/Δ*lacZ*) after incubation corrected by the input ratio. (D) Swimming motility of the wild type and Δ*flrA* expressed as diameter (mm) of the zone travelled from point of inoculation grown overnight on semi-solid LB agar plates. (E) Biofilm biomass of the wild type and Δ*flrA* quantified by CV staining. (F) Haemolytic activity of the wild type and Δ*flrA* expressed as percent haemolysis of 1 % sheep erythrocyte suspension (G) Protease activity in culture supernatants of the wild type and Δ*flrA* measured by azocasein hydrolysis assay. (H) Swimming motility of the wild

type and Δ*flrA* complemented with either pBAD24 or pBAD24 containing wild type *flrA* and/or mutated copies of the *flrA* (A213V and V261G). Values are expressed as diameter (mm) of the zone travelled from point of inoculation by bacteria grown overnight on semi-solid LB agar plates containing ampicillin and with or without arabinose. All data are from nine independent biological replicates and are shown as the mean ± standard deviation. Statistical significance was determined by two-tailed, non-parametric Mann–Whitney test (A-G), one-way ANOVA and Kruskal-Wallis test (H) and is indicated by ∗∗∗, $p < 0.001$.

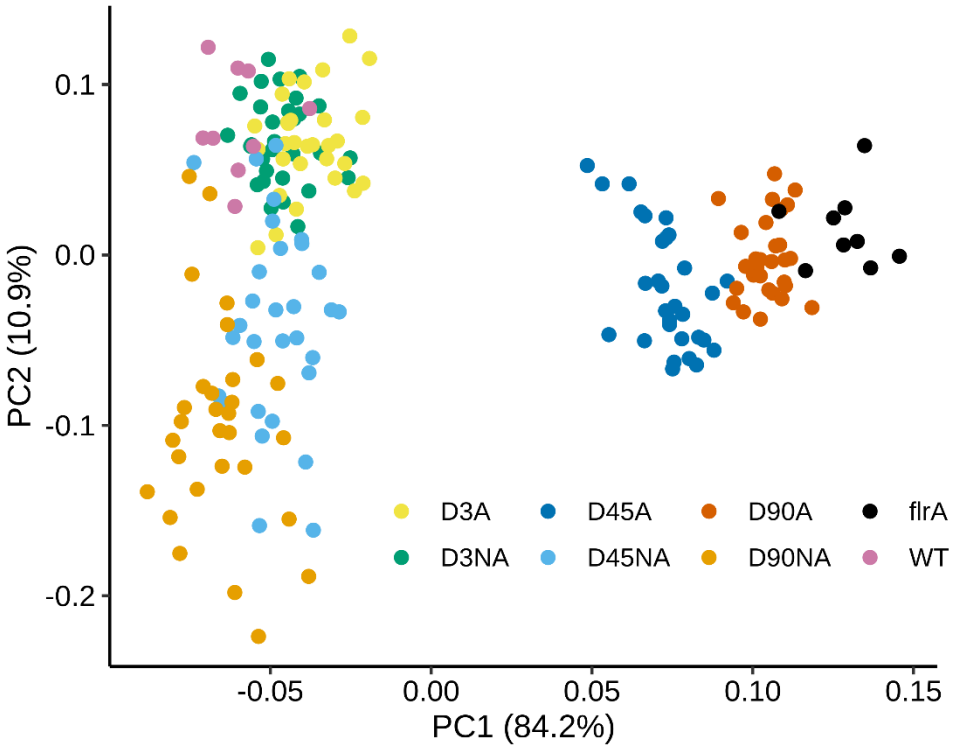

Figure 2.5. Principal component analysis of the four virulence phenotypes. The PCA of the changes in motility, biofilm, haemolysin and protease phenotypes across adapted isolates, non-adapted isolates, wild type and Δ*flrA* mutant are shown. Legend abbreviations, Day (D), adapted (A), non-adapted (NA).

2.3.6 Adaptation leads to enhanced colonisation of an aquatic host

Since the adapted isolates showed differences in production of multiple virulence related traits, we hypothesised that they were primed for colonisation of higher eukaryotic organisms. To test this, the adult zebrafish model was employed as this model supports a natural route of transmission and has been used for colonisation and transmission of *V. cholerae* [202-204]. To measure the colonisation of the adapted isolates harbouring mutations in the *flrA* (A213V and V261G) relative to the Δ*lacZ* strain competition assays were performed. The CI was calculated from the cells recovered from each fish intestine after 24 h of infection. The results indicated that Δ*flrA* colonised adult zebrafish 10-fold better than the Δ*lacZ* strain. The strains harbouring point mutations (A213V and V261G) in *flrA* colonised similarly to the Δ*flrA* (Figure 2.6A). Zebrafish were infected with GFP-tagged test strains (Wild type, Δ*flrA, flrA* A213V, *flrA* V261G) and an RFP-tagged Δ*lacZ* strain. Imaging revealed greater binding to fish intestinal epithelial cells of *V. cholerae flrA* mutants compared to the Δ*lacZ* strain (Figure 2.6B-C). The proportion of GFP and RFP fluorescence associated with fish intestinal epithelium cells recapitulated the trends seen in the CFU recovery assay. Hence, adaptation in amoeba increases the potential of *V. cholerae* to colonise higher eukaryotic organisms in the natural environment and contributes to the persistence and dissemination of the bacterium.

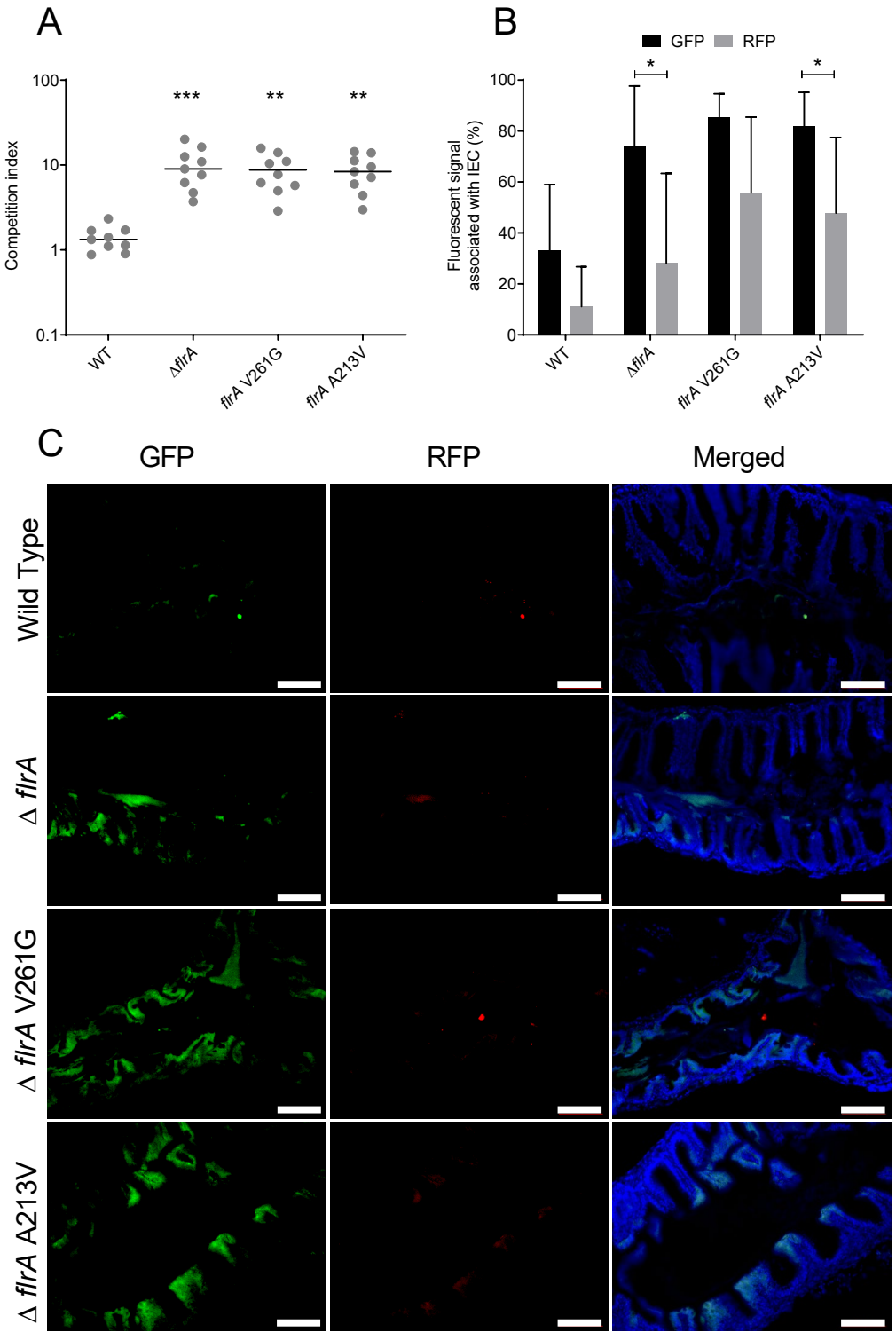

Figure 2.6. Enhanced colonisation of adapted isolates in a zebrafish infection model. (A) CI of adapted isolates with mutations in *flrA* in zebrafish infection model was calculated by

dividing the output ratio of test strain (e.g. *flrA* mutants) to Δ*lacZ* after infection corrected by the input ratio. Data are from nine independent biological replicates and are shown as the median. Statistical significance was determined by one-way ANOVA and Kruskal-Wallis test and is indicated by ∗∗∗, $p < 0.001$ and ∗∗, $p < 0.01$. (B) Quantification of bacterial fluorescence associated with intestinal epithelial cells of zebrafish after infection. Data are presented as percentages of GFP (test strain) and RFP (Δ*lacZ* mutant) signal quantified by fluorescent pixel count of tissue sections in ImageJ. Statistical significance was determined by one-way ANOVA and Tukey's multiple comparison test and is indicated by ∗, $p < 0.05$. (C) Colonisation of adapted isolates in adult zebrafish intestine. The four panels show representative fluorescence microscopy images of intestinal epithelial cell of adult zebrafish colonised with the indicated bacteria tagged with GFP and Δ*lacZ* strain tagged with RFP. Scale bars: 100μm.

2.4 Discussion

The results described here have important implications for understanding the molecular mechanisms of bacterial adaptation in the environment and how that may result in changes in pathogenicity. During intense predation pressure by free-living protozoa, *V. cholerae* can adapt to predation pressure, and this may lead to increased fitness. The results presented here show that this is achieved through a trade-off among multiple virulence traits that ultimately lead to increased fitness. The loss of motility may protect *V. cholerae* by reducing the frequency of contact with predators. It has been previously reported that motile bacteria experience increased rates of contact with raptorial feeding protists and hence are more susceptible to being ingested than non-motile cells [183, 184]. In addition, the flagellin protein functions as a pathogen-associated molecular pattern (PAMP) that binds to pattern-recognition receptors on a variety of defence cells, including macrophage and amoeba, thereby activating phagocytosis [205, 206].

Reports suggest that the production of the protease in *V. cholerae* is critical for neutralisation of the haemolysin. The haemolysin causes lysis of amoeba and by degrading the haemolysin, premature lysis of the amoeba host is prevented, hence ensuring a successful replication niche [15]. Here, we report that co-adaptation with amoeba led to an increase in protease activity and a concomitant decrease in haemolysin activity, further supporting the hypothesis that expression of haemolysin in amoeba is not advantageous for *V. cholerae* when residing in amoeba.

The loss of motility has been shown to have a negative impact on biofilm formation, and it is likely that the decrease in immunogenic impacts of flagella outweigh the benefits of biofilm formation during long-term co-adaptation and is thus the result of a trade-off to ensure successful replication within the amoeba host. Further, as amoeba selectively graze on biofilm cells the long-term adaptation leads to less biofilm, further reducing predation. The increase in intracellular survival and competitive fitness of adapted isolates in amoeba are the effect of synergistic actions of multiple traits in the adapted isolates.

Genome analysis of the amoeba-adapted *V. cholerae* revealed that mutations in *flrA* were responsible for the increased fitness and changes in phenotypic traits (Chapter Four). FlrA is the main regulator of the flagellar regulon and its inactivation leads to loss of flagellar synthesis [200, 201]. The regulator is widespread in bacteria and regulates diverse functions including motility, biofilm formation, virulence factor expression and sensing of small molecules. [207-209]. The absence of a flagellum hampers early stages of biofilm formation in *V. cholerae* [210]. Consistent with our study, Syed et al. showed that absence of *flrA* increases the expression of the secreted proteases, HapA and PrtV, and the haemolysin, HlyA [201]. It is likely that increased protease production in *V. cholerae* degrades the secreted haemolysin explaining our observations in the late stage amoeba-adapted isolates [211].

The phenotypes observed in the late-stage amoeba-adapted isolates are an indication of increased HapR activity. HapR is a quorum-sensing master regulator in *V. cholerae* which positively regulates production of proteases while negatively regulating biofilm formation [212]. Future studies will be needed to identify the putative link between *flrA* and *hapR*. However, it has been previously shown that FliA, a downstream target of FlrA, represses *hapR* expression [213]. Hence, in absence of FlrA the repression is likely be relieved and the increased protease and decreased biofilm formation in late-stage adapted isolates might be due to increased HapR activity.

Significantly, this study demonstrated that selection of multiple virulence-related traits in *V. cholerae* during adaptation with an amoebal host leads to increased colonisation in the zebrafish model of infection. As fish are potential reservoirs of *V. cholerae,* the increased colonisation may further contribute to persistence of the bacterium in the environment and may play an important role in dissemination [214-216]. Our results support the hypothesis that adaptation to amoeba drives selection of multiple phenotypic traits which improved fitness and increased colonisation in a higher eukaryotic host. Surprisingly, point mutations in a single gene, *flrA*, associated with regulation of flagella, recapitulated the changes in phenotypes observed in adapted isolates as well as colonisation of zebrafish. This highlights how predation can select for strains with enhanced capacity to colonise other hosts, which may be the result of only one or two nucleotide changes. A previous study showed that absence of *flrA* in *V. cholerae* leads to colonisation defects in infant mouse model which is a gold standard model for cholera infection [200]. Thus, the varied effects of colonisation in these two different models might be a trade-off that make it less successful in human context while increasing the potential for transmission and dissemination in the environment. Together, these phenotypic and genotypic changes contribute to our understanding of defensive and adaptive mechanisms of *V. cholerae* exhibits in the environment under predatory pressure.

Chapter Three

Increased iron acquisition and oxidative stress tolerance in a *Vibrio cholerae* *flrA* mutant confers resistance to amoeba predation

Chapter Three

Increased iron acquisition and oxidative stress tolerance in a *Vibrio cholerae* *flrA* mutant confers resistance to amoeba predation

3.1 Introduction

Cholera is an acute life-threatening diarrhoeal disease that continues to impact many regions in the world, especially in parts of Asia, Africa and Latin America [217, 218]. The causative agent of cholera, *Vibrio cholerae,* has adapted to survive in aquatic ecosystems as well as in the human gastrointestinal tract [72]. To persist in aquatic environments, this bacterium must survive predation by bacterivorous protists [165]. Many bacteria, including *V. cholerae,* are able to survive predation by some unicellular eukaryotic protist hosts and are released back into the environment [13, 131, 178]. However, our understanding of the mechanisms involved in survival and persistence in protist hosts is limited.

Iron is an essential nutrient required for pathogen survival and growth [219]. However, biological sources of iron are scarce due to the insoluble nature of iron at neutral pH and due to the fact that iron is chelated with high affinity iron-binding proteins in the host [220]. Hence, to overcome iron-withholding defences in the eukaryotic host, *V. cholerae* must utilise host-associated iron. *V. cholerae* possesses multiple iron acquisition systems, including receptors and transporters of haem as well as the siderophore, vibriobactin [220]. Although iron is a crucial element for survival, excess amounts of free iron (Fe^{2+}) can cause oxidative cell damage by the generation of reactive oxygen species (ROS) due to Fenton reactions [221, 222]. Hence, cells must tightly control the cellular pool of iron to maintain proper homeostasis.

In *V. cholerae,* expression of many of the iron acquisition genes are tightly controlled by the ferric uptake regulator (Fur) [223]. Fur-iron (Fe^{2+}) complexes repress iron acquisition genes in order to mitigate iron-mediated cellular toxicity caused by ROS, thereby ensuring expression

of these genes only when iron is limited [223]. Interestingly, Fur regulation has also been reported to modulate the expression of genes involved in antioxidant defences [224-226]. *V. cholerae* also possesses multiple defence systems to mitigate ROS, including the oxidative stress-related transcriptional activator, OxyR, catalases (KatB, KatG) and several peroxidases [227, 228]. Phagocytic protists, such as amoebae, exhibit many similarities to mammalian phagocytic cells and use ROS to destroy internalised bacteria [176, 229]. Hence to survive predation inside amoebae, phagocytosed bacterial cells must use mechanisms to counteract ROS mediated damage.

Another important anti-predation mechanism expressed by *V. cholerae* is the type-six secretion system (T6SS) that has been shown to kill both prokaryotic and eukaryotic cells [127, 168]. The structure of T6SS resembles tailed bacteriophages that direct toxic effector proteins to target cells [168, 230]. There are several clusters of genes present in *V. cholerae* genome that encode T6SS. Each of the clusters encode different T6SS effector proteins including VgrG3, TseL and VasX which are used to kill neighbouring cells [231, 232] TseL is a lipase effector, VgrG3 is a peptidoglycan degrading effector while VasX is a membrane disrupting effector [231, 233]. *V. cholerae* expresses immunity genes (*tsiV1, tsiV2, tsiV3*) which protect the cells from T6SS effectors [233]. These effector and immunity genes are encoded in different T6SS gene clusters as toxin-antitoxin pairs [233]. Bacteria also have other mechanisms beyond immunity gene-mediated protection from the T6SS [234]. Several stress responses in bacteria including oxidative, periplasmic and osmotic stress confers critical protection against T6SS effector-mediated killing [235-237]. In addition, spatial distribution of bacterial communities plays a crucial role in mediating immunity-independent protection against T6SS effectors [238].

Chapter Two reported that long-term co-incubation of *V. cholerae* with amoeba resulted in increased survival and fitness of the bacterium in amoeba. Increased survival and fitness were associated with inactivation of the flagellar transcriptional regulator, FlrA. This chapter focuses on the mechanisms of increased survival and fitness of the *V. cholerae flrA* mutants in amoeba. Results show that increased survival and fitness of *V. cholerae flrA* is related to increased expression of iron acquisition-related genes and enhanced tolerance to oxidative stress.

3.2 Materials and methods

3.2.1 Organisms and growth conditions

Organisms used in this study are listed in Supplementary Table 1. Bacterial and amoebal strains were grown as described in Section 2.2.1. To measure the optical density (OD) in iron-limited condition an iron chelator 2,2′-Bipyridyl (BP) were added in LB medium with a final concentration mentioned in the result section 3.3.7.

3.2.2 Intracellular survival assay

The intracellular survival of *V. cholerae* in amoeba was carried out according to the method described in Section 2.2.3.

3.2.3 Generation of mutants

The *V. cholerae* in-frame deletion mutants used in this chapter were constructed as described in Section 2.2.9.

3.2.4 RNA extraction and sequencing

V. cholerae wild type and Δ*flrA* mutants were grown with *A. castellanii* as described in 2.2.2. After overnight co-incubation, cells were washed 3 times in 2M medium, and amoeba were lysed with 1% Triton-X to release intracellular bacteria. RNA protect (Qiagen, Hilden, Germany) was added immediately to the cell lysate and total RNA was extracted using the

RNeasy plus mini kit (Qiagen, Hilden, Germany). A combination of lysozyme and proteinase K was used to ensure complete lysis. RNeasy plus mini kit's gDNA shearer column as well as RNase free DNase (Qiagen, Hilden, Germany) on column DNA digest were used to ensure sufficient degradation of the contaminant DNA in the sample. The quantity and purity ratios of samples were determined with Nanodrop One™. A Clean & Concentrator kit was used to purify the extracted RNA (Zymo Research). RNA samples were quantified fluorometrically using a Qubit fluorometer (Thermo Fisher) and quality was evaluated using TapeStation (Agilent Technologies). Only samples with a RIN number higher than 8 were used for analysis. RNA-seq libraries were prepared using Illumina TruSeq Stranded mRNA kit according to the manufacturer's protocol (Illumina, San Diego, CA, USA). The libraries were sequenced on the Illumina HiSeq2500 platform (V2 100 x 100 bp) at the Singapore Centre for Environmental Life Sciences Engineering, Nanyang Technological University, Singapore.

3.2.5 Transcriptomic analysis

The RNA sequencing reads were filtered to remove adapter contamination and low-quality bases (≤ Q20) using TrimGalore and were checked using FastQC before analysis [239, 240]. Clean reads were aligned to the reference genome of *V. cholerae* O1 El Tor strain N16961 (RefSeq accession numbers NC_002505 and NC_002506 for chromosome I and II respectively) using Subread aligner [241]. The mapped reads per gene count were quantified using featureCount [242]. The count matrices were uploaded to R version 4.1.0 and differential expression and PCA analysis was performed using DEseq2 [243]. The heat map was generated using variance stabilising transformation (vst) method and visualised by pheatmap package in R [244]. Other visualisation was generated with ggplot2 package in R [245]. All the codes have been deposited in the Github repository (https://github.com/mozammel47/PhD_Thesis).

3.2.6 Oxidative stress sensitivity assay

To assess oxidative stress sensitivity, the viability of *V. cholerae* strains was measured after exposure to hydrogen peroxide (H_2O_2). Exponential-phase cultures were normalised to an OD_{600} of 0.6 and treated with 2 mM H_2O_2 for 60 min. The viability of the cells was assessed by enumerating CFU after over-night growth on LB agar. Survival was determined by normalising CFU to the H_2O_2 non-treated group. The assay was performed in triplicate in 3 independent experiments.

3.2.7 Catalase activity assay

Catalase activity was determined as previously described [246]. Briefly, *V. cholerae* strains were grown in LB at 37 °C with shaking at 200 rpm. Cells were washed and adjusted to OD_{600} of 1.5 in phosphate-buffered saline (PBS). Equal volumes of normalised cells were mixed with catalase reaction buffer (1% Triton X-100 and 3% hydrogen peroxide in PBS) in tubes. The tubes were incubated at room temperature and the height of the bubbles was measured when bubbling subsided (approximately after 10 min). A standard curve was generated using purified bovine catalase (Sigma) mixed with catalase reaction buffer for 10 min (Figure 3.4D). Catalase activities of the samples were determined by linear regression equation calculated by "geom_smooth" function of ggplot2 package in R using the standard curve.

3.2.8 Quantitative real-time PCR (qRT-PCR)

RNA for qRT-PCR was isolated as described in section 3.2.4. The reverse transcription reaction and real-time PCR was carried out using the iTaq Universal SYBR Green One-Step Kit (Bio-Rad) according to the manufacturer's instructions. Briefly, 100 ng of RNA was mixed with iTaq universal SYBR green reaction mix and iScript reverse transcriptase in a 20 µL final volume. The assay was carried out in 96-well plates in a QuantStudio 6 Flex Real-Time PCR System (Applied Biosystems) with specific primer pairs for target genes. The *relA* gene was

used as a housekeeping reference gene and the relative gene expression were determined by the $2^{-\Delta\Delta Ct}$ method [247]. All the primers used for qRT-PCR are listed in Supplementary Table 1.

3.2.9 Statistical analyses

The R software package and GraphPad Prism software version 9 La Jolla California USA, (www.graphpad.com) were used for statistical analyses. Two-tailed student's t-tests (non-parametric Mann–Whitney tests) were used to compare means between wild type and mutants. Statistical analysis for experiments with multiple samples were performed using either two-way ANOVA and Sidak's multiple comparisons test or one-way ANOVA and Kruskal-Wallis test.

3.3 Results

3.3.1 The flagellar transcriptional regulator, *flrA*, mutant exhibited altered growth in amoeba

The uptake and survival of the flagellar transcriptional regulator Δ*flrA* mutant strain differed when compared to the wild type (Figure 3.1A). Equal numbers of bacterial cells (approximately 1.0×10^7 CFU ml^{-1}) were used to infect approximately 10^5 cells of amoeba at a MOI of 1:100. The number of intracellular bacterial cells was quantified using the gentamicin protection assay at different time intervals over 24 h. The results showed that the numbers of intracellular Δ*flrA* increased throughout the experiment from an average of 3.0×10^3 CFU ml^{-1} at 2 hours to 8.6×10^7 CFU ml^{-1} at 24 hours. In contrast, the numbers of the wild type remained relatively constant with an average of 2.2×10^5 CFU ml^{-1} at 2 hours and 6.5×10^5 CFU ml^{-1} at 24 hours. Analysis of survival at 2 and 4 hours of incubation showed that the Δ*flrA* mutant showed 4 to 5-fold increased survival compared to the wild type (Figure 3.1B).

3.3.2 The loss of motility is responsible for reduced uptake by amoeba

Although the Δ*flrA* mutant exhibited increased intracellular survival and growth after uptake, there was reduced uptake of the mutant by amoeba compared to the wild type at 2 hours (Figure 3.1A). After 2 hours of co-incubation, approximately 2.2×10^5 CFU ml^{-1} wild type cells and 3.0×10^3 CFU ml^{-1} Δ*flrA* cells were detected in amoeba. Hence, the mutant was 100-fold reduced for uptake by amoeba compared to the wild type. The *flrA* mutation leads to the loss of the flagellum and motility. To determine if it is the loss of motility or the loss of flagella that is responsible for reduced uptake, non-motile genetic mutants targeting either the major flagellin subunit, FlaA, resulting in non-flagellated bacteria, or the flagellar motor protein, MotX, resulting in rotation-deficient but fully flagellated bacterium, were generated. The results of the gentamicin protection assay indicated that all non-motile mutants showed reduced uptake by amoeba compared to the wild type (Figure 3.1C). Hence, the results suggested that the reduced uptake of Δ*flrA* was not due to the loss of flagella but due to the loss of motility.

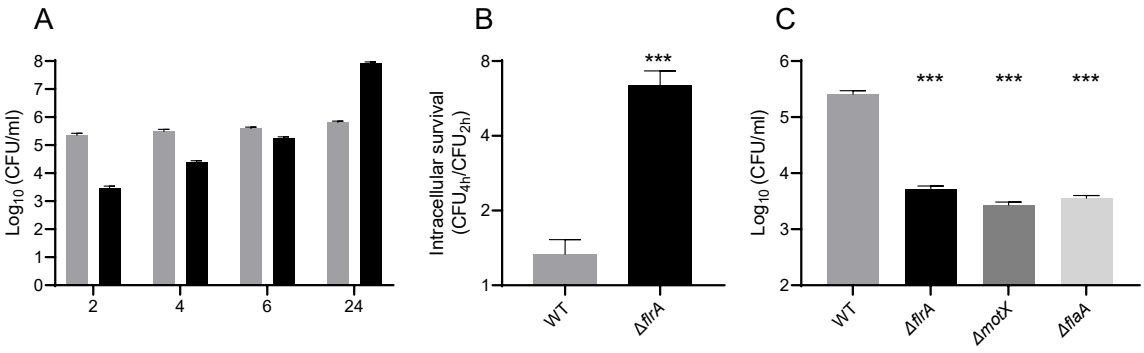

Figure 3.1. Intracellular growth, survival and uptake of Δ*flrA* mutant and wild type in amoeba. (A) Intracellular growth of wild type (grey) and Δ*flrA* (black) in *A. castellanii.* (B) Fold change in intracellular survival of wild type (grey) and Δ*flrA* (black) in *A. castellanii* calculated by dividing the CFU at 4 h by the CFU at 2 h of the assay. (C) Uptake of wild type and non-motile mutants by amoeba quantified by a modified gentamicin protection assay. Data are shown as the median of three independent experiments. Statistical analysis was performed

using student t-test or one-way ANOVA and Dunnett's multiple comparisons test. Statistical significance is indicated by ***, $p < 0.001$ compared to wild type.

3.3.3 Transcriptome of the Δ*flrA* mutant during predation by amoeba

To identify potential mechanisms contributing to the increased survival of the Δ*flrA* mutant, RNA sequencing (RNA-seq) was used to compare mutant and wild type strains during amoeba predation. A strong correlation was observed between the RNA-seq for biological replicates of both the wild type and the Δ*flrA* samples as depicted by principal component analysis (PCA) (Figure 3.2A). The PCA also revealed a marked difference in gene expression in the Δ*flrA* compared to the wild type. Differentially expressed transcripts were determined using the DEseq2 pipeline and transcripts with $\log_2$ fold change 1.5 and p-value < 0.05 were considered to be differentially expressed. In total, 516 genes corresponding to approximately 13% of the *V. cholerae* genome were differentially expressed in the Δ*flrA* strain (Figure 3.2B and Supplementary Data 3.1). Of these 516 differentially expressed genes, 140 and 376 were found to be up- and down-regulated, respectively in Δ*flrA* compared to the wild type.

V. cholerae encodes multiple iron acquisition systems, including several receptors, transporters and binding proteins. The RNA-seq revealed that nearly all the genes involved in the uptake of haem as well as the siderophore, vibriobactin, were significantly upregulated in Δ*flrA* relative to the wild type *V. cholerae* during amoeba predation. Of 140 up-regulated genes 20.7% (n=29) were involved in the uptake of haem and vibriobactin-mediated acquisition of iron. Haem and vibriobactin-associated genes showed approximately 2- and 1.4-fold induction respectively (Figure 3.2C). Expression of many of the iron acquisition genes are tightly controlled by the ferric uptake regulator (Fur). All the Fur-controlled genes that are known to be induced under iron-limiting conditions were also up-regulated in Δ*flrA* relative to wild type (Figure 3.2D). In addition to iron acquisition genes, several amino acid metabolism genes related to methionine

and arginine were also highly up regulated in Δ*flrA*. The two catalase-encoding genes, *katB* and *katG* showed opposite patterns of expression. The *katB* gene was significantly up-regulated in the *flrA* mutant while *katG* was significantly down-regulated during co-incubation with amoeba.

Of the 516 transcripts altered in the *flrA* mutant relative to WT, 376 were down-regulated, indicating that FlrA acts primarily as a transcriptional activator in *V. cholerae*. Genes involved in flagellar assembly, chemotaxis and two-component systems were mostly down-regulated in Δ*flrA*. The highest log-fold change among the down-regulated genes were observed for the *makDCBA* (motility associated killing) operon that encodes the MakA toxin, which was predicted to be released through flagellar channels and elicit toxicity towards vertebrae hosts [248].

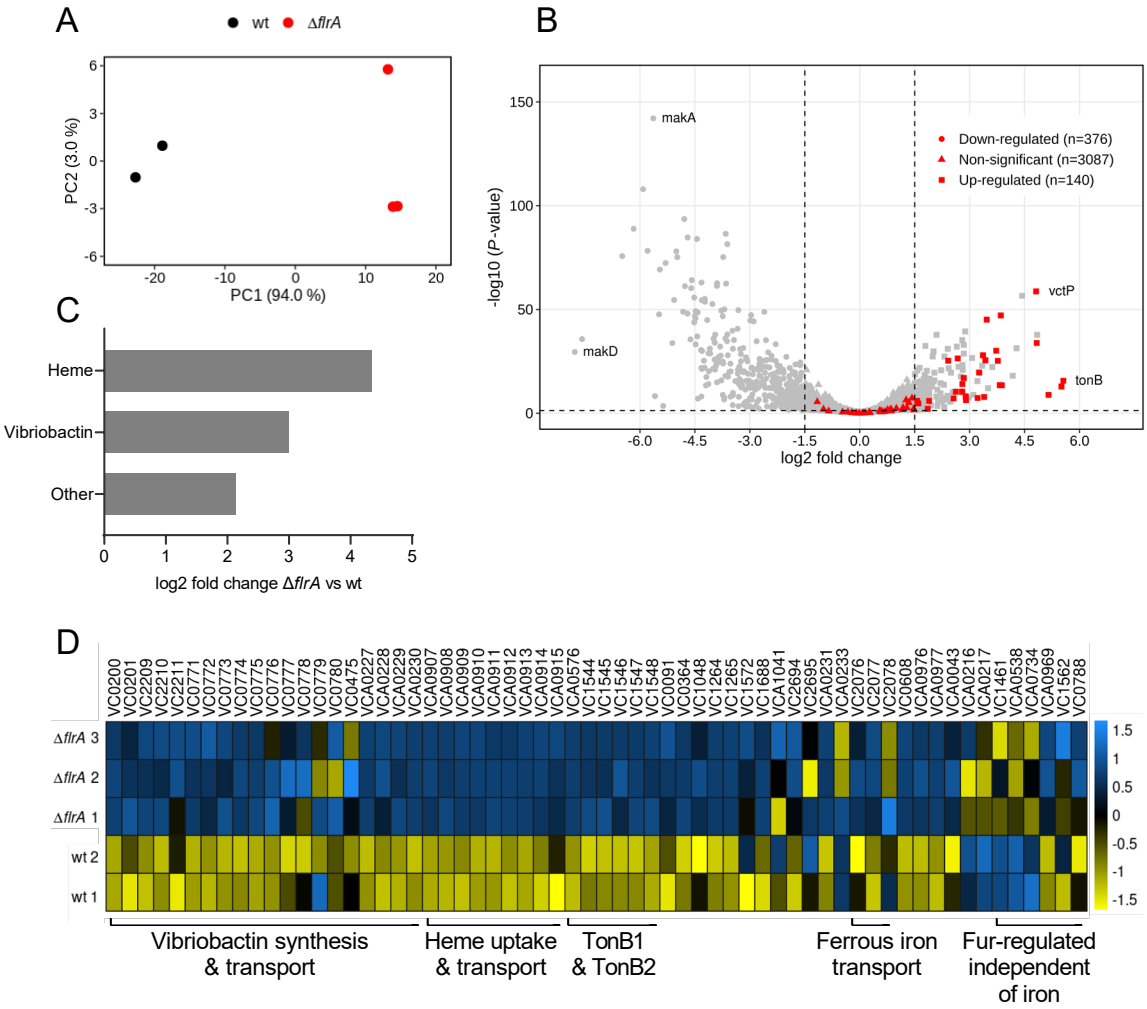

Figure 3.2. Transcriptional analysis of Δ*flrA* mutant compared to the wild type strain during amoeba predation reveals up-regulation of iron acquisition genes. (A) PCA plot for RNA-seq data from biological replicates of two wild type and three Δ*flrA* replicates. (B) Volcano plot representations of differential expression analysis of the Δ*flrA* mutant versus wild type. The negative log of *p*-value (base 10) is plotted on the y axis, and the log of the fold change (base 2) is plotted on the X axis. Genes predicted to be regulated by Fur and low iron are indicated by red. The two genes with the highest fold change and *p*-value are annotated for both up and down-regulated genes. (C) Average log fold change of up-regulated genes categorised as haem-utilisation genes, vibriobactin genes and others. (D) Heat map of RNA-

seq data from normalised expression (Variance stabilising transformation) of *V. cholerae* fur-regulated genes in Δ*flrA* mutant compared to the wild type.

3.3.4 Differential expression of Type VI secretion genes.

V. cholerae encodes one major (VCA0105-VCA0124) and three auxiliary clusters (VC1415-VC1421, VCA0017-VCA0021 and VCA0284-VCA0286) of genes involved in T6SS. Transcriptome analysis revealed that FlrA also regulates several T6SS genes (Figure 3.3). Notably, two genes in the auxiliary cluster 2, *vasX* (1.6) and *vasW* (2.8) were significantly upregulated in Δ*flrA* compared to the wild type. The *vasX* encodes a pore-forming effector protein and *vasW* aids in the secretion of VasX. In addition, the cognate immunity gene, *tsiV2* showed a log-fold change of 0.8. The gene encoding *tseL,* a lipase effector (1.2) and VC1421 (1.4) in auxiliary cluster 1 and VCA108 (0.7) in the major cluster also showed relatively high expression values compared to other T6SS genes.

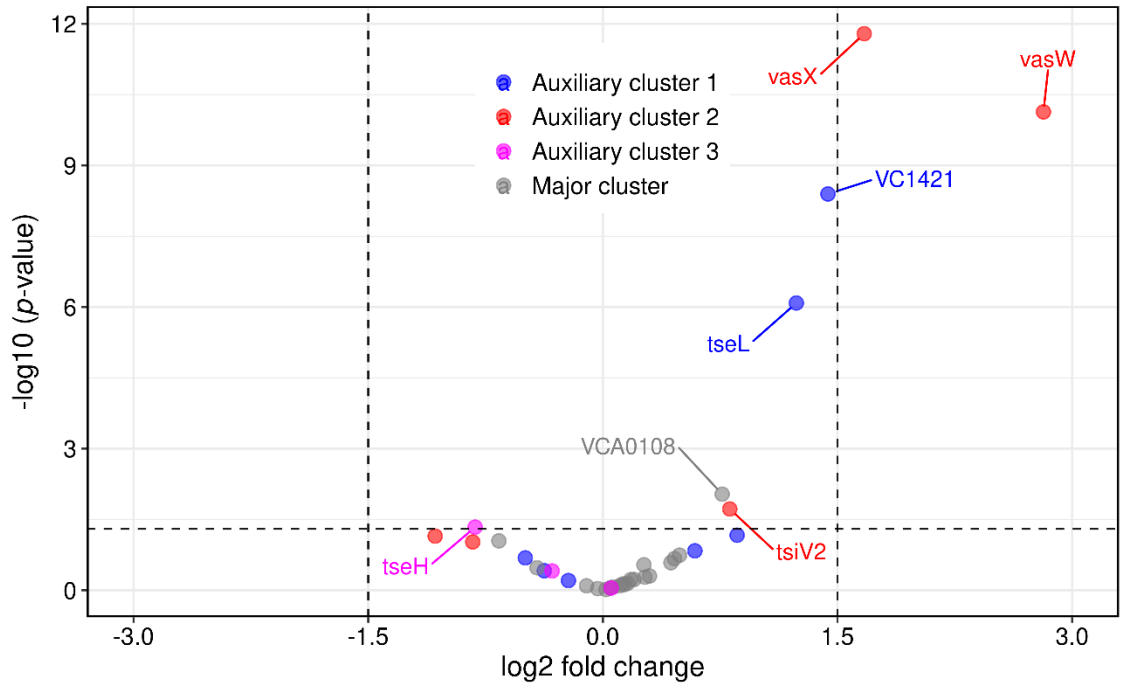

Figure 3.3. Expression of Type VI secretion genes in the Δ*flrA* relative to wild type. Volcano plot representations of differential expression analysis of the T6SS genes in the Δ*flrA* mutant relative to wild type. The negative log of *p*-value (base 10) is plotted on the Y-axis, and

the log of the fold change (base 2) is plotted on the X-axis. Genes in different T6SS clusters are categorised with different colours as indicated in the legend. Genes with the significant *p*-value (< 0.05) are annotated.

3.3.5 KEGG pathway analysis of up- and down-regulated genes

The KEGG (Kyoto Encyclopedia of Genes and Genomes) pathway abundance analysis revealed that most of the down-regulated genes are involved in chemotaxis (55%, n=39), flagellar assembly (54%, n=27), two-component systems (34%, n=57) and butanoate (37%, n=11) and pyruvate (20%, n=10) metabolism (Figure 3.4). Twelve percent (n=13) of the genes involved in biofilm formation were also significantly down-regulated. In contrast, most of the up-regulated genes are involved in amino acid metabolism, including arginine, alanine, aspartate, glutamate, cysteine, methionine, glycine, serine and threonine (Figure 3.4). The genes involved in iron acquisition are categorised mainly into ABC transporters (11%, n=15) and biosynthesis of secondary metabolites pathways (9%, n=28).

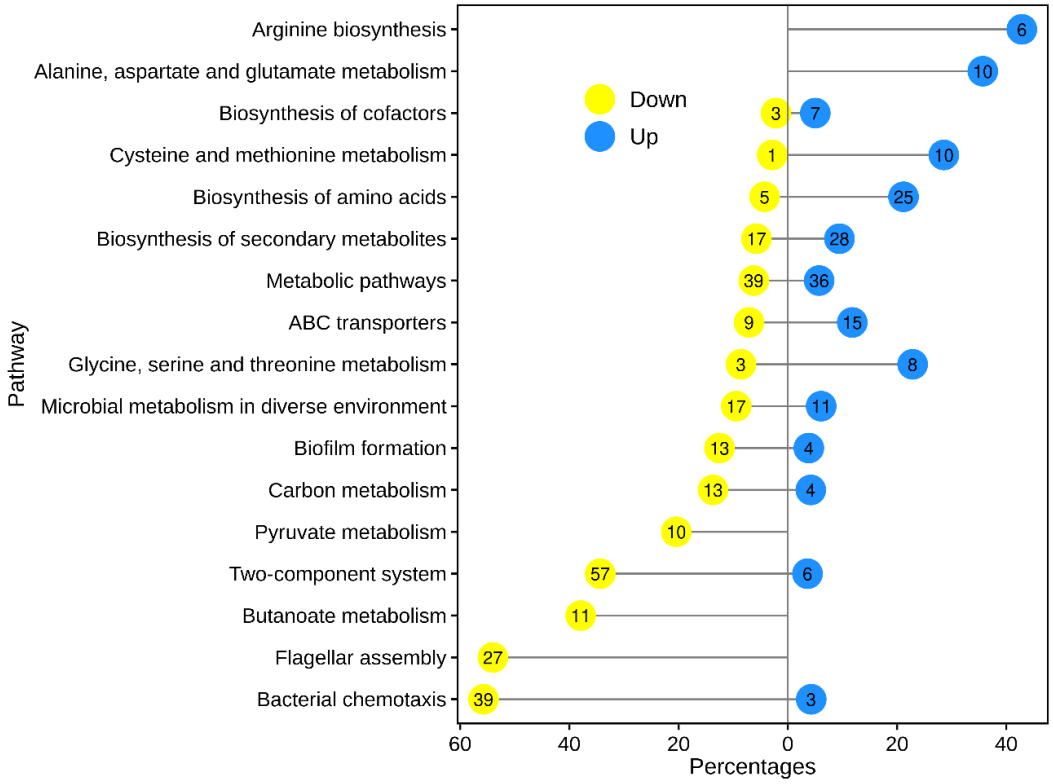

Figure 3.4. KEGG pathway analysis of the differentially expressed genes in Δ*flrA* mutant compared to the wild type. The length of the lollipop shows the percentages of *V. cholerae* genes in each pathway that are either up- or down-regulated. The number of the genes in each pathway are shown in the circles. Only pathways with six or more genes in either one of the categories are shown for simplicity.

3.3.6 The Δ*flrA* mutant exhibits increased oxidative stress resistance due to increased KatB expression

Amoebae increase levels of ROS in phagosomes to kill internalised bacterial cells [229]. We speculated that long-term adaptation in amoeba might lead to increased resistance to ROS as the late-stage amoeba-adapted isolates showed increased survival in amoeba. To identify the molecular mechanisms of increased survival of Δ*flrA* in amoeba, oxidative stress resistance assays with hydrogen peroxide were performed. The Δ*flrA* showed 4-5-fold increased resistance to hydrogen peroxide compared to wild type (Figure 3.5A). To identify the mechanism of increased oxidative stress resistance of Δ*flrA,* catalase activity was evaluated by extrapolating from a standard catalase activity curve (Figure 3.5B). Quantification of catalase activity revealed that the Δ*flrA* showed a 4-fold increased catalase activity compared to wild type (Figure 3.5C). The analysis of expression of genes related to oxidative stress resistance revealed that only the catalase encoded by *katB* was significantly up-regulated compared to the wild type, as observed in both RNA-seq and RT-qPCR data (Figure 3.5D). The *katG* catalase was down-regulated and the expression of *oxyR* and *sodC* were not significantly different compare to wild type.

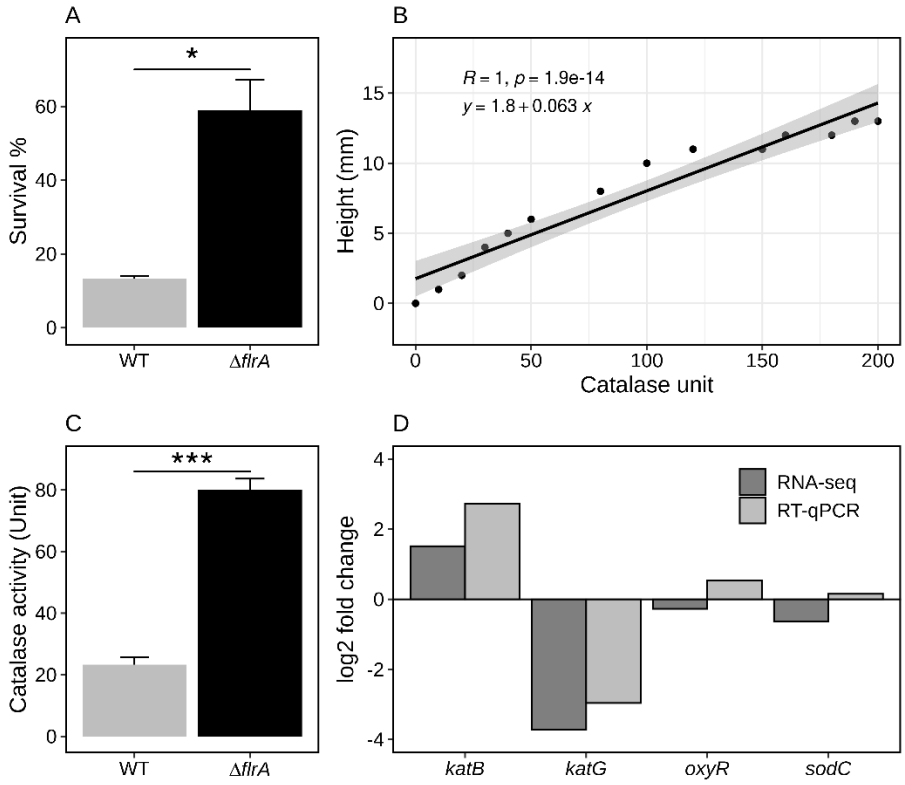

Figure 3.5. Oxidative stress resistance is due to increased catalase activity and KatB expression. (A) Wild type and Δ*flrA* were grown in LB to mid-log phase. The cells were resuspended in PBS and exposed to a final concentration of 2 mM H_2O_2 for 60 minutes and survival determined. Data are shown as the median of 3 independent experiments. Statistical analysis was performed using student t-test. Statistical significance is indicated by $*$, $p < 0.05$ compared to wild type. (B) Catalase activity standard curve. The points represent the height of the bubble produce by degradation of H_2O_2 corresponding to catalase units specified in x-axis. The shaded area represents 95% confidence interval. The linear regression equation is depicted in the plot. (C) Catalase activity in wild type and Δ*flrA* extrapolated from the standard curve. Statistical analysis was performed using student t-test. Statistical significance compared to wild type is indicated by $***$, $p < 0.001$. (D) Fold change of expression of genes related to oxidative stress resistance in Δ*flrA* compared to wild type.

3.3.7 The Δ*flrA* mutant exhibits increased growth under iron-limited conditions

Most of the genes involved in iron acquisition were up-regulated in the Δ*flrA* mutant compared to the WT, thus, the mutant may have an increased capacity for utilisation of iron. A growth assay was performed in LB with and without the presence of an iron chelator 2,2′-bipyridyl (BP). The addition of BP reduced the growth of both WT and Δ*flrA* strains (Figure 3.6). The addition of 200 µM of BP reduced the growth approximately 2.5-fold compared to the control. The Δ*flrA* mutant maintained increased growth (OD_{600}) compared to WT in the presence of BP which indicates an increased capacity to utilise iron (Figure 3.6).

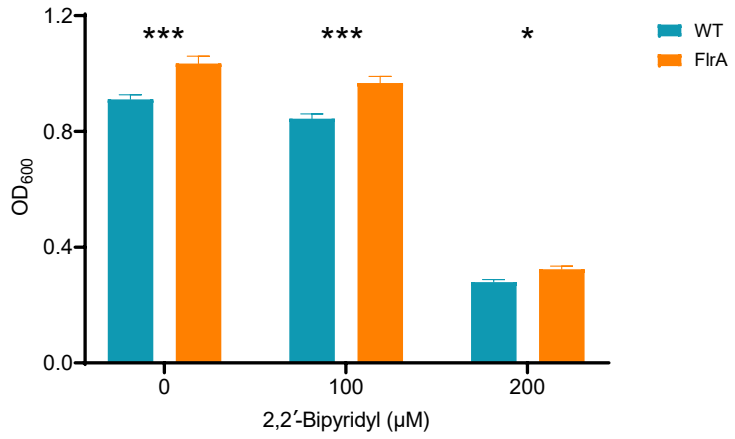

Figure 3.6. Growth of wild type and Δ*flrA* under iron-limited conditions. The wild type and Δ*flrA* were grown in LB with and without the presence of the iron-chelator 2,2′-bipyridyl. The OD_{600} was taken after 8 hours of growth. Statistical analysis was performed using two-way ANOVA and Sidak's multiple comparisons test. Statistical significance is indicated by ***, $p < 0.001$; **, *, $p < 0.05$; compared to wild type

3.4 Discussion

The results presented in this chapter highlight mechanisms that allow bacteria to adapt to predators in the environment. Analysis of the transcriptome of the amoeba-adapted strains that exhibited increased intracellular survival during amoeba predation revealed strategies that allow for acquisition of essential nutrients, including iron and protection against ROS. The

transcriptome also revealed metabolic changes associated with increased intracellular survival and revealed putative mechanisms of intra-species competition in the face of predation pressure.

Expression of genes involved in iron acquisition in mammalian hosts has been linked to enhanced fitness and virulence in *V. cholerae* [249]. Here, a similar pattern was observed where there was up-regulation of iron acquisition genes leading to increased fitness and survival inside the unicellular eukaryotic host, *A. castellanii*. The increased expression of genes in the Δ*flrA* strain involved in iron acquisition reflect the iron-restrictive environment inside the amoeba host. Iron acquisition genes are under tight control by the Fur-Fe^{2}+ complex and increased expression of these genes in a Δ*flrA* background indicates potential regulatory interactions between Fur and FlrA.

The Fur-Fe^{2+} complex has been reported to regulate genes involved in antioxidant defence, both positively and negatively [225, 250]. It is possible that *katG*, *sodA*, *sodB* and *sodC* are under positive regulation, while *katB* is under negative regulation by Fur-Fe^{2+} in *V. cholerae* as was observed in the transcriptomic analysis. The differential expression of the two catalases KatB and KatG indicated that the use of only one system may be metabolically advantageous under the conditions used here. In addition, *flrA* may have a regulatory role in expression of catalases. In fact, the signalling molecule cyclic-di-GMP increases KatB expression but not KatG [251]. In *V. cholerae,* cyclic-di-GMP modulates gene expression through three transcriptional regulators, VpsT, VpsR and FlrA. The cyclic-di-GMP mediated expression of KatB is dependent on the transcription factors VpsT and VpsR [251]. However, role of FlrA in the expression of catalases can't be rule out as cyclic-di-GMP also acts as a modulator of FlrA [69]. Binding of cyclic-di-GMP inactivates the transcriptional factor FlrA and inhibits the downstream signalling cascade of flagellar synthesis [69]. Hence, the absence of FlrA might

lead to the co-ordinate regulation of catalases through combined effects of other transcriptional regulators VpsT and VpsR.

The Δ*flrA* strain showed up-regulation of genes involved in metabolism of many amino acids, including cysteine and methionine. Up-regulation of cysteine and methionine reflects additional anti-oxidant mechanisms of the *flrA* mutant in addition to catalase as both of the amino acids are involved in anti-oxidant defences [252]. *V. cholerae* is a facultative anaerobic pathogen and capable of fermenting diverse carbohydrates including glucose [253]. Low levels of oxygen inside amoeba might induce switching to anaerobic metabolism, indicated by the down-regulation of carbon and pyruvate metabolism. This downregulation is indicative of an anaerobic metabolic life-style, producing less energy through cycling of carbon through the TCA cycle while favouring synthesis of essential amino acids. The fermentative pathway enables bacteria to produce low levels of energy by altering the flux of pyruvate to produce organic acids and other molecules like amino acids. Chapter Two discussed the potential activation of *hapR*/quorum sensing (QS) activity in Δ*flrA*. QS activity favours the flux of pyruvate to production of the neutral molecule acetoin which benefits bacteria at low pH [254]. Thus, by reducing carbon-pyruvate flux to energy production the Δ*flrA* produces molecules/amino acids that enhance their ability to survive ROS and low pH encountered inside the amoeba.

Transcriptomic analysis also revealed up-regulation of genes involved in the T6SS; *vasX* (effector), *vasW*, and *tsiV2* (immunity). Increased expression of these genes might play a role in the fitness advantage of *flrA* mutants during co-incubation with amoeba. The effects of the expression of T6SS genes are not clear as previous studies reported that expression of VasX resulted in killing of *Dictyostelium discoideum* but had no killing effect on *Acanthamoeba castellanii* [15, 231]. Thus, the T6SS genes may mediate intra-species competition inside

amoeba. The increased expression of VasX may lead to the selective killing of sister wild type cells in the phagosomal environment, providing a competitive advantage to the *flrA* mutant. This competitive advantage could result in enrichment of the *flrA* mutant as seen in Figure 4.2 and 4.4 (Chapter Four). VasW expression ensures successful killing by VasX as it is essential for the secretion of the VasX [255]. In addition, increased expression of TsiV2 would confer immunity to the *flrA* mutant. The molecular mechanism of the increased expression of the genes involved in iron acquisition and T6SS is not known, but this study is the first step in identification of other genes regulated by FlrA. VasH, which is located in the primary T6SS cluster, acts as a transcriptional activator of σ^{54} (RpoN) and is needed for VasX expression [256]. FlrA is also a transcriptional activator of σ^{54} like VasH, and σ^{54} is involved in expression of a number of T6SS genes as depicted by a ChiP-Seq study [200, 257]. It suggests that the absence of one sigma-54-dependent transcriptional regulator (FlrA) might "free up" sigma-54 for binding by VasH. Hence, the possible connection between FlrA and T6SS needs to be further elucidated.

A previous report showed secretion of a cytotoxin encoded by the *makDCBA* (motility-associated killing factor) operon was flagella-mediated in *V. cholerae* [248]. Down-regulation of all the genes in this operon in Δ*flrA* suggested that flagella are not only involved in secretion of the toxin but are also involved in its regulation. As the toxin has effects on both vertebrates and invertebrates, down-regulation would ensure a successful replication niche for *V. cholerae* inside amoeba. Future studies are needed to elucidate the regulatory pathway of this toxin and its role in diverse protozoan hosts.

Taken together, the results presented in this chapter highlight how adaption of *V. cholerae* to predation increases resistance to oxidative stress and acquisition of iron which ensure successful survival under predation pressure.

Chapter Four

Adaptation of *Vibrio cholerae* in an amoeba host leads to mutations in the flagellar transcriptional regulator, *flrA*

Chapter Four

Adaptation of *Vibrio cholerae* in an amoeba host leads to mutations in the flagellar transcriptional regulator, *flrA*

4.1 Introduction

Vibrio cholerae naturally inhabits the aquatic environment and is transmitted through contaminated water causing the acute diarrhoeal illness, cholera [23]. Adaptation in the aquatic environment is a key factor leading to persistence and dissemination of the bacterium. Genetic adaptation is a major driver of *V. cholerae* evolution leading to multiple worldwide pandemics and epidemics of cholera [258]. Acquisition of foreign DNA elements through horizontal gene transfer (HGT) contributes significantly to the genetic diversity of *V. cholerae* [27]. The major toxins and virulence factors of *V. cholerae* are encoded by genes in mobile genetic elements, including the cholera toxin CT, the Vibrio pandemic island 1 (VPI), and the Vibrio seventh pandemic islands (VSP-1, VSP2) that were acquired by HGT [259, 260]. However, genomic mutations also drive genetic variation leading to evolution [261]. But the environmental factors that lead to genomic mutations are not well understood. It is known that environmental stressors drive rapid mutation in bacteria leading to adaptive evolution [262]. As *V. cholerae* persists long-term in aquatic ecosystems [263], elucidating the role of aquatic reservoirs in genomic evolution through adaptive mutations is important for understanding how the organism persists.

Mutations can be defined as changes in genetic material either by substitution, deletion, insertion, or rearrangement of single or multiple nucleotides as well as rearrangements of large sections of the genome [264]. Single nucleotide changes often lead to either no change (synonymous) or changes (non-synonymous or frameshift) in an amino acid sequence of a protein. Although these mutations are often harmful, they can also be beneficial, increasing genetic diversity and allowing adaptation to changing environments. Such beneficial mutations

include gain of function [265], immune evasion [266], acquisition of antimicrobial resistance [267, 268], increased fitness [269] and virulence [270]. Experimental evolution coupled with genome sequencing offers a powerful tool for the study of mutations and many studies have elucidated their role in bacterial evolution, host adaptation and pathogenicity [271, 272]. The pioneering work on experimental evolution lead by Richard Lenski and his team showed that gain of citrate utilisation (Cit^+ phenotypes) in Cit^- *Escherichia coli* occurred through accumulation of adaptive mutations [273]. Another example of experimental evolution of *Burkholderia cenocepacia* biofilms revealed that mixed communities of variants that arose were more productive than individual members [274].

A growing number of publications [131, 155, 156, 158, 275] have reported the role of protozoa predation in evolution of virulence-associated traits of pathogenic bacteria. For example, predation of *Aeromonas hydrophila* by *Tetrahymena thermophila* enhances environmental adaptation through alteration of diverse traits, including biofilm formation, motility and increased resistance to reactive oxygen species (ROS) [158]. Within host evolution of *Legionella pneumophila* in mouse macrophages leads to mutations that are beneficial in that environment while being detrimental in other hosts [275]. Experiments with multispecies communities revealed that ciliate and amoeba predation leads to attenuation of virulence in *Pseudomonas aeruginosa* [276] and *Serratia marcescens* [277]. These examples of short-term adaptation indicate that protists have been shown to be drivers of evolution of pathogenicity [8] and often these are mediated through genomic diversification due to adaptive mutations.

To understand the consequences of bacterial-protozoal interactions, an experimental evolution approach was undertaken here to assess the effects of long-term amoeba predation on *V. cholerae*. This chapter presents results on the genetic variations that arose in *V. cholerae* during long-term co-incubation with and without the amoeba, *Acanthamoeba castellanii*. The

mutations that arose in amoeba-adapted and non-adapted *V. cholerae* were assessed in both whole populations and in single clones obtained from the adapted and non-adapted populations. Sequence analysis revealed that amoeba-adapted isolates possess unique non-synonymous mutations in highly conserved amino acid residues in the *flrA* gene. This chapter further illustrates the temporal appearance of mutations in *flrA* gene over the course of long-term evolution experiment.

4.2 Materials and Methods

4.2.1 Organisms and growth conditions

Organisms used in this study are listed in Supplementary Table 1. Bacterial and amoebal strains were grown as described in Section 2.2.1.

4.2.2 Experimental co-evolution of *V. cholerae* in *A. castellanii*

Experimental co-evolution of *V. cholerae* in *A. castellanii* was carried out as described in Section 2.2.2.

4.2.3 Extraction of genomic DNA

V. cholerae were sequenced to determine genotypic changes that occurred in response to co-adaptation with amoeba. Genomic DNA was extracted from the three replicate lineages (P1, P2, P3) of each adapted and non-adapted population as well as from single isolates derived from days 3, 45 and 90 using the QIAamp DNA mini kit (Qiagen) according to manufacturer's instructions. Briefly, LB cultures grown overnight were pelleted and resuspended in ATL buffer (supplied in the QIAamp DNA Mini Kit). The suspension was treated with 20 µL of proteinase K and 4 µL of RNase A (100 mg ml^{-1}) to remove protein and RNA contamination before mixing with buffer AL. Ethanol precipitation and subsequent washing steps were carried out and genomic DNA isolated using a QIAamp Mini spin column. DNA concentration was

determined using the Qubit dsDNA high sensitivity assay kit (Life Technologies). DNA was stored in -80^0 C until sequencing.

4.2.4 Sequencing and genomic analysis

DNA libraries were prepared using the TruSeq DNA sample preparation kit (Illumina, San Diego, CA, USA), and sequenced on a MiSeq (Illumina, USA) to generate 2 × 150 bp paired-end reads at the Singapore Centre for Environmental Life Sciences Engineering, Nanyang Technological University, Singapore. Sequenced reads were trimmed to remove adapter contamination and low-quality bases (≤ Q20) using TrimGalore and were checked using FastQC before analysis [239, 240]. Filtered reads were mapped to the *V. cholerae* O1 El Tor strain A1552 (NCBI GenBank accession no CP025936 and CP025937 for chromosome I and II respectively) and genetic variants including single nucleotide polymorphisms (SNPs) and insertion and deletions (INDELS) were called along with the respective genotype information of all samples using the polymorphism mode of breseq pipeline with default parameters [278]. Mutations with ≥ 10% frequency in at least one replicate community were analysed. Mutation calls were manually curated to remove false positives. Single isolates of *V. cholerae* from the co-evolution experiment were also subjected to sequencing to determine genotypic changes. Three randomly selected *V. cholerae* isolates from one of the lineages from both adapted and non-adapted populations from days 3, 45 and 90 were sequenced and analysed using the same method that was used for population sequencing. Short paired-end reads from the single isolates were assembled into contig using SPAdes 3.11.1 [279]. The assembled genomes were used to analyse the mutations by alignment using blastn program.

4.2.5 Amplification refractory mutation system (ARMS)-PCR

ARMS-PCR were used to detect the single point mutations in the *flrA* gene. The online primer1 tool (http://primer1.soton.ac.uk/primer1.html) was used to design allele specific primers.

Briefly, a mismatch at the -2 position of the 3′ end of the primer was introduced following wild type or mutant alleles using principles establish for ARMS-PCR [280]. In addition, common primers located at the 5′ and 3′ terminus of the *flrA* gene were designed. These four sets of primers were used in a single PCR reaction to detect the wild type and mutant alleles. The presence of a particular allele was confirmed by the size differences of the allele specific amplicons by agarose gel electrophoresis. All the primers targeting the A213V (C638T) and V261G (T782G) mutations of the *flrA* gene are listed in Supplementary Table 1.

4.2.6 Functional classification of the mutated genes

The locus tag of the mutated genes was uploaded onto the input panel of Microbial Genomic context Viewer (MGcV) server (https://mgcv.cmbi.umcn.nl/). Clusters of Orthologous Groups (COGs) information of each locus tag was retrieved from output tab. The COGs were verified by the NCBI COG database for *V. cholerae* O1 biovar El Tor str. N16961 https://ftp.ncbi.nih.gov/pub/COG/COG2014/static/lists/listVibcho.html. Finally, COGs were further divided by their general function as defined by the CloVR website. http://clovr.org/docs/clusters-of-orthologous-groups-cogs/

4.2.7 Data availability

Sequence data generated in this study are available from the NCBI Sequence Read Archive with accession number PRJNA685017.

4.3 Results

4.3.1 Dynamics of mutations arising in *V. cholerae* during co-incubation with amoeba

The altered phenotypes of the adapted isolates were stable, thus, genomic DNA from three replicate populations (P1, P2, P3) of amoeba-adapted and non-adapted *V. cholerae* populations from the different time points (3, 45 and 90 days) were subjected to sequencing (Supplementary Data 1 and Supplementary Data 2). In addition to whole population sequencing, 18 individual

amoeba-adapted and non-adapted isolates (three from each population) were sequenced and analysed (Supplementary Data 3 and Supplementary Data 4). The genome sequences of adapted and non-adapted populations were compared to the WT strain and the allelic frequencies of mutations that occurred at a minimum of a 10% frequency in populations were determined using the breseq pipeline [278]. Point mutations including synonymous single nucleotide polymorphisms (sSNPs), non-synonymous SNPs (nsSNPs), intergenic mutations and INDELs (<50 bp) were identified (Supplementary Data 1 and Supplementary Data 2). The numbers and types of genetic alterations identified in adapted and non-adapted populations and single isolates are depicted in Figure 4.1A and B.

Briefly, the total number of mutations in adapted and non-adapted populations did not differ significantly over time. A slight decrease in the number of mutations was observed in adapted populations while the number was relatively constant in the non-adapted populations over the time course of the experiment. Interestingly, a gradual increase in the percentage of nsSNP from days 3 to 90 were observed in adapted populations. The percentages of nsSNP in days 3, 45 and 90 adapted populations were 42.5%, 45.8% and 49.2% respectively, while the percentages of nsSNP in 3, 45, and 90-day non-adapted populations were 41.7%, 45.1% and 41.4% respectively. The percentages of sSNP were relatively similar in both adapted and non-adapted populations over time. Intergenic mutations and INDELS were more common in non-adapted populations than in adapted populations.

A total of 144 and 146 different mutations (nsSNPs and sSNPs) and INDELs were observed in coding regions of adapted and non-adapted populations affecting 37 and 35 genes, respectively. Twenty-five genes were common in both populations while 12 and 10 genes were unique to adapted and non-adapted populations, respectively (Supplementary Table 2 and Supplementary Table 3). The *flrA* gene was the only gene that was consistently mutated across days 45 and 90

in the replicate adapted populations (6 nSNP and 1 INDEL). The unique mutations that were detected in the coding regions in amoeba-adapted populations but not in non-adapted populations are presented in Figure 4.2. Overall, most of the mutations fluctuate throughout the experiment and are ultimately lost in both adapted and non-adapted populations with very few of the mutations that appeared in the day 45 adapted populations persisting in day 90 adapted populations. Notably, four nsSNPs (L201W at 41.7 %, S204R at 21.9 %, A213V at 16.7 % and V261G at 29.5 % frequency) in the flagellar transcriptional master regulator, *flrA,* (VC2137) were detected in the day 45 adapted populations. The same four mutations persisted in the day 90 adapted populations and the mutational frequencies increased to L201W at 74.3%, S204R at 46.6%, A213V at 29.2% and V261G at 63.3%. Analysis of genomes of single isolates from the adapted population revealed two nsSNPs (A213V and V261G) in *flrA* on days 45 and 90 as well. These two mutations occurred at 100% frequency in the adapted isolates (Supplementary Data 3 and Supplementary Figure 1). Unique and common genes that were mutated in adapted and non-adapted isolates are listed in Supplementary Table 4 and Supplementary Table 5, respectively.

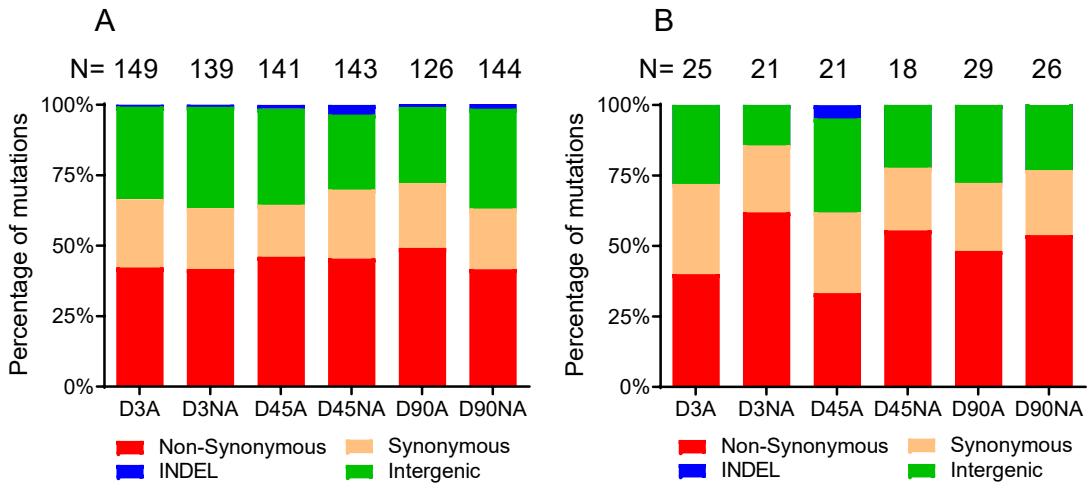

Figure 4.1. Mutations in adapted and non-adapted populations (A) and isolates (B). Shaded bars show the distribution of different types of genetic changes for all independent mutations found in the adapted (A) and non-adapted (NA) populations at different time points (D3, D45 and D90). The total number of mutations (N) are shown above each column. Base substitutions shown are nsSNP, sSNP, INDELs and intergenic mutations.

Locus tag	Gene/ Gene Function	Mutation	Day 3 P1	Day 3 P2	Day 3 P3	Day 45 P1	Day 45 P2	Day 45 P3	Day 90 P1	Day 90 P2	Day 90 P3
VC0760	histidine tRNA ligase	E270G (GAG→GGG)*									
VC0791	sensor histidine kinase *citA*	I202I (ATC→ATT)‡									
VC0791	sensor histidine kinase *citA*	I202F (ATC→TTC)*									
VC0913	MexH multidrug efflux RND transporter	D71G (GAC→GGC)*									
VC0913	MexH multidrug efflux RND transporter	G84S (GGT→AGT)*									
VC0998	Polar transmembrane protein *hubP*	N953S (AAT→AGT)*									
VC0998	Polar transmembrane protein *hubP*	V986A (GTC→GCC)*									
VC0998	Polar transmembrane protein *hubP*	L1061L (TTA→TTG)‡									
VC0998	Polar transmembrane protein *hubP*	S1073A (TCG→GCG)*									
VC0998	Polar transmembrane protein *hubP*	L1089L (TTA→TTG)‡									
VC0998	Polar transmembrane protein *hubP*	L1135L (CTA→TTA)‡									
VC0998	Polar transmembrane protein *hubP*	A1136V (GCA→GTA)*									
VC0998	Polar transmembrane protein *hubP*	A1140A (GCT→GCC)‡									
VC0998	Polar transmembrane protein *hubP*	D1160D (GAT→GAC)‡									
VC0998	Polar transmembrane protein *hubP*	D1184E (GAT→GAG)*									
VC0998	Polar transmembrane protein *hubP*	A1265S (GCG→TCG)*									
VC0998	Polar transmembrane protein *hubP*	L1277P (CTC→CCC)*									
VC0998	Polar transmembrane protein *hubP*	T1341T (ACT→ACC)‡									
VC1015	electron transport complex subunit RsxC	A721A (GCT→GCC)‡									
VC1015	electron transport complex subunit RsxC	R661R (CGT→CGC)‡									
VC1180	cysteine/glutathione ABC transporter	L559P (CTC→CCC)*									
VC1571	cytochrome ubiquinol oxidase subunit I	L238V (TTA→GTA)*									
VC1590	acetolactate synthase *alsS*	G72G (GGA→GGG)‡									
VC1927	C4 dicarboxylate ABC transporter permease	V140G (GTG→GGG)*									
VC2137	σ 54 dependent transcriptional regulator *flrA*	coding (1247 1257 nt)									
VC2137	σ 54 dependent transcriptional regulator *flrA*	V261G (GTG→GGG)* #									
VC2137	σ 54 dependent transcriptional regulator *flrA*	R260W (CGG→TGG)*									
VC2137	σ 54 dependent transcriptional regulator *flrA*	G223D (GGC→GAC)*									
VC2137	σ 54 dependent transcriptional regulator *flrA*	A213V (GCG→GTG)* #									
VC2137	σ 54 dependent transcriptional regulator *flrA*	S204R (AGT→AGA)*									
VC2137	σ 54 dependent transcriptional regulator *flrA*	L201W (TTG→TGG)*									
VC2376	glutamate synthase large subunit	F88F (TTT→TTC)‡									
VC2376	glutamate synthase large subunit	L89H (CTC→CAC)*									
VC2376	glutamate synthase large subunit	S90N (AGC→AAC)*									
VC2376	glutamate synthase large subunit	P93L (CCA→CTA)*									
VC2384	hypothetical protein	G16G (GGA→GGG)‡									
VC2534	magnesium transporter *mgtE*	D272G (GAT→GGT)*									
VC0093	glycerol 3 phosphate 1 O acyltransferase	L508P (CTC→CCC)*									
VC0215	phosphopantothenate cys decarboxylase ligase	S213P (TCA→CCA)*									
VC0180	2 dehydropantoate 2 reductase	E234G (GAG→GGG)*									
VCA0101	EAL domain containing protein	L357L (CTT→CTA)‡									

Figure 4.2. Unique mutations in coding regions of adapted populations. The locus tag and gene designation are indicated in the first and second columns, respectively. The third column indicates the amino acid change with positions in the protein and affected base changes highlighted with underscore. The black horizontal bars in the heatmap represent the frequency

of respective mutations in each population (P1, P2, P3) with values ranging from 10 to 100%. The symbols represent * non-synonymous mutation, ‡ synonymous mutation, # same mutation also found in single clones at 100% frequency.

4.3.2 Long-term predation by amoeba drives mutations in conserved regions of the flagellar master regulator, *flrA*

Mutational analysis of adapted populations and single isolates from the populations indicated that mutations in the *flrA* gene of *V. cholerae* arose at high frequency. In depth analysis of the mutations revealed that the central ATPase associated domain with diverse cellular activities (AAA+) harbours all the nsSNPs while one deletion mutation occurred in the flanking region of the central and C-terminal DNA binding helix turn helix (HTH) domain (Figure 4.3). The observed mutations resulted in leucine being replaced with tryptophan, serine with arginine, alanine with valine, glycine with aspartic acid, arginine with tryptophan, and valine with glycine at positions 201, 204, 213, 223, 260 and 261of the AAA+ domain of the FlrA protein, respectively.

The AAA+ domain converts chemical energy by hydrolysing ATP into mechanical force for a wide variety of activities, including gene expression, genome replication, protein folding and unfolding. AAA+ domains consist of a central β-sheet flanked by two α-helices to form an α-β-α sandwich. The domain has walker A and walker B motifs which are highly conserved three-dimensional structures [281]. The walker A motif binds the phosphate of ATP and positions the triphosphate group. Its general structure is GXXXXGK(T/S) where X denotes any amino acid and G, K, T, S denote glycine, lysine, threonine and serine residues respectively. The walker B motif is responsible for hydrolysis of ATP. It consists of hhhhD where D denotes aspartic acid residues and h denotes any hydrophobic amino acid. In addition to these two motifs, AAA+ proteins also possess a second region of homology SRH that consists of sensor

1 and R-finger elements. Sensor 1 consists of the polar residues asparagine or threonine and the R-finger is a trans-acting arginine residue adjacent to SRH that stabilises the ATP during hydrolysis.

To identify what region of the FlrA protein was affected by the mutations, the FlrA protein sequences of several species of *Vibrio* and other Gram-negative bacteria were aligned (Figure 4.3). The full-length alignment of the FlrA protein is available in Supplementary Figure 2. Sequence alignment results show that all the amino acids affected by the nSNPs are highly conserved within *Vibrio* species and other Gram-negatives.

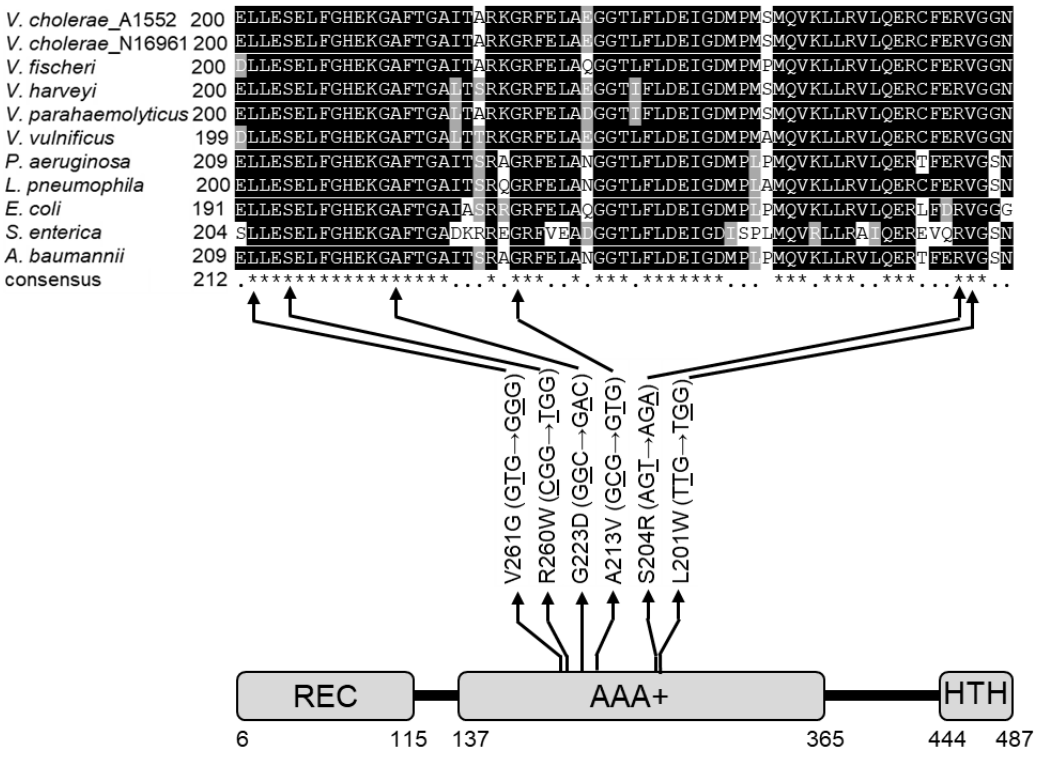

Figure 4.3. Schematic representation of the non-synonymous mutations affecting the conserved region of the FlrA protein. The FlrA protein has three domains as indicated, an N-terminal signal receiver (REC) domain, a central ATPase Associated domain with diverse cellular Activities (AAA+) and a C-terminal DNA binding helix turn helix (HTH) domain.

Positions of the mutations in the central domain are indicated with respective amino acid and nucleotide base substitution in the codon. Affected amino acids in the sequence alignment of FlrA protein are also shown by the black arrows. Protein sequences retrieved from the NCBI database are *V. cholerae* A1552 (AUR70352), *V. cholerae* N16961 (NP_231768), *V. fischeri* (WP_011262363), *V. parahaemolyticus* (WP_025525752), *V. vulnificus* (WP_039545791), *P. aeruginosa* (NP_249788), *L. pneumophila* (WP_027221215), *E. coli* (MHO05571), *S. enterica* (WP_064013385) and *A. baumannii* (SCY06189). Multiple sequence alignment was done on the T-coffee server and annotated using Expasy Box shade tool. Identical amino acids in the FlrA protein sequences are shown in the consensus using symbols.

4.3.3 Temporal mutation of *flrA* during co-adaptation

Sequencing data reveals mutations in the *flrA* gene on days 45 and 90 in adapted populations. To characterise the emergence of the *flrA* mutant during co-adaptation, an amplification refractory mutation system (ARMS)-PCR assay was performed. Template DNA was prepared from the populations and subjected to ARMS-PCR. ARMS-PCR were designed to detect the single point mutation A213V (C638T) in the *flrA* gene according to the method described in the materials and method section. Four sets of primers were used in a single reaction and wild type and mutant alleles were distinguished from the size differences of the allele specific amplicon. The assay revealed that a sub-population carrying A213V (C638T) mutation in the *flrA* gene first appeared on day 9 and remained throughout the co-culture experiment (Figure 4.4). The banding intensity of the allele specific amplicon showed enrichment of the *flrA* mutant from days 9 to 90 populations.

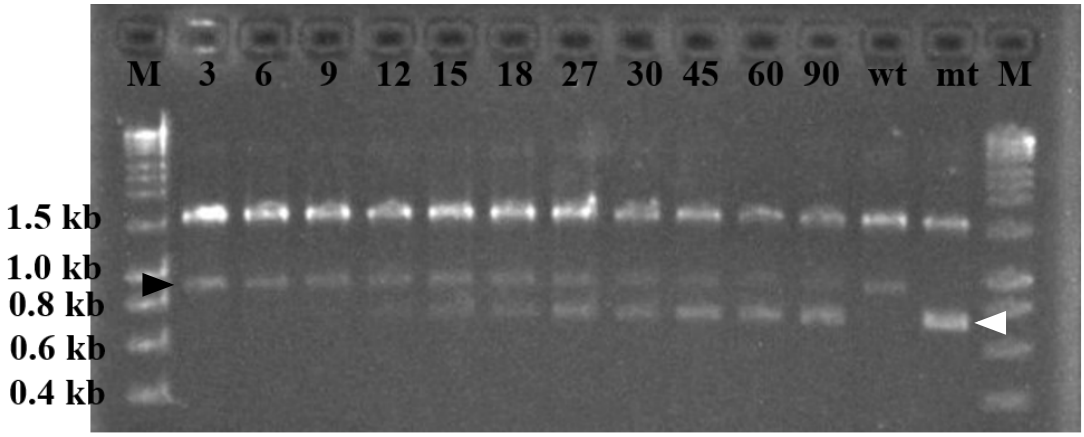

Figure 4.4. Temporal appearance of the A213V (C638T) mutation in *flrA* gene during adaptation. The gel image shows the temporal appearance of the A213V (C638T) mutation in the *flrA* gene in adapted populations at indicated times of isolation. The ARMS-PCR results show a 912 bp amplicon band (black arrow) corresponding to the wild type allele (C) and a 712 bp amplicon band (white arrow) corresponding to the mutant allele (T) at position 638 of the *flrA* gene. The assay also shows a common amplicon (1587 bp) at the top of the gel.

4.3.4 Functional classification of mutated genes in adapted and non-adapted populations

The mutated genes were classified according to their functions based on COGs. The classification revealed that 50% of the affected genes in adapted populations were involved in metabolism followed by cellular processes and signalling (31%), information storage and processing (9.5%) and poorly characterised (9.5%). Most of the mutated genes in non-adapted populations were involved in cellular processes and signalling (36.1%) followed by metabolism (33.3%), poorly characterised (16.7%) and information storage and processing (13.9%) (Figure 4.5A). The classification also revealed that the mutated genes were distributed in 17 different COG sub-categories (Figure 4.5B). The frequencies of 8 out of the 17 categories were higher in adapted populations compared to non-adapted populations. In contrast, the frequencies of 5 out of the 17 categories were higher in non-adapted populations compared to adapted populations, while the distributions were equal in 4 of the COG categories between

adapted and non-adapted populations. The highest number of mutated genes in adapted populations are involved in signal transduction followed by amino acid and carbohydrate metabolism. Mutations in genes associated with coenzyme transport and metabolism occurred solely in adapted populations.

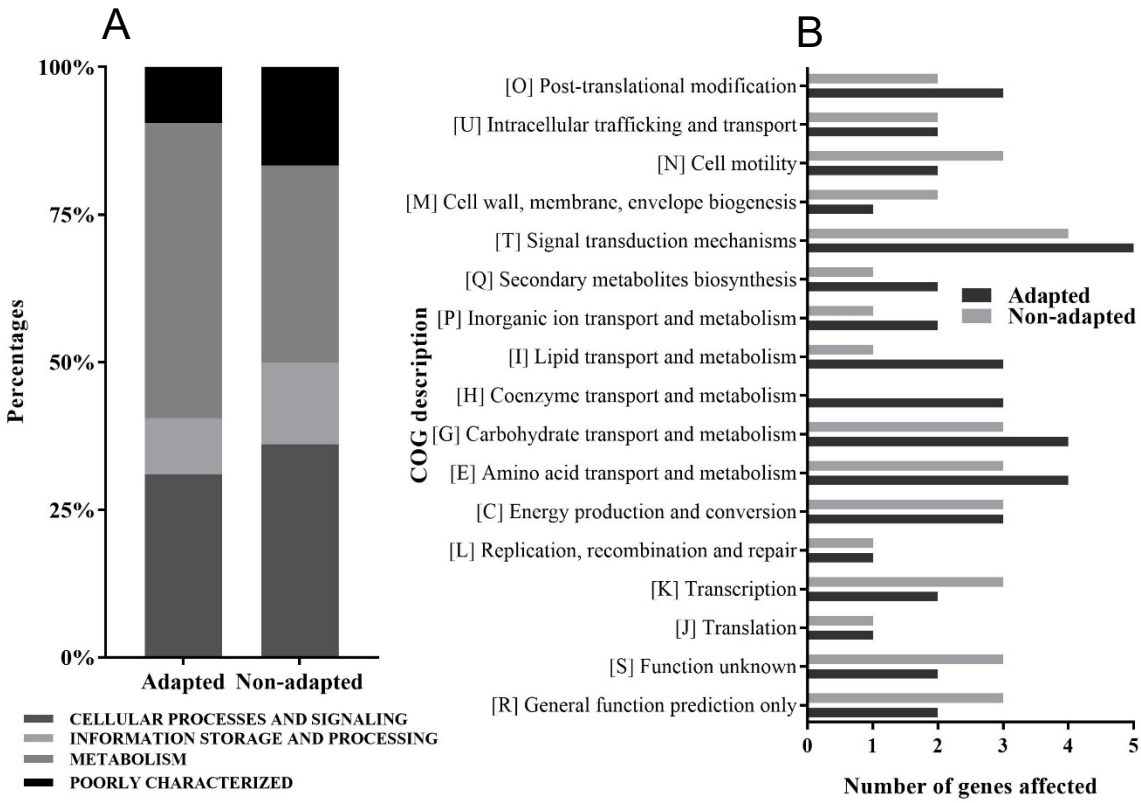

Figure 4.5. Functional annotation of mutated genes in adapted and non-adapted populations. (A) Distribution of COG categories and (B) subcategories of the mutated genes of adapted and non-adapted populations. Each category and sub-category are shown as a percentage of the total number of affected genes.

4.3.5 Analysis of the genes under selection in adapted and non-adapted populations

To determine the genes under selection in both amoeba-adapted and non-adapted conditions the ratio of the nonsynonymous substitutions (dN) to synonymous substitutions (dS) was determined. A dN/dS ratio of more than one implies positive selection whereas a ratio of less than one implies purifying selection and dN/dS ratio equal to one indicates neutral selection. The mutations in this study revealed many genes contained only sSNP or nsSNP which made it difficult to calculate the ratio. To overcome this, the numbers of nsSNPs and sSNPs were plotted in an x-y graph (Figure 4.6) with the values closer to the x-axis representing genes under positive selection and values closer to y-axis representing genes under purifying selection. The values closer to the dissecting line denote genes under neutral selection. Careful observation led to the identification of five genes (*citA*-VC0791, *hubP*-VC0998, *rsxC*-VC1015, imidazolonepropionase-VC1205 and *fruA*-VC1821) whose position in the graph is similar for both adapted and non-adapted populations. These five genes are likely to be mutated due to the experimental conditions in both adapted and non-adapted populations. Among the genes with at least five mutations in the adapted populations, *flrA*-VC2137 (six nsSNPs and no sSNPs) shows positive selection. In contrast, *rtxA*-VC1451(five nsSNPs and no sSNPs) is under positive selection in non-adapted populations.

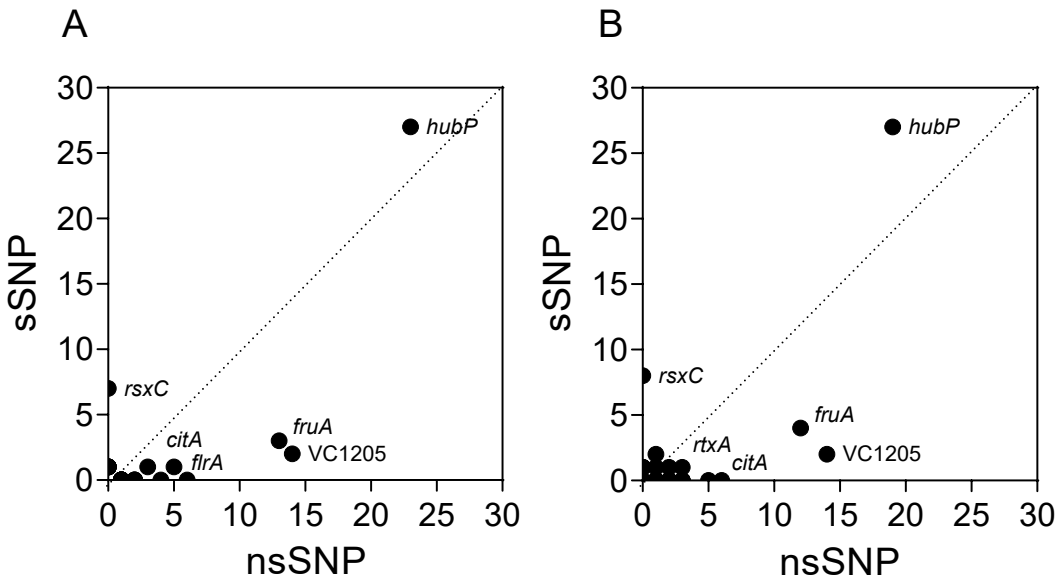

Figure 4.6. The genes with nsSNP and sSNP in adapted (A) and non-adapted (B) populations. Only genes with at least five mutations are labelled according to their locus tag. Diagonal intersection represent same number of sSNP and nsSNP.

4.4 Discussion

In Chapter One it was reported that long-term adaptation of *V. cholerae* in *A. castellanii* leads to isolates that exhibited increased intracellular survival in amoeba and increased competitive fitness *in vitro*. To investigate the underlying mechanisms allowing for these phenotypes, four virulence-associated factors, motility, biofilm formation and haemolysin and protease production were assessed in adapted and non-adapted isolates. The assays revealed a significant change in virulence factor production in the amoeba-adapted isolates from days 3 to 90. Motility, biofilm formation and haemolysin activity decreased significantly from day 3 to day 90 in adapted isolates. In contrast, protease production increased significantly from day 3 to

day 90 in adapted isolates. This chapter focuses on mutational analysis to link the altered phenotypic patterns with putative genomic changes in amoeba-adapted *V. cholerae*.

Genomic analysis of amoeba-adapted and non-adapted populations led to the identification of mutations in all the experimental lineages. A slight decrease was observed in the total number of mutations in adapted populations over the course of the experiment (from day 3 to day 90), while the total number of mutations was relatively constant in non-adapted populations. This suggested that during initial interaction with amoeba *V. cholerae* accumulated many mutations and over time most of them are lost, with only beneficial mutations that confer fitness advantage are being fixed in the populations. Although there was a decrease in the total number of mutations observed in adapted populations, the percentages of nsSNPs mutations increased. This suggested that selection pressure exerted by amoeba predation drives adaptation. Mutational and PCR analysis revealed clonal enrichment of sub-populations within the same lineage of adapted populations (Figure 4.2 and Figure 4.4). Persistence and enrichment of sub-populations carrying four nsSNPs in the *flrA* gene were detected in days 45 and 90 adapted populations (Figure 4.2). Analysis of single clones derived from each lineage confirmed the presence of these mutations (A213V and V261G) in the *flrA* gene. The enrichment of the sub-populations with mutations in *flrA* indicates selection of the advantageous clones during long-term predation stress. As discussed in Chapter Three, the competitive advantages may be related to enhanced capacity to acquire essential nutrients, resistance to oxidative stress and T6SS-dependent intra-species competition.

FlrA, the flagellar transcriptional master regulator, is a σ^{54} dependent enhancer binding protein (EBP) in *V. cholerae* that regulates the flagellar genetic cascade [282]. The FlrA protein has three domains, an N-terminal signal receiver (REC) domain, a central ATPase Associated domain with diverse cellular Activities (AAA+) and a C-terminal DNA binding helix turn helix

(HTH) domain (Figure 4.3). These regulators are widespread in bacteria and regulate diverse functions such as motility, biofilm formation and virulence factor expression. [207, 208]. The FlrA protein senses external cues such as cyclic-di-GMP and binding results in repression of downstream transcription, and point mutations in the *flrA* gene relieves the repression [69]. Interestingly, when incubated long-term in filter sterilised lake water a 49 bp deletion mutation was detected in *flrA* [283], indicating that this gene is prone to loss of function mutations under long-term stress. In this project, sequence alignment of FlrA proteins showed that mutations that arise in adapted isolates affected highly conserved residues in the walker domain (Figure 4.3). Previous reports also suggest that mutation in this domain of the FleQ protein which is a homologue of FlrA leads to aflagellated strains of *P. aeruginosa* [284].

In conclusion, this chapter demonstrates that mutations arise in *V. cholerae* during long-term predation by a natural predator. The data presented here linked the altered phenotypic pattern of late-stage adapted isolates to the point mutation in *flrA* gene. Collectively, this chapter showed that point mutations in key regulatory genes in response to predation could lead to the enhanced fitness of a bacterium.

Chapter Five

General Discussion and Future Perspective

Chapter Five

General Discussion and Future Perspective

5.1 Prelude

This project aimed to elucidate effects of long-term predation of *Vibrio cholerae* by the amoeba, *Acanthamoeba castellanii.* There have been many reports on the short-term interactions between various pathogens and environmental predators. Short-term predation pressure (7 days or less) often results in the expression of acute virulence traits such as production of toxins, secondary metabolites and effector proteins. For example, Shiga toxin (Stx) producing *Escherichia coli* showed broad spectrum cytotoxicity against different protist hosts, including amoeba and ciliates, while Stx negative strains displayed reduced toxicity [129, 285]. Secondary metabolites such as pyomelanin, diacetyl phloroglucinol (DAPG), pyrrolnitrin, hydrogen cyanide, and pyoluteorin are involved in predation resistance [14, 286]. However, much less is known about the effects of long-term predation pressure that would be experienced where pathogen and predator loads are high or under increased temperature resulting in increased predation rates. Here, the experimental evolution of the model pathogen *V. cholerae* with *A. castellanii* was performed with the aim to increase our understanding of the effects on adaptation and evolution of virulence-related traits. A combination of methods including phenotypic screening, genomic sequencing, transcriptomics and mutational analysis was conducted to characterise the effects of the adaptation.

Chapter One of this thesis provided a comprehensive literature review highlighting the possible mechanisms of environmental persistence of *V. cholerae* and the role of protozoan predation in the evolution of bacteria. The literature review also identified knowledge gaps and future research directions. Chapter Two, the first results chapter, revealed the phenotypic variation that arose in *V. cholerae* during co-incubation with an amoeba host and how that phenotypic variation impacted fitness and colonisation of the zebrafish host. Chapter Three explored the

mechanisms of enhanced fitness and survival in amoeba of amoeba-adapted *V. cholerae* and presented evidence that oxidative stress resistance and the acquisition of essential nutrients was involved. Chapter Four, the last results chapter, characterised the genetic variation that arose in amoeba-adapted and non-adapted populations and isolates of *V. cholerae* during the co-evolution experiments.

In this final discussion chapter, key points drawn from the overall project will be discussed. These points will highlight the role of different traits in *V. cholerae* that arise during adaptation to predation on maintenance of fitness and persistence in the environment as well as on further interactions with eukaryotic hosts. In addition, this chapter will address how adaptation to protozoan hosts serves as a key driver of evolution of bacteria in natural environments.

5.2 Adaptation strategies during long-term co-evolution

Adaptation to ever changing environments is an evolutionary challenge for every organism. Bacteria experience fluctuations in temperature, pH, oxygen levels, nutrient availability and predation stress in the environment. Adaptation shapes the course of evolution, hence understanding how bacteria adapt to these changes is important for predictions of evolutionary trajectories of microorganisms. Experimental evolution studies coupled with high-throughput sequencing has revealed some emerging trends that arise during microbial adaptation processes in response to changing environmental conditions. Firstly, adaptation often leads to fitness trade-offs in different environments and is due to genetic changes. For example, under carbon limitation, *Saccharomyces cerevisiae* increased the number of genes involved in sugar transport, which increased its fitness in low carbon environments but reduced its fitness in rich carbon media since increased influx of sugar leads to abnormal cellular homeostasis [287, 288].

Secondly, transcriptional and signalling pathways carefully control gene expression during adaptation processes perhaps to limit energy expenditure while maximising the utilisation of

low abundance resources. For example, *E. coli* exhibits reduced gene expression during nutrient starvation thereby optimising cellular functions [289]. Thirdly, adaptive changes are often associated with pleiotropic effects. For example, *rpoB* mutations in *E. coli* result in enhanced fitness during starvation and temperature stress and also confer resistance to rifampicin [290].

In this study, we observed these three effects of adaptation strategies arose in *V. cholerae* during long-term adaptation with amoeba. Point mutations in a gene, *flrA,* led to pleiotropic effects resulting in perturbation of multiple phenotypic traits leading to enhanced fitness in amoeba. This is not surprising as FlrA is not only the transcriptional master regulator of flagella but also an activator protein of RpoN (σ^{54}) which regulates diverse cellular functions [200].

Phagocytic cells like amoeba and macrophage deliver several antimicrobial effectors towards ingested prey bacteria, including reactive oxygen and nitrogen species [229]. Prey bacteria use catalases and peroxidases, for example, to neutralise reactive oxygen species (ROS) [227]. Adaptation to amoeba hosts leads to *V. cholerae* isolates with increased oxidative stress resistance reflecting adaptation to the ROS-containing environment which results in predation resistance and enhanced persistence. ROS defence activates the SOS response and is thus, a driver of adaptive mutations [291].

Colonisation of a host by bacterial pathogens is challenging because of the iron-limited conditions in the host. Often depletion of iron at the site of infection is a strategy used by a host against invading pathogens [219]. Moreover, in mammals, the level of freely available iron is far below the level that is required for bacterial multiplication [219]. However, bacterial pathogens deploy diverse tactics to tackle iron limitation, thereby allowing successful colonisation. Likewise, *V. cholerae* have evolved a wide array of iron acquisition systems that allow successful replication of the bacterium in diverse eukaryotic hosts [220]. In fact, the

cholera toxin promotes up-regulation of genes involved in acquisition of iron ensuring successful colonisation [249]. A very similar strategy was observed in this study where adapted isolates showed up-regulation of iron acquisition genes. The molecular mechanism of up-regulation of iron acquisition genes in *flrA* mutant is yet to be investigated. Also, how exactly iron is involved in increased survival inside amoeba is yet to be elucidated.

5.3 Fitness trade-off and evolution of virulence

Adaptation to protist hosts can impact bacterial virulence in multiple ways. Adaptation to predation may result in increased or decreased virulence depending on the bacterial pathogen, protist host, experimental conditions and infection model utilised as depicted by several previous studies [131, 153, 156-158, 276, 277, 292]. For example, intracellular adaptation of *Legionella pneumophila* and *Mycobacterium avium* in *A. castellanii* results in increased virulence in a mouse model of infection [153, 157]. In contrast, protist-driven attenuation of virulence was observed in *Pseudomonas aeruginosa* and *Serration marcescens* in wax moth larvae and a fruit fly (*Drosophila melanogaster*) oral infection model as reported in two independent studies [276, 277].

Here, we observed that the amoeba-adapted *V. cholerae* harbouring mutations in the *flrA* gene showed increased colonisation of the intestines in an adult zebrafish model of infection compared to the wild type. Since fishes serve as reservoirs of *V. cholerae,* especially in cholera endemic areas, increased colonisation might contribute to enhanced potential for persistence and dissemination [214, 216, 293]. A previous report has suggested that *V. cholerae* lacking *flrA* were defective for colonisation in an infant mouse model of infection [201]. The contrasting effects are likely the result of the varied mechanisms of colonisation and innate differences in mammalian mouse and vertebrate *Danio rerio* animal models. In addition, the different results may be due to the fact that the study by Syed et. al. was conducted with a *V.*

cholerae strain O395 which was defective in the production of quorum-sensing master regulator, HapR [201]. HapR impacts colonisation by down-regulation of cholera toxin (CT) and toxin co-regulated pilus (TCP) [61]. *V. cholerae* does not require CT or TCP to colonise zebrafish [203], but does require those factors to colonise the infant mouse and human hosts [38]. The underlying mechanism of increased colonisation in zebrafish by the adapted isolates with *flrA* mutations can be explained by increased oxidative stress resistance. Increased oxidative stress resistance contributes to enhanced colonisation in zebrafish while it does not affect colonisation in the infant mouse model as reported in previous studies [227]. Future studies will be needed to identify the exact mechanism of enhanced colonisation in zebrafish and examine colonisation potential in mouse models.

The potential effects on virulence of amoeba-adapted *V. cholerae* in different hosts might reflect a fitness trade-off resulting in increased environmental persistence and dissemination while compromising virulence in the human context. Similar fitness trade-offs in different hosts are also observed in *L. pneumophila.* Adaptation of *L. pneumophila* in a macrophage host resulted in decreased fitness in amoeba hosts [275]. The T6SS effector protein VasX has been reported to have a killing effect in the soil-bourne amoeba, *Dictyostelium discoideum* but not in the water-bourne amoeba, *A. castellanii* [15, 231]. Hence, the up-regulation of VasX might be an indication of a niche specific fitness trade-off between these closely related amoebal hosts. Loss of motility and biofilm formation by the late-stage amoeba-adapted *V. cholerae* may reflect a fitness trade-off in different environments since both of the phenotypes are crucial for infection in humans [72, 78, 190]. Loss or reduction of these two phenotypes facilitates phagocytic resistance, as seen by reduced uptake by amoeba. Proteases have been shown to confer increased resistance of *V. cholerae* against lysis by lytic bacteriophages [294]. Thus, high protease production by the amoeba-adapted *V. cholerae* have the potential to confer enhanced fitness against bacteriophages. Survival of *V. cholerae* against bacteriophage attack

is crucial for persistence in the environment since bacteriophages play an important role in the epidemiology of cholera [295]. *V. cholerae* proteases are also involved in the killing of ciliated and flagellated protists [167]. Therefore, proteases are critically important for the evolution of fitness of *V. cholerae* in different environments and hosts. Future studies to assess the fitness of amoeba-adapted *V. cholerae* against bacteriophages and other protists host to identify the exact role of virulence-related traits such as proteases are needed.

5.4 Shift from antagonistic to neutral interaction

According to a literature survey documented in the protist interaction database (PIDA), predation is the major outcome of protist-bacteria interactions accounting for 39% of all records analysed [296]. However, this interaction also led to symbiosis (29%), parasitism (18%) and some unrecognised relationships (14%) [296]. Here, we observed that long-term predation drives antagonistic to more neutral interactions between amoeba and *V. cholerae*. This neutral interaction could be a mutualistic or commensal interaction that facilitates increased survival of both the predator and prey. The free-living amoeba, *A. castellanii,* is a heterotrophic protist that feeds on bacteria [2, 106]. Many pathogenic bacteria can survive intracellularly in amoeba hosts and hence amoeba have been referred to as the "Trojan horse" of the microbial world [134]. This long-term co-adaptation study enabled us to explore possible mechanisms allowing for adaptation and resulting in enhanced fitness. These interactions also benefit the amoeba host by providing a steady supply of a food source.

The loss of motility in late-stage amoeba-adapted *V. cholerae* possibly enhances the persistence of the bacterium inside the amoeba host and perhaps contributes to the commensal interaction between them. Reduced haemolysin and increased protease expression ensures that the host is not lysed by the haemolysin, allowing for maintenance of the replication niche [15, 297]. The

decreased expression of the Mak cytotoxin possibly prevents unnecessary toxicity towards amoeba cells as the toxin is involved in the killing of eukaryotic cells [248].

There may also be metabolic co-ordination of nutrient utilisation by *V. cholerae* inside the host amoeba as seen from the transcriptomic data. Iron is regarded as part of the innate immune defence, and phagocytic cells require iron to mediate antimicrobial effectors against internalised bacteria, including NADPH-dependent oxygen and nitrogen radicals [298]. Thus, the increased capacity to acquire iron by *V. cholerae* might prevent reactive oxygen and nitrogen radical-mediated killing by the amoeba, providing further predation resistance and persistence. *L. pneumophilia* is capable of activating host proteasomes to degrade host protein, ensuring access to essential amino acids [299]. The co-ordination of amino acid auxotrophy between *L. pneumophilia* and *A. castellanii* ensure the amino acid needs of both predator and prey are met. It would be interesting to explore amino acid auxotrophy in *V. cholerae* in coordination with amoeba and how that might impact on survival. This could lead to exploration of metabolic perturbation as a control for infection.

5.5 Potential impact of global warming on the evolution of virulence

Global warming impacts on marine ecosystems as temperature influences several water parameters including nutrient content and productivity [300]. Thus, increased seawater temperature is associated with blooms of microbial organisms in the environment. Many reports have reported that the abundance of phytoplankton and zooplankton are positively correlated with increased surface water temperature [301-303]. Temperature also impacts the seasonality of the waterbourne disease cholera, which follows a distinct epidemiological pattern in endemic areas with biannual peaks of the disease observed every year [11, 28]. The seasonal peaks are associated with warmer months of the year thus elucidating the role of increased temperature on the outbreak of cholera cases. There are many biotic and abiotic

factors that drive this seasonality. For example, increased abundance of planktonic communities are associated with increased cholera cases during warmer months [85]. Like *V. cholerae,* many other *Vibrio* species are associated with chitinous surfaces of planktonic organisms in the marine environment [23, 83]. Vezzulli *et al*. showed that warmer climates also influence the abundance of *Vibrio* spp. in many parts of the world [304]. The abundance of *Vibrio* spp. not only increased with the rise of temperature but also became dominant planktonic communities in marine waters [305]. This is potentially due to the fact that increased temperature results in upregulation of chitin binding appendages such as the N-acetylglucosamine-binding protein A (GbpA) and the mannose-sensitive haemagglutinin [306]. Hence, this study provides a model for how potential rises in temperature may affect the outcome of predator-prey interactions and the impact on virulence in pathogens.

5.6 Conclusion

The coincidental evolution hypothesis states that pathogens acquire virulence traits during adaptation in ecological niches other than the host where they cause infection [155]. It is now widely acknowledged that protozoan predation serves as a key driver of the adaption process and to the evolution of virulence [8, 9]. Identifying molecular mechanisms and key factors of the adaptation processes of virulence traits is important for understanding how pathogens adapt in the environment and for devising control strategies to prevent transmission and infection. In this study, experimental evolution of the model pathogen, *V. cholerae,* with a potential aquatic reservoir, *A. castellanii* led to an understanding of how the pathogen adapts under predation pressure. Long-term predation selects for *V. cholerae* isloates with improved fitness, possibly enhancing commensalism with the host amoeba. This study also elucidated a number of adaptative strategies used by the bacterium, including trade-offs among multiple virulence-related traits, an enhanced ability to derive essential micro-nutrients, and resistance to oxidative

stress. These adaptation strategies presumably enhance the fitness of the bacterium and serve as molecular drivers of evolution at the host-pathogen interface.

Supplementary Information

Supplementary Figure 1

Locus tag	Gene/ Gene function	Mutation	A			NA		
			3	45	90	3	45	90
VC0744	protein translocase subunit	E101G (GAG→GGG)						
VC0766	exodeoxyribonuclease	S148P (TCA→CCA)						
VC0778	siderophore transporter permease	E246G (GAG→GGG)						
VC0791	sensor histidine kinase	Y183S (TAC→TCC)						
VC0905	met transporter binding protein	N58K (AAT→AAA)						
VC0913	multidrug efflux RND transporter	N78K (AAT→AAA)						
VC0998	Polar transmembrane protein	D948E (GAT→GAG)						
VC0998	Polar transmembrane protein	D996E (GAT→GAG)						
VC0998	Polar transmembrane protein	T1033A (ACA→GCA)						
VC0998	Polar transmembrane protein	V1094A (GTC→GCC)						
VC0998	Polar transmembrane protein	T1095A (ACG→GCG)						
VC0998	Polar transmembrane protein	V1125A (GTA→GCA)						
VC0998	Polar transmembrane protein	S1145F (TCT→TTT)						
VC0998	Polar transmembrane protein	L1185P (CTC→CCC)						
VC0998	Polar transmembrane protein	V1217A (GTC→GCC)						
VC0998	Polar transmembrane protein	T1229S (ACT→AGT)						
VC0998	Polar transmembrane protein	P1238T (CCC→ACC)						
VC1205	imidazolonepropionase	P60Q (CCG→CAG)						
VC1205	imidazolonepropionase	P60T (CCG→ACG)						
VC1205	imidazolonepropionase	T59K (ACA→AAA)						
VC1205	imidazolonepropionase	V58F (GTC→TTC)						
VC1205	imidazolonepropionase	L57* (TTA→TGA)						
VC1205	imidazolonepropionase	G55V (GGC→GTC)						
VC1451	multifunctional autoprocessing toxin	V1112G (GTA→GGA)						
VC1455	XRE family transcriptional regulator	A68D (GCT→GAT)						
VC1798	ATPase AAA	E292G (GAG→GGG)						
VC1821	PTS fructose transporter IIC	A190S (GCG→TCG)						
VC1821	PTS fructose transporter IIC	I191F (ATT→TTT)						
VC1821	PTS fructose transporter IIC	G193D (GGT→GAT)						
VC1821	PTS fructose transporter IIC	G194D (GGT→GAT)						
VC1821	PTS fructose transporter IIC	F198Y (TTC→TAC)						
VC1821	PTS fructose transporter IIC	D199E (GAT→GAG)						
VC2021	beta ketoacyl ACP reductase	I244L (ATC→CTC)						
VC2137	σ 54 dependent transcriptional regulator *flrA*	V261G (GTG→GGG)						
VC2137	σ 54 dependent transcriptional regulator *flrA*	A213V (GCG→GTG)						

Supplementary Figure 4.1. Non-synonymous mutations in coding regions of adapted and non-adapted isolates. The locus tag and name of the affected gene are indicated in the first and second columns, respectively. The third column shows the type of amino acid changes with position in the

protein with affected base changes highlighted with underscore. The heatmap shows the presence (deep colour) and absence (shaded colour) of nsSNPs found in coding region of adapted and non-adapted isolates respectively in the three replicates from days 3, 45 and 90. The symbols are A, for adapted and NA for non-adapted.

Supplementary Figure 2

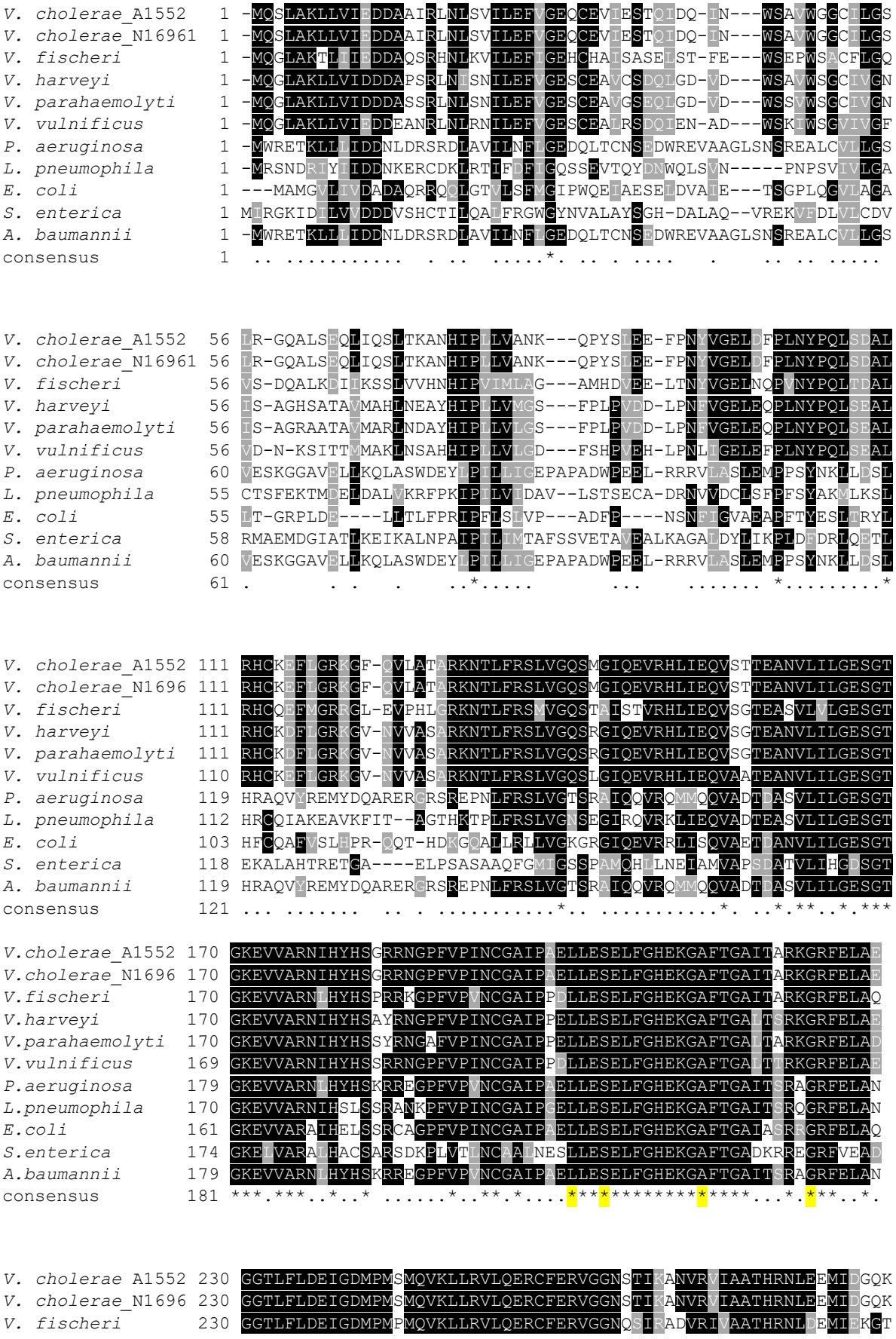

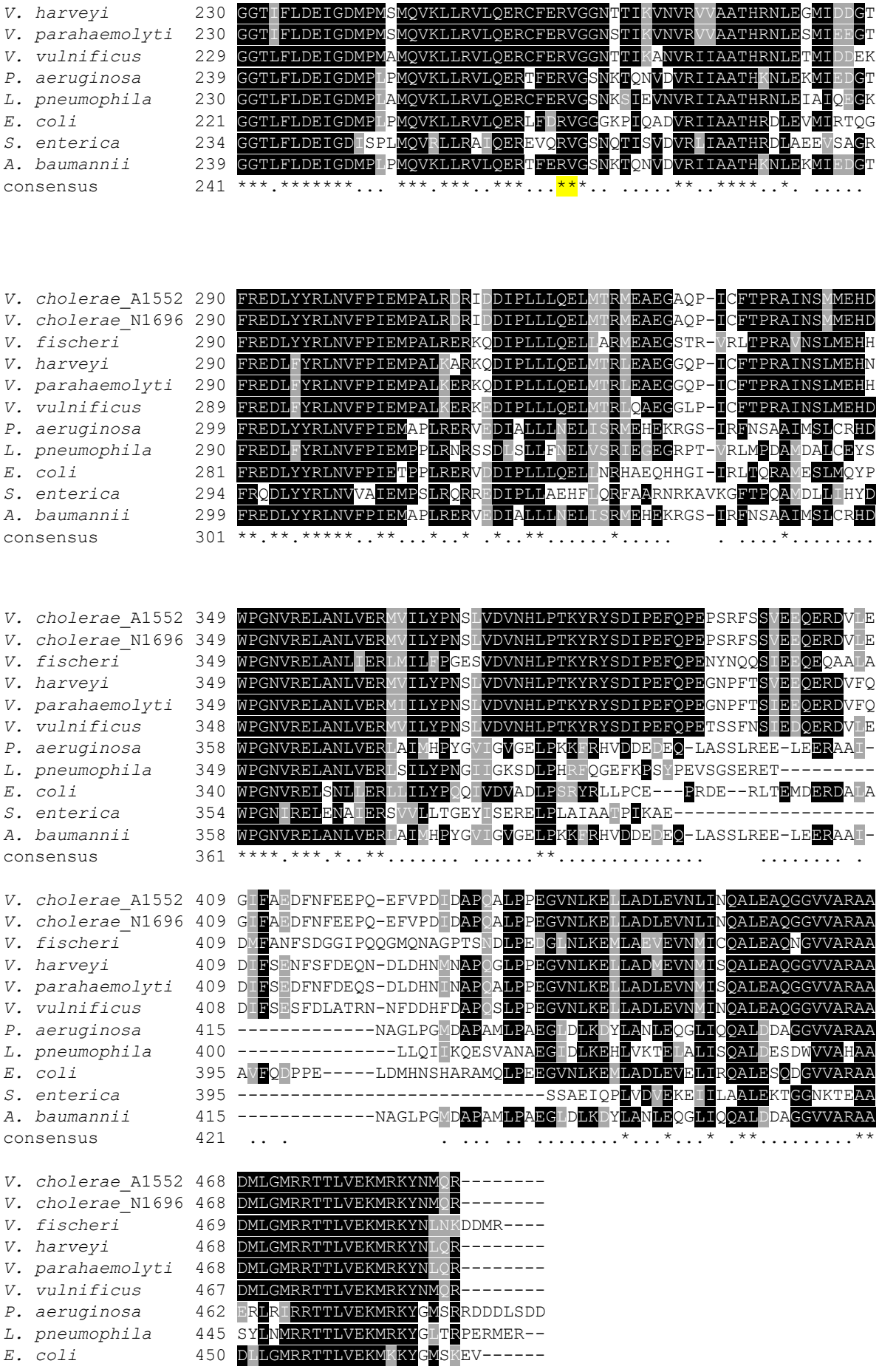

Supplementary Figure 4.2. Amino acid sequence alignment of the FlrA protein. Protein sequences were retrieved from the NCBI protein database: *V. cholerae* A1552 (AUR70352), *V. cholerae* N16961 (NP_231768), *V. fischeri* (WP_011262363), *V. parahaemolyticus* (WP_025525752), *V. vulnificus* (WP_039545791), *P. aeruginosa* (NP_249788), *L. pneumophila* (WP_027221215), *E. coli* (MHO05571), *S. enterica* (WP_064013385), *A. baumannii* (SCY06189) respectively. Multiple sequence alignment was done on T-coffee server and annotated using Expasy Box shade tool. Affected amino acids are highlighted with yellow shadings. Identical amino acids in all of these FlrA protein sequences are shown in the consensus.

Supplementary Table 1. List of strains, plasmids, and primers

Organisms/Strains	**Description**	**Reference**
Vibrio cholerae A1552	Wild type, O1, El Tor, Inaba, smooth, Rif^r	[307]
V. cholerae A1552 Δ*lacZ*	In-frame deletion mutant of *lacZ* gene on wild type	[131]
V. cholerae A1552 Δ*flrA*	In-frame deletion mutant of *flrA* gene on wild type	This Study
Escherichia coli DH5α	F endA1 hsdR17 supE44 thi-1 recA1 gyrA96 relA1 (argF-lacZYA) U169 (80lacM15)	Laboratory collection
E. coli BW20767	RP42tet::Mu1kan::Tn7- integrant uidA(DMlu1)::pir+ recA1 creB510 leu63 hsdR17 endA1 zbf5 thi	ATCC 47084
E. coli S17-1 λ pir	recA thi pro rK- mK+ RP4::2-Tc::MuKm Tn7 Tpr Smr λ pir	ATCC 47055
Acanthamoeba castellanii		ATCC 30234
Zebrafish (*Danio rerio*)		[197]
Oligonucleotide/Primer		
Primers for construction of *flrA* mutant		
flrA-up-F	GAAGAAGAACTCGACGCTCAA	This study
flrA -up-R	CCAGCCTACACGGCATCGTCCTCAATCA CAAGT	This study
flrA -cat-F	GGACGATGCCGTGTAGGCTGGAGCTGC TTC	This study
flrA -cat-R	TGCGCATCTTCTCAACCATATGAATATC CTCCTTAG	This study
flrA -down-F	GAGGATATTCATATGGTTGAGAAGATG CGCAAATACA	This study
flrA -down-R	TTCAAGTCACGGTTACTGGTTG	This study
Primers for gibson cloning		
pBAD-F	CAGTAGAGAGTTGCGATAAA	This study
pBAD-R	GATGAGAGAAGATTTTCAGC	This study
flrA-pBAD-gibson-F	TTTTTATCGCAACTCTCTACTGATGCAG AGTTTAGCGAAACT	This study
flrA-pBAD-gibson-R	GGCTGAAAATCTTCTCTCATCCTAGCGT TGCATGTTGTATT	This study
Primers for ARMS-PCR		
flrA -outer-F	ATGATGTTCAAACGGTGCAA	This study
flrA -outer-R	GCCAAGCCATTCATGTTTAA	This study
*flrA*213-innerC-F	TTTGGTCATGAAAAAGGTGC	This study
*flrA*213-innerT-R	GTAATCGCTCCGGTAACCA	This study
*flrA*261-innerG-F	GCGCTGTTTTGAACGAGG	This study

*flrA*261-innerT-R	ATGGTGCTGTTGCCTCTCA	This study
Primers for RT-qPCR		
katB-F	ACCAGCAAAGGCAAAATCAC	This study
katB-R	CCAGTTGCCTTGTTCGGTAT	This study
katG-F	CACCGTCACCAGTGGTATTG	This study
katG-R	ACCTGCAGGGCTCTTAGTGA	This study
sodC-F	CAAGCAAATCAACCCGTTTT	This study
sodC-R	TGGATGGTCGGAATGGTTAT	This study
oxyR-F	CATGAAGCGCAGACTAACCA	This study
oxyR-R	GCACTGCAATGCTCAACACT	This study
relA-F	ATGCAGAAAAAGAGCCTCGC	[247]
relA-R	TCGGTTTTGGGTTTGCTACA	[247]
Plasmid		
pBAD24	Cloning vector with arabinose inducible promoter, Amp^r	[131]
pBAD24::*flrA*	*flrA* gene of WT cloned into MCS site of pBAD24	This study
pBAD24::*flrA* A213V	*flrA* gene containing point mutation affecting amino acid at position 213 cloned into MCS site of pBAD24	This study
pBAD24::*flrA* V261G	*flrA* gene containing point mutation affecting amino acid at position 261 cloned into MCS site of pBAD24	This study
pKD3	FRT-flanked cat gene in oriRγ replicon requiring the *pir* gene product, Addgene plasmid # 45604	[308]
miniTn7(Gm)PrrnB1 – gfpASV	a Gm→,Cm→ PrrnB1 GFP-ASV→ Prr-gfp-ASV cloned into NotI site of pBKminiTn7-ΩGm, *Escherichia coli* AKN139	[309]
miniTn7(Gm)PA1/04/03 – DsRedExpress	A Gm→,Cm→ PA1/04/03 DsRedExpress → PA1/04/03- DsRedExpress (AKN122) cloned into NotI site of pBK-miniTn7-ΩGm, *Escherichia coli* AKN132	[309]
pUX-BF13	oriR6K helper plasmid, mob/oriT, provides Tn7 transposition function in trans, *Escherichia coli* AKN69	[309]
pBR-flp	FLP+, k cI857+, k pR from pCP20 integrated into EcoRV site of pBR322	[193]

Supplementary Table 2. Unique genes mutated in adapted and non-adapted populations.

	Locus tag	Gene/Gene function	Number	nsSNP	sSNP	INDEL	Same lineage	Day 3	Day 45	Day 90
Unique to Adapted	VC0760	histidine tRNA ligase	1	1	0	0	-	+	-	-
	VC1180	cysteine/glutathione ABC transporter CydC	1	1	0	0	-	-	-	+
	VC1590	acetolactate synthase AlsS	1	0	1	0	-	+	+	-
	VC1927	C4-dicarboxylate ABC transporter permease	1	1	0	0	-	-	-	+
	VC2021	beta-ketoacyl-ACP reductase	1	1	0	0	-	+	-	-
	VC2137	sigma-54-dependent transcriptional regulator, *flrA*	7	6	0	1	+	-	+	+
	VC2384	hypothetical protein VC2384	1	0	1	0	-	-	-	+
	VC2534	magnesium transporter	1	1	0	0	-	+	-	-
	VC0093	glycerol-3-phosphate 1-O-acyltransferase	1	1	0	0	-	+	-	-
	VC0215	cysteine ligase and decarboxylase CoaBC	1	1	0	0	-	+	-	-
	VC0180	2-dehydropantoate 2-reductase	1	1	0	0	-	+	-	-
	VCA0101	EAL domain-containing protein	1	0	1	0	-	-	-	+
Unique to Non-adapted	VC0534	RNA polymerase sigma factor RpoS	2	0	0	2	-	-	+	-
	VC0893	flagellar motor protein MotB	3	2	0	1	-	-	+	+
	C1H56_06465	resolvase	1	1	0	0	-	-	-	+
	C1H56_07180	ABC transporter permease	1	0	0	0	-	-	+	-
	VC1710	PAS domain S-box protein	1	1	0	0	-	-	+	-
	VC2156	outer membrane protein assembly factor BamC	1	0	1	0	-	-	+	-
	VC2185	redox-regulated ATPase YchF	1	0	1	0	-	-	-	+
	VC2601	Sodium type flagellar protein MotX	1	0	0	1	+	-	+	+
	VCA0171	VWA domain-containing protein	1	1	0	0	-	-	-	+
	VCA0678	periplasmic nitrate reductase subunit alpha	1	1	0	0	-	+	-	-

Supplementary Table 3. Common genes mutated in adapted and non-adapted populations.

		Adapted								Non-adapted							
Locus tag	**Gene/Gene function**	**Number**	**nsSNP**	**sSNP**	**INDEL**	**Same lineage**	**Day 3**	**Day 45**	**Day 90**	**Number**	**nsSNP**	**sSNP**	**INDEL**	**Same lineage**	**Day 3**	**Day 45**	**Day 90**
VC0027	threonine ammonia-lyase, biosynthetic	1	1	0	0	-	+	-	-	2	1	1	0	-	+	+	-
VC0766	exodeoxyribonuclease VII large subunit	1	1	0	0	-	-	+	-	1	1	0	0	+	-	+	+
VC0791	sensor histidine kinase citA	6	5	1	0	+	+	+	+	6	6	0	0	+	+	+	+
VC0905	methionine ABC transporter MetQ	1	1	0	0	-	+	-	+	4	3	1	0	+	+	+	+
VC0913	MexH family multidrug efflux RND transporter	4	4	0	0	+	+	+	+	3	3	0	0	+	+	+	+
VC0995	PTS N-acetylmuramic acid transporter IIBC	1	0	1	0	-	+	+	-	3	1	2	0	+	+	+	+
VC0998	Polar transmembrane protein	50	23	27	0	+	+	+	+	46	19	27	0	+	+	+	+
VC1015	electron transport complex subunit RsxC	7	0	7	0	+	+	+	+	8	0	8	0	+	+	+	+
VC1162	ATP-dependent Zn protease	2	0	1	1	+	+	+	+	4	2	1	1	-	+	+	+
VC1205	imidazolonepropionase	16	14	2	0	+	+	+	+	16	14	2	0	+	+	+	+
VC1386	molecular chaperone	2	2	0	0	+	+	+	+	3	3	0	0	+	+	+	+
VC1451	multifunctional autoprocessing toxin RtxA	2	2	0	0	-	-	+	+	5	5	0	0	+	+	+	+
VC1455	XRE family transcriptional regulator	1	1	0	0	-	-	+	+	1	1	0	0	-	+	-	-
VC1571	cytochrome ubiquinol oxidase subunit I	2	2	0	0	-	+	+	+	2	2	0	0	+	+	+	+
VC1580	LysR family transcriptional regulator	1	0	1	1	-	+	-	-	1	0	1	0	-	-	-	+
VC1665	ABC transporter permease	1	1	0	0	+	+	+	+	2	2	0	0	+	+	+	+
VC1798	ATPase AAA	1	1	0	0	-	-	+	-	1	1	0	0	-	+	+	+
VC1821	PTS fructose transporter subunit IIC	16	13	3	0	+	+	+	+	16	12	4	0	+	+	+	+
VC2376	glutamate synthase large subunit	4	3	1	0	-	+	+	-	1	1	0	0	-	+	-	-
VC2618	aspartate aminotransferase family protein	1	1	0	0	+	-	+	+	2	2	0	0	-	-	+	+
VC2749	nitrogen regulation protein NR(I)	1	0	1	0	+	-	+	+	1	0	1	0	+	+	+	+
VC0143	hypothetical protein, VC0143	1	1	0	0	-	-	+	+	1	1	0	0	-	+	-	-
VC0171	nickel/dipeptide/oligopeptide ABC transporter	2	2	0	0	-	+	-	-	3	3	0	0	-	-	-	+
VCA0268	methyl-accepting chemotaxis protein	1	1	0	0	-	+	-	-	1	1	0	0	-	+	+	-
VCA0517	1-phosphofructokinase	1	1	0	0	-	+	-	-	1	1	0	0	-	+	-	-

Supplementary Table 4. Unique genes mutated in adapted and non-adapted isolates.

	Locus tag	Gene/Gene function	Number	nsSNP	sSNP	INDEL	Day 3	Day 45	Day 90
Unique to Adapted	VC0744	protein translocase subunit SecF	1	1	0	0	-	-	+
	VC0778	Fe(3+)-siderophore ABC transporter permease	1	1	0	0	+	-	-
	VC2137	sigma-54-dependent transcriptional regulator, *flrA*	2	2	0	0	-	+	+
	VCA0283	hypothetical protein	1	0	0	1	-	+	-
Unique to Non-adapted	VC0766	exodeoxyribonuclease VII large subunit	1	1	0	0	+	-	-
	VC0791	sensor histidine kinase	1	1	0	0	-	-	+
	VC0905	methionine ABC transporter MetQ	1	1	0	0	-	-	+
	VC0913	MexH family multidrug efflux RND transporter	1	1	0	0	-	+	+
	VC1451	multifunctional autoprocessing toxin RtxA	1	1	0	0	+	-	-
	VC1798	ATPase AAA	1	1	0	0	+	-	-
	VC2185	redox-regulated ATPase YchF	1	0	1	0	-	-	+
	VC2677	DNA-binding transcriptional regulator CytR	1	0	1	0	+	-	-

Supplementary Table 5. Common genes mutated in adapted and non-adapted isolates.

		Adapted							Non-adapted						
Locus tag	**Gene/Gene function**	**Number**	**nsSNP**	**sSNP**	**indel**	**Day 3**	**Day 45**	**Day 90**	**Number**	**nsSNP**	**sSNP**	**indel**	**Day 3**	**Day 45**	**Day 90**
VC0998	Polar transmembrane protein	19	9	10	0	+	+	+	12	7	5	0	+	+	+
VC1015	electron transport complex subunit RsxC	2	0	2	0	+	+	+	3	0	3	0	+	-	+
VC1205	imidazolonepropionase	3	3	0	0	-	+	+	4	4	0	0	+	+	-
VC1455	XRE family transcriptional regulator	1	1	0	0	+	-	+	1	1	0	0	+	-	+
VC1821	PTS fructose transporter subunit IIC	6	4	2	0	-	+	+	7	5	2	0	+	+	+
VC2021	beta-ketoacyl-ACP reductase	1	1	0	0	+	+	+	1	1	0	0	-	+	-

Supplementary Data 1. Mutations detected in adapted populations.

chromosome: position	annotation	Day 3			Day 45			Day 90			description
		P1	P2	P3	P1	P2	P3	P1	P2	P3	
Chl:17087	E201G (GAG→GGG)	14.0%		13.9%							threonine ammonia lyase, biosynthetic
Chl:85242	intergenic (+13/ 22)					13.4%					tRNA Met/tRNA Gly
Chl:85254	intergenic (+25/ 10)				10.1%						tRNA Met/tRNA Gly
Chl:85592	noncoding (67/77 nt)	15.1%	19.9%	18.1%	24.3%		31.1%	12.1%	18.0%	11.6%	tRNA Met
Chl:85696	noncoding (52/77 nt)	20.9%	25.9%	18.7%	21.1%		17.4%	20.7%	14.7%	15.8%	tRNA Met
Chl:126127	noncoding (1550/1553 nt)	21.9%	30.4%	36.4%	32.3%	37.2%			41.6%	42.0%	16S ribosomal RNA
Chl:131685	intergenic (+15/ 49)					51.1%					16S ribosomal RNA/tRNA Glu
Chl:131976	noncoding (43/76 nt)	28.1%	49.9%	48.6%	69.0%	48.0%		45.6%	55.5%	46.5%	tRNA Val
Chl:309374	intergenic (+12/ 11)					10.7%	11.9%	11.8%			tRNA Arg/tRNA Ser
Chl:309674	intergenic (+54/ 2)	14.2%									tRNA Arg/tRNA Arg
Chl:379609	intergenic (32/+25)					10.3%					chitobiase/ABC transporter
Chl:541243	E270G (GAG→GGG)		10.1%								histidine tRNA ligase
Chl:547560	S148P (TCA→CCA)						11.5%				exodeoxyribonuclease VII large subunit
Chl:575571	I202I (ATC→ATT)				12.6%				12.0%		sensor histidine kinase citA
Chl:575573	I202F (ATC→TTC)				11.4%						sensor histidine kinase citA
Chl:575578	A200V (GCT→GTT)		12.0%	14.5%	16.9%	15.3%	10.1%		11.7%		sensor histidine kinase citA
Chl:575594	L195F (CTT→TTT)		10.9%	16.8%			11.0%				sensor histidine kinase citA
Chl:575606	L191F (CTT→TTT)				11.7%		11.0%				sensor histidine kinase citA
Chl:575621	I186F (ATT→TTT)		11.1%		11.2%	13.6%					sensor histidine kinase citA
Chl:694022	N58K (AAT→AAA)	10.1%							12.6%		metQ
Chl:696131	intergenic (198/ 38)	13.3%									MetN/phosphatase
Chl:701454	intergenic (6/+79)		12.9%	10.8%		10.5%			13.9%		tRNA Tyr/tRNA Tyr
Chl:701518	intergenic (70/+15)									10.4%	tRNA Tyr/tRNA Tyr
Chl:701700	intergenic (83/+2)		11.2%						18.3%		tRNA Tyr/tRNA Tyr
Chl:701730	noncoding (57/85 nt)				11.8%						tRNA Tyr
Chl:701863	intergenic (77/+9)	14.3%	12.3%								tRNA Tyr/tRNA Tyr
Chl:701867	intergenic (81/+5)						15.8%				tRNA Tyr/tRNA Tyr
Chl:702453	D71G (GAC→GGC)		12.8%								MexH family RND transporter
Chl:702475	N78K (AAT→AAA)		10.2%		10.7%	10.7%	14.2%	11.2%			MexH family RND transporter
Chl:702491	G84S (GGT→AGT)			14.0%							MexH family RND transporter
Chl:702524	A95T (GCT→ACT)				10.7%						MexH family RND transporter
Chl:789999	G158G (GGA→GGG)		11.0%		14.0%		14.7%				PTS N acetylmuramic acid transporter
Chl:796023	D948E (GAT→GAG)		10.9%	11.8%	10.5%		12.2%	13.8%		10.0%	Polar transmembrane protein
Chl:796037	N953S (AAT→AGT)							10.7%			Polar transmembrane protein
Chl:796136	V986A (GTC→GCC)		10.6%	11.4%							Polar transmembrane protein
Chl:796155	E992E (GAA→GAG)		10.6%	15.9%						10.7%	Polar transmembrane protein
Chl:796167	D996E (GAT→GAG)		13.6%					10.6%			Polar transmembrane protein
Chl:796213	K1012E (AAG→GAG)		16.9%			14.5%				17.4%	Polar transmembrane protein
Chl:796270	S1031P (TCC→CCC)				13.2%					14.0%	Polar transmembrane protein
Chl:796362	L1061L (TTA→TTG)							10.1%			Polar transmembrane protein
Chl:796371	Y1064Y (TAT→TAC)							12.0%	11.2%		Polar transmembrane protein
Chl:796374	T1065T (ACA→ACC)			12.5%				13.0%			Polar transmembrane protein
Chl:796383	D1068D (GAC→GAT)	14.3%	14.6%								Polar transmembrane protein
Chl:796396	S1073A (TCG→GCG)				10.5%			16.0%			Polar transmembrane protein
Chl:796416	A1079A (GCC→GCA)	16.2%									Polar transmembrane protein
Chl:796444	L1089L (TTA→CTA)		14.7%	10.1%				13.2%	10.8%		Polar transmembrane protein
Chl:796446	L1089L (TTA→TTG)		10.0%								Polar transmembrane protein
Chl:796448	V1090A (GTA→GCA)		10.0%		11.4%			12.7%			Polar transmembrane protein
Chl:796460	V1094A (GTC→GCC)				15.2%			12.1%			Polar transmembrane protein
Chl:796462	T1095A (ACG→GCG)	11.8%	15.4%	12.8%	12.9%		11.8%		11.2%		Polar transmembrane protein
Chl:796467	E1096E (GAG→GAA)		12.3%	11.2%	14.7%			10.5%	13.1%		Polar transmembrane protein
Chl:796491	E1104E (GAA→GAG)			14.3%	15.7%		12.5%	13.8%	12.7%		Polar transmembrane protein
Chl:796553	V1125A (GTA→GCA)	12.4%	10.8%	10.0%	10.5%		16.8%	12.5%			Polar transmembrane protein
Chl:796582	L1135L (CTA→TTA)						11.7%				Polar transmembrane protein
Chl:796584	L1135L (CTA→CTG)	14.0%			15.9%						Polar transmembrane protein
Chl:796586	A1136V (GCA→GTA)						14.9%				Polar transmembrane protein
Chl:796596	P1139P (CCT→CCA)			12.1%				12.1%	14.1%		Polar transmembrane protein
Chl:796599	A1140A (GCT→GCC)				10.4%						Polar transmembrane protein
Chl:796613	S1145F (TCT→TTT)	11.2%	16.4%	16.4%	13.0%	12.5%	15.2%	12.9%	17.6%		Polar transmembrane protein
Chl:796632	L1151L (CTT→CTC)	16.7%	11.2%				15.1%	11.6%	10.5%	13.4%	Polar transmembrane protein
Chl:796641	P1154P (CCC→CCT)	14.5%				12.5%	16.4%	10.1%			Polar transmembrane protein
Chl:796659	D1160D (GAT→GAC)	11.7%									Polar transmembrane protein
Chl:796708	S1177P (TCC→CCC)	18.1%	12.1%		10.8%		12.9%		12.5%		Polar transmembrane protein
Chl:796728	S1183S (AGC→AGT)		10.1%								Polar transmembrane protein
Chl:796731	D1184E (GAT→GAG)						10.2%				Polar transmembrane protein
Chl:796733	L1185P (CTC→CCC)	10.9%	10.9%	12.1%			15.3%				Polar transmembrane protein
Chl:796747	P1190A (CCC→GCC)		14.5%	10.4%			17.5%				Polar transmembrane protein
Chl:796800	A1207A (GCT→GCC)				11.0%						Polar transmembrane protein
Chl:796806	A1209A (GCA→GCG)	16.5%	13.1%	12.5%			18.1%	10.5%	18.3%	10.4%	Polar transmembrane protein

Chl:796812	A1211A (GCA→GCG)	10.2%		11.0%							Polar transmembrane protein
Chl:796829	V1217A (GTC→GCC)	12.9%	13.5%		13.3%			15.0%		12.4%	Polar transmembrane protein
Chl:796836	S1219S (TCT→TCG)	19.5%	22.8%	14.0%	12.5%	10.6%	16.2%	15.5%		19.3%	Polar transmembrane protein
Chl:796865	T1229S (ACT→AGT)	14.8%	15.0%		10.7%						Polar transmembrane protein
Chl:796890	F1237F (TTC→TTT)	18.9%	16.3%		17.8%				10.4%	12.3%	Polar transmembrane protein
Chl:796891	P1238T (CCC→ACC)	20.4%	14.5%	21.4%	12.2%				13.8%		Polar transmembrane protein
Chl:796938	A1253A (GCT→GCC)		12.9%					10.6%		13.4%	Polar transmembrane protein
Chl:796972	A1265S (GCG→TCG)								14.7%		Polar transmembrane protein
Chl:797009	L1277P (CTC→CCC)							10.9%			Polar transmembrane protein
Chl:797017	K1280E (AAA→GAA)							11.4%			Polar transmembrane protein
Chl:797031	T1284T (ACT→ACC)		17.2%	15.7%		10.0%		10.7%	13.2%		Polar transmembrane protein
Chl:797202	T1341T (ACT→ACC)			10.7%							Polar transmembrane protein
Chl:811852	A721A (GCT→GCC)		11.0%		10.5%	12.5%		14.4%			electron transport complex RsxC
Chl:811858	T719T (ACT→ACA)	16.5%	16.0%					15.6%			electron transport complex RsxC
Chl:811924	A697A (GCG→GCC)								13.7%		electron transport complex RsxC
Chl:811927	A696A (GCT→GCC)					10.8%					electron transport complex RsxC
Chl:811951	A688A (GCT→GCA)	16.8%		17.7%							electron transport complex RsxC
Chl:812032	R661R (CGT→CGC)	15.3%									electron transport complex RsxC
Chl:812068	D649D (GAT→GAC)	12.6%						12.0%	14.4%		electron transport complex RsxC
Chl:962858	coding (242/738 nt)	16.7%	16.7%	16.9%	16.1%	10.9%	11.5%	18.9%		15.7%	ATP dependent Zn protease
Chl:962890	T70T (ACT→ACC)			17.9%		12.7%					ATP dependent Zn protease
Chl:980246	L559P (CTC→CCC)							11.8%			CydC
Chl:1009784	L62M (TTG→ATG)	34.0%	45.0%	37.0%	15.0%	25.7%	29.4%	20.5%	19.6%	22.7%	imidazolonepropionase
Chl:1009786	G61E (GGA→GAA)	36.6%	48.9%	46.3%	29.7%	28.8%	31.3%	20.2%	22.1%	24.4%	imidazolonepropionase
Chl:1009787	G61R (GGA→AGA)	36.4%	43.9%	42.3%	23.6%	20.1%	35.7%	19.6%	17.4%	28.2%	imidazolonepropionase
Chl:1009788	P60P (CCG→CCA)	42.4%	50.9%	50.6%	25.3%	27.9%	29.3%	21.2%	25.2%	32.0%	imidazolonepropionase
Chl:1009789	P60Q (CCG→CAG)	31.0%	37.4%	43.9%	15.6%	19.8%	26.7%		24.9%		imidazolonepropionase
Chl:1009790	P60T (CCG→ACG)	34.4%	47.2%	43.7%	25.3%	24.0%	24.4%	20.8%	18.0%	21.8%	imidazolonepropionase
Chl:1009792	T59K (ACA→AAA)	30.8%	44.2%	41.0%	16.1%	28.4%	34.1%	24.9%	20.5%	19.1%	imidazolonepropionase
Chl:1009794	V58V (GTC→GTG)	42.0%	49.9%	46.6%	28.8%	29.9%	36.9%	21.6%	23.6%	23.3%	imidazolonepropionase
Chl:1009796	V58F (GTC→TTC)	33.5%	48.2%	43.6%	30.3%	31.8%	30.7%	16.9%	19.7%	25.2%	imidazolonepropionase
Chl:1009797	L57F (TTA→TTC)	39.2%	52.2%	54.2%	28.2%	29.8%	38.5%	27.9%	25.9%	25.5%	imidazolonepropionase
Chl:1009798	L57* (TTA→TGA)	39.2%	37.0%	42.4%	23.7%	24.8%	34.9%	19.9%	24.7%	27.2%	imidazolonepropionase
Chl:1009800	K56N (AAA→AAC)	48.7%	53.1%	52.9%	25.4%	30.8%	44.1%	24.4%	31.9%	28.2%	imidazolonepropionase
Chl:1009801	K56I (AAA→ATA)	41.1%	51.9%	49.5%	27.1%	34.5%	36.2%	19.2%	26.1%	24.5%	imidazolonepropionase
Chl:1009802	K56* (AAA→TAA)	44.4%	53.6%	50.3%	23.6%	34.2%	37.9%	21.3%	25.8%	30.1%	imidazolonepropionase
Chl:1009804	G55V (GGC→GTC)	42.9%	45.3%	49.8%	23.2%	29.1%	30.7%	16.8%	25.3%	23.1%	imidazolonepropionase
Chl:1009810	C53Y (TGT→TAT)	51.4%	53.4%	59.3%	35.3%	42.6%	41.9%	31.0%	31.2%	35.1%	imidazolonepropionase
Chl:1207845	V447G (GTC→GGC)				12.7%			12.9%			molecular chaperone
Chl:1207853	R450C (CGC→TGC)	10.6%						10.4%	10.5%		molecular chaperone
Chl:1207903	intergenic (+45/ 80)			11.0%							molecular chaperone/lipoate ligase A
Chl:1282254	V1106G (GTG→GGG)						10.0%				rtxA
Chl:1282272	V1112G (GTA→GGA)							11.5%			rtxA
Chl:1295059	A68D (GCT→GAT)					100%				100%	XRE family transcriptional regulator
Chl:1295272	intergenic (+77/ 265)	49.2%	47.6%		50.0%	50.9%		44.7%	44.9%		XRE transcriptional regulator/lipoate ligase
Chl:1302195	intergenic (+76/ 265)	40.4%									XRE transcriptional regulator/lipoate ligase
Chl:1302195	intergenic (+76/ 265)						43.3%				XRE transcriptional regulator/lipoate ligase
Chl:1335141	intergenic (488/ 461)	10.3%				14.7%	12.1%				MarR regulator/hypothetical protein
Chl:1335146	intergenic (493/ 456)						14.0%	10.3%			MarR regulator/hypothetical protein
Chl:1361001	intergenic (312/+159)	22.9%	22.6%	20.0%	22.0%		20.0%	14.5%	21.3%	18.9%	phage terminase/hypothetical protein
Chl:1361005	intergenic (316/+155)	18.6%			13.7%		13.6%	14.6%		13.8%	phage terminase/hypothetical protein
Chl:1361010	intergenic (321/+150)	14.5%	15.7%	14.3%	18.9%	15.0%	19.9%	19.4%	19.5%	20.1%	phage terminase/hypothetical protein
Chl:1361012	intergenic (323/+148)	21.3%	28.5%	24.4%	24.1%	18.2%	19.7%	17.8%	31.7%	17.1%	phage terminase/hypothetical protein
Chl:1361014	intergenic (325/+146)	15.1%	16.9%			10.3%	11.2%	13.1%	12.3%		phage terminase/hypothetical protein
Chl:1361016	intergenic (327/+144)		21.2%	15.0%							phage terminase/hypothetical protein
Chl:1361019	intergenic (330/+141)	13.0%									phage terminase/hypothetical protein
Chl:1361033	intergenic (344/+127)	16.8%	12.5%						11.5%	11.1%	phage terminase/hypothetical protein
Chl:1361047	intergenic (358/+113)	18.4%	16.7%	13.5%	13.7%	15.2%	12.8%	12.0%	18.4%	12.9%	phage terminase/hypothetical protein
Chl:1361054	intergenic (365/+106)	23.4%	16.8%		19.7%	16.2%	14.5%	19.0%	20.5%	13.3%	phage terminase/hypothetical protein
Chl:1361058	intergenic (369/+102)	17.0%						11.1%		15.2%	phage terminase/hypothetical protein
Chl:1361064	intergenic (375/+96)	16.2%					12.3%	15.8%		13.9%	phage terminase/hypothetical protein
Chl:1361068	intergenic (379/+92)	10.1%					14.0%				phage terminase/hypothetical protein
Chl:1361086	intergenic (397/+74)	13.0%	11.0%		14.8%				13.5%		phage terminase/hypothetical protein
Chl:1361090	intergenic (401/+70)		11.2%				12.3%	10.6%	16.6%		phage terminase/hypothetical protein
Chl:1361101	intergenic (412/+59)									10.7%	phage terminase/hypothetical protein
Chl:1361105	intergenic (416/+55)			10.2%		12.4%		12.0%			phage terminase/hypothetical protein
Chl:1361115	intergenic (426/+45)		14.1%								phage terminase/hypothetical protein
Chl:1361140	intergenic (451/+20)		12.7%		10.5%						phage terminase/hypothetical protein
Chl:1361144	intergenic (455/+16)	13.4%	16.4%	13.0%	14.6%	11.2%	15.5%			10.8%	phage terminase/hypothetical protein
Chl:1461009	L238V (TTA→GTA)			13.5%							cytochrome ubiquinol oxidase subunit I
Chl:1461027	Q232* (CAG→TAG)	12.0%		11.3%	11.8%					11.2%	cytochrome ubiquinol oxidase subunit I
Chl:1469052	V65V (GTG→GTT)			11.9%							LysR family transcriptional regulator
Chl:1479319	G72G (GGA→GGG)			14.7%		11.9%					acetolactate synthase AlsS
Chl:1573197	S61F (TCT→TTT)			100%			100%			100%	ABC transporter permease
Chl:1719984	E292G (GAG→GGG)				11.8%						ATPase AAA
Chl:1738516	G189V (GGT→GTT)				16.0%		21.5%		14.5%		PTS fructose transporter subunit IIC
Chl:1738518	A190S (GCG→TCG)		20.1%	22.3%	27.0%	17.8%	17.3%	29.2%			PTS fructose transporter subunit IIC
Chl:1738519	A190V (GCG→GTG)	27.7%	29.5%	31.7%	28.4%	26.3%	37.9%	32.0%	23.9%	29.1%	PTS fructose transporter subunit IIC
Chl:1738520	A190A (GCG→GCT)	22.3%	26.2%	22.5%	26.2%	18.5%	24.5%	29.6%	18.9%		PTS fructose transporter subunit IIC

ChI:1738521	I191F (ATT→TTT)	32.2%	37.7%	33.9%	30.6%	28.5%	41.2%	42.9%	31.1%	30.1%	PTS fructose transporter subunit IIC
ChI:1738524	L192F (CTT→TTT)	31.8%	31.4%	26.5%	32.8%	28.6%	36.1%	34.0%	28.0%	23.6%	PTS fructose transporter subunit IIC
ChI:1738526	L192L (CTT→CTC)	28.5%	30.8%	30.3%	26.1%	26.5%	33.6%	34.4%	27.6%	23.8%	PTS fructose transporter subunit IIC
ChI:1738527	G193S (GGT→AGT)	22.9%	23.7%	26.2%	22.0%	19.3%	20.3%	24.5%	12.8%	12.4%	PTS fructose transporter subunit IIC
ChI:1738528	G193D (GGT→GAT)	11.9%	26.8%	25.3%	18.5%	15.0%	22.4%		17.2%	17.1%	PTS fructose transporter subunit IIC
ChI:1738529	G193G (GGT→GGG)	34.9%	37.9%	37.4%	32.8%	38.0%	35.8%	32.6%	32.4%	32.4%	PTS fructose transporter subunit IIC
ChI:1738530	G194R (GGT→CGT)	26.8%	31.2%	23.8%	22.3%	28.1%	28.8%	37.6%	22.5%	18.5%	PTS fructose transporter subunit IIC
ChI:1738531	G194D (GGT→GAT)	21.8%	19.4%	25.9%	22.8%	16.6%	20.9%	30.1%	21.4%	12.8%	PTS fructose transporter subunit IIC
ChI:1738532	G194G (GGT→GGG)	32.5%	34.8%	29.9%	30.1%	30.3%	37.4%	33.7%	33.0%	22.8%	PTS fructose transporter subunit IIC
ChI:1738534	M195K (ATG→AAG)	31.2%	35.5%	26.8%	30.8%	21.5%	37.8%	33.8%	21.2%	27.3%	PTS fructose transporter subunit IIC
ChI:1738543	F198Y (TTC→TAC)	37.7%	34.2%	32.9%	34.3%	32.3%	40.2%	39.7%	35.2%	35.2%	PTS fructose transporter subunit IIC
ChI:1738547	D199E (GAT→GAG)	31.3%	24.2%	29.2%	26.6%	25.4%	23.6%	26.7%	29.6%		PTS fructose transporter subunit IIC
ChI:1856353	V140G (GTG→GGG)									14.2%	ABC transporter permease
ChI:1906959	intergenic (+77/ 76)			10.7%							aminotransferase/5' deoxynucleotidase
ChI:1951003	I244L (ATC→CTC)			12.5%							beta ketoacyl ACP reductase
ChI:2067941	coding (1247 1257/1467 nt)						22.7%				σ 54 dependent transcriptional regulator
ChI:2068416	V261G (GTG→GGG)				29.5%	20.9%		63.3%	19.4%		σ 54 dependent transcriptional regulator
ChI:2068420	R260W (CGG→TGG)									12.3%	σ 54 dependent transcriptional regulator
ChI:2068530	G223D (GGC→GAC)									24.1%	σ 54 dependent transcriptional regulator
ChI:2068560	A213V (GCG→GTG)				16.7%	11.4%		29.2%			σ 54 dependent transcriptional regulator
ChI:2068586	S204R (AGT→AGA)						21.9%			46.6%	σ 54 dependent transcriptional regulator
ChI:2068596	L201W (TTG→TGG)					41.7%			74.3%		σ 54 dependent transcriptional regulator
ChI:2314339	F88F (TTT→TTC)						11.2%				glutamate synthase large subunit
ChI:2314341	L89H (CTC→CAC)				10.5%		10.7%				glutamate synthase large subunit
ChI:2314344	S90N (AGC→AAC)				10.6%						glutamate synthase large subunit
ChI:2314353	P93L (CCA→CTA)	10.7%			11.2%						glutamate synthase large subunit
ChI:2325554	G16G (GGA→GGG)								11.0%		hypothetical protein VC2384
ChI:2329775	intergenic (66/ 123)	14.1%				13.0%	12.0%			15.0%	hypothetical protein/hypothetical protein
ChI:2329785	intergenic (76/ 113)			12.9%							hypothetical protein/hypothetical protein
ChI:2329787	intergenic (78/ 111)			11.0%							hypothetical protein/hypothetical protein
ChI:2329790	intergenic (81/ 108)								11.1%		hypothetical protein/hypothetical protein
ChI:2329802	intergenic (93/ 96)	11.5%		14.4%		10.8%					hypothetical protein/hypothetical protein
ChI:2329804	intergenic (95/ 94)		12.6%	15.1%	14.8%				13.8%		hypothetical protein/hypothetical protein
ChI:2329815	intergenic (106/ 83)		10.1%	13.8%					19.9%		hypothetical protein/hypothetical protein
ChI:2329889	intergenic (180/ 9)		12.2%								hypothetical protein/hypothetical protein
ChI:2329893	intergenic (184/ 5)								10.2%		hypothetical protein/hypothetical protein
ChI:2440408	intergenic (306/+179)				10.2%						acetolactate synthase/CoA ligase
ChI:2440409	intergenic (307/+178)				10.7%						acetolactate synthase/CoA ligase
ChI:2440410	intergenic (308/+177)				11.1%						acetolactate synthase/CoA ligase
ChI:2440413	intergenic (311/+174)				11.6%						acetolactate synthase/CoA ligase
ChI:2440434	intergenic (332/+153)				12.1%						acetolactate synthase/CoA ligase
ChI:2440435	intergenic (333/+152)				10.8%						acetolactate synthase/CoA ligase
ChI:2440436	intergenic (334/+151)				10.1%						acetolactate synthase/CoA ligase
ChI:2440440	intergenic (338/+147)				15.6%			10.7%			acetolactate synthase/CoA ligase
ChI:2492693	D272G (GAT→GGT)	10.4%									magnesium transporter
ChI:2564137	S10G (AGT→GGT)					13.1%			11.8%	10.1%	Asp aminotransferase family protein
ChI:2564312	intergenic (148/+250)	12.1%	13.6%	15.0%	13.5%	13.1%					Asp aminotransferase/deoxychorismate
ChI:2564313	intergenic (149/+249)				11.8%						Asp aminotransferase/deoxychorismate
ChI:2564316	intergenic (152/+246)		10.8%	13.2%			11.2%				Asp aminotransferase/deoxychorismate
ChI:2564321	intergenic (157/+241)			11.8%	11.6%					10.1%	Asp aminotransferase/deoxychorismate
ChI:2646776	pseudogene (2113/3599 nt)		10.1%								DUF3372 domain containing protein
ChI:2699564	V224V (GTG→GTT)					12.1%			10.6%		nitrogen regulation protein NR(I)
ChI:2731231	I59F (ATT→TTT)			10.6%						12.3%	hypothetical protein, VC0143
ChI:2773757	L508P (CTC→CCC)			10.9%							glycerol 3 phosphate 1 O acyltransferase
ChI:2912738	S213P (TCA→CCA)		13.2%								CoaC/CoaB
ChI:2954216	E234G (GAG→GGG)		11.5%								2 dehydropantoate 2 reductase
ChI:2965511	T267A (ACT→GCT)		10.3%								nickel ABC transporter
ChI:2965514	F266V (TTC→GTC)		12.2%								nickel ABC transporter
ChI:2969248	intergenic (36/+26)		16.5%								tRNA Pro/tRNA His
ChI:2983998	noncoding (43/76 nt)	43.1%			30.0%		62.3%				tRNA Val
ChII:108234	L357L (CTT→CTA)							10.4%			EAL domain containing protein
ChII:286269	E607G (GAG→GGG)		10.3%								methyl accepting chemotaxis protein
ChII:445274	A54E (GCA→GAA)			10.1%							1 phosphofructokinase
ChII:458584	intergenic (115/ 352)			11.7%							H(+)/Cl( )transporter/GTP binding protein
ChII:458603	intergenic (134/ 333)	11.2%				12.0%			10.4%	12.0%	H(+)/Cl( )transporter/GTP binding protein
ChII:458604	intergenic (135/ 332)			12.2%		13.8%			10.7%	11.5%	H(+)/Cl( )transporter/GTP binding protein

Supplementary Data 2. Mutations detected in non-adapted populations.

chromosome: position	annotation	Day 3			Day 45			Day 90			description
		P1	P2	P3	P1	P2	P3	P1	P2	P3	
Chl:16981	G236G (GGT→GGG)						13.9%				threonine ammonia lyase, biosynthetic
Chl:17087	E201G (GAG→GGG)			13.5%							threonine ammonia lyase, biosynthetic
Chl:85253	intergenic (+24/ 11)		13.8%				12.4%				tRNA Met/tRNA Gly
Chl:85592	noncoding (67/77 nt)	17.2%	14.4%			20.0%	18.6%		13.2%	24.1%	tRNA Met
Chl:85696	noncoding (52/77 nt)	17.8%	14.0%	20.3%	13.6%		21.5%	17.6%	16.5%	15.1%	tRNA Met
Chl:85730	intergenic (+9/ 34)								13.6%		tRNA Met/tRNA Met
Chl:126127	noncoding (1550/1553 nt)	50.1%	44.9%	37.0%	36.2%	35.4%	37.3%	50.5%	25.4%	42.3%	16S ribosomal RNA
Chl:126174	intergenic (+44/ 10)								32.5%		16S ribosomal RNA/tRNA Ile
Chl:131976	noncoding (43/76 nt)	46.5%	39.7%	51.8%		38.3%	30.8%		37.7%	42.9%	tRNA Val
Chl:293234	coding (311/1008 nt)						14.8%				RNA polymerase sigma factor RpoS
Chl:293235	coding (312/1008 nt)					16.8%					RNA polymerase sigma factor RpoS
Chl:309274	intergenic (+22/ 12)				17.4%						tRNA Ser/tRNA Arg
Chl:309374	intergenic (+12/ 11)						10.0%			11.2%	tRNA Arg/tRNA Ser
Chl:309612	noncoding (69/77 nt)			11.5%							tRNA Arg
Chl:309687	noncoding (12/77 nt)						16.9%		16.9%		tRNA Arg
Chl:309796	intergenic (+44/ 29)					15.9%			19.1%		tRNA Arg/tRNA Arg
Chl:309820	intergenic (+68/ 5)						17.6%		21.4%		tRNA Arg/tRNA Arg
Chl:309836	noncoding (12/77 nt)		19.0%								tRNA Arg
Chl:310027	noncoding (70/77 nt)	10.9%									tRNA Arg
Chl:379609	intergenic (32/+25)		10.5%	12.1%						11.2%	chitobiase/ABC transporter
Chl:547560	S148P (TCA→CCA)						12.4%			13.0%	exodeoxyribonuclease VII large subunit
Chl:575578	A200V (GCT→GTT)				10.7%		10.5%	12.4%			sensor histidine kinase citA
Chl:575594	L195F (CTT→TTT)	12.8%									sensor histidine kinase citA
Chl:575606	L191F (CTT→TTT)	11.5%		11.9%		11.2%					sensor histidine kinase citA
Chl:575621	I186F (ATT→TTT)	10.0%								11.9%	sensor histidine kinase citA
Chl:575642	R179G (CGG→GGG)							12.4%			sensor histidine kinase citA
Chl:575719	A153G (GCG→GGG)									11.2%	sensor histidine kinase citA
Chl:679969	F32C (TTC→TGC)							10.3%			flagellar motor protein MotB
Chl:680440	I189S (ATC→AGC)									31.7%	flagellar motor protein MotB
Chl:680550	coding (676/957 nt)				16.9%						flagellar motor protein MotB
Chl:694022	N58K (AAT→AAA)				11.5%	10.1%		11.0%			MetQ
Chl:694050	A49G (GCG→GGG)						13.0%				MetQ
Chl:694071	E42G (GAA→GGA)						13.0%		10.9%		MetQ
Chl:694076	G40G (GGT→GGG)		10.2%								MetQ
Chl:696093	intergenic (160/ 76)									10.3%	MetN/phosphatase
Chl:701454	intergenic (6/+79)			11.9%				12.6%	11.0%	12.5%	tRNA Tyr/tRNA Tyr
Chl:701700	intergenic (83/+2)								16.6%		tRNA Tyr/tRNA Tyr
Chl:701863	intergenic (77/+9)	15.9%									tRNA Tyr/tRNA Tyr
Chl:701863	intergenic (77/+9)									14.2%	tRNA Tyr/tRNA Tyr
Chl:702450	V70G (GTG→GGG)						11.4%				MexH family multidrug efflux transporter
Chl:702475	N78K (AAT→AAA)	10.1%					10.9%			12.7%	MexH family multidrug efflux transporter
Chl:702524	A95T (GCT→ACT)		13.1%			10.5%					MexH family multidrug efflux transporter
Chl:789945	F140F (TTC→TTT)			10.2%							PTS N acetylmuramic acid transporter
Chl:789976	I151F (ATC→TTC)	10.2%									PTS N acetylmuramic acid transporter
Chl:789999	G158G (GGA→GGG)	12.8%		10.6%	11.5%			11.4%			PTS N acetylmuramic acid transporter
Chl:796023	D948E (GAT→GAG)						12.3%	11.6%			Polar transmembrane protein
Chl:796155	E992E (GAA→GAG)	11.0%								12.7%	Polar transmembrane protein
Chl:796167	D996E (GAT→GAG)	16.4%	15.1%	10.3%							Polar transmembrane protein
Chl:796213	K1012E (AAG→GAG)	11.8%			10.4%					11.5%	Polar transmembrane protein
Chl:796260	A1027A (GCA→GCG)			10.4%							Polar transmembrane protein
Chl:796270	S1031P (TCC→CCC)			11.2%	13.1%						Polar transmembrane protein
Chl:796276	T1033A (ACA→GCA)			12.7%							Polar transmembrane protein
Chl:796371	Y1064Y (TAT→TAC)						10.6%		12.4%	11.2%	Polar transmembrane protein
Chl:796374	T1065T (ACA→ACC)			10.0%					12.9%		Polar transmembrane protein
Chl:796383	D1068D (GAC→GAT)					10.7%				13.9%	Polar transmembrane protein
Chl:796410	P1077P (CCC→CCT)					11.9%					Polar transmembrane protein
Chl:796416	A1079A (GCC→GCA)			12.5%							Polar transmembrane protein
Chl:796444	L1089L (TTA→CTA)	11.6%		13.1%			17.7%				Polar transmembrane protein
Chl:796448	V1090A (GTA→GCA)		10.5%				11.0%				Polar transmembrane protein
Chl:796460	V1094A (GTC→GCC)			14.6%	13.4%		11.5%	14.3%			Polar transmembrane protein
Chl:796462	T1095A (ACG→GCG)		15.6%	10.3%	11.1%		14.3%	13.3%		13.7%	Polar transmembrane protein
Chl:796467	E1096E (GAG→GAA)		17.2%	15.6%	15.5%		14.2%		10.7%	11.6%	Polar transmembrane protein
Chl:796491	E1104E (GAA→GAG)			11.3%	18.2%	12.3%	13.1%	11.9%		10.4%	Polar transmembrane protein
Chl:796548	P1123P (CCT→CCC)				11.0%						Polar transmembrane protein
Chl:796553	V1125A (GTA→GCA)				12.9%			13.3%	10.6%	14.6%	Polar transmembrane protein
Chl:796584	L1135L (CTA→CTG)		11.5%		12.4%	13.1%	13.3%	11.8%		11.0%	Polar transmembrane protein
Chl:796596	P1139P (CCT→CCA)							17.0%	12.9%	12.9%	Polar transmembrane protein
Chl:796596	P1139P (CCT→CCC)						14.5%				Polar transmembrane protein
Chl:796613	S1145F (TCT→TTT)			12.8%		19.6%	14.7%	14.1%	18.0%	12.7%	Polar transmembrane protein

Chl:796624	N1149D (AAT→GAT)						12.0%				Polar transmembrane protein
Chl:796632	L1151L (CTT→CTC)	10.1%	14.5%				18.8%	12.6%	11.4%		Polar transmembrane protein
Chl:796641	P1154P (CCC→CCT)	10.0%	13.1%		11.7%		10.0%	10.6%	10.1%		Polar transmembrane protein
Chl:796708	S1177P (TCC→CCC)						12.8%			12.0%	Polar transmembrane protein
Chl:796710	S1177S (TCC→TCA)					18.7%	15.8%				Polar transmembrane protein
Chl:796728	S1183S (AGC→AGT)										Polar transmembrane protein
Chl:796733	L1185P (CTC→CCC)	10.0%		10.1%		14.1%	12.1%		16.7%		Polar transmembrane protein
Chl:796747	P1190A (CCC→GCC)				10.9%		13.8%			11.1%	Polar transmembrane protein
Chl:796800	A1207A (GCT→GCC)						10.3%				Polar transmembrane protein
Chl:796806	A1209A (GCA→GCG)			10.6%			18.4%			12.1%	Polar transmembrane protein
Chl:796812	A1211A (GCA→GCG)			11.0%			12.0%	12.4%			Polar transmembrane protein
Chl:796829	V1217A (GTC→GCC)		13.6%	12.0%	10.9%	10.6%	22.3%	14.8%		15.5%	Polar transmembrane protein
Chl:796836	S1219S (TCT→TCG)	13.2%		19.0%	17.3%	14.2%	13.9%	15.0%	16.9%		Polar transmembrane protein
Chl:796865	T1229S (ACT→AGT)	13.0%		11.8%	13.3%	11.5%	19.6%		15.1%	13.1%	Polar transmembrane protein
Chl:796875	A1232A (GCC→GCA)		11.0%								Polar transmembrane protein
Chl:796890	F1237F (TTC→TTT)	19.0%	13.4%	12.5%	12.0%	12.7%	13.2%			15.4%	Polar transmembrane protein
Chl:796891	P1238T (CCC→ACC)	10.8%	14.1%		18.2%				16.3%		Polar transmembrane protein
Chl:796938	A1253A (GCT→GCC)				10.9%	10.2%					Polar transmembrane protein
Chl:797017	K1280E (AAA→GAA)				11.1%						Polar transmembrane protein
Chl:797031	T1284T (ACT→ACC)	11.1%				11.0%		11.4%	10.8%		Polar transmembrane protein
Chl:797112	S1311S (TCA→TCG)							11.0%			Polar transmembrane protein
Chl:797132	E1318G (GAG→GGG)		12.7%								Polar transmembrane protein
Chl:811732	A761A (GCT→GCC)							11.5%			electron transport complex subunit RsxC
Chl:811747	A756A (GCT→GCC)	10.3%								13.5%	electron transport complex subunit RsxC
Chl:811858	T719T (ACT→ACA)					10.8%					electron transport complex subunit RsxC
Chl:811867	A716A (GCT→GCC)			12.1%							electron transport complex subunit RsxC
Chl:811924	A697A (GCG→GCC)						10.9%	10.4%	15.3%		electron transport complex subunit RsxC
Chl:811927	A696A (GCT→GCC)	12.6%	10.7%				10.0%		14.9%		electron transport complex subunit RsxC
Chl:811951	A688A (GCT→GCA)						11.7%				electron transport complex subunit RsxC
Chl:812068	D649D (GAT→GAC)	12.6%				13.4%	11.7%	12.2%			electron transport complex subunit RsxC
Chl:962856	A82P (GCC→CCC)							12.1%			ATP dependent Zn protease
Chl:962858	coding (242/738 nt)	16.9%	14.9%	10.3%			14.3%	14.3%	10.5%		ATP dependent Zn protease
Chl:962890	T70T (ACT→ACC)					21.8%					ATP dependent Zn protease
Chl:962900	E67G (GAG→GGG)	17.0%									ATP dependent Zn protease
Chl:1009784	L62M (TTG→ATG)		27.9%	28.9%	25.1%	27.9%	23.0%	20.9%	23.1%	24.8%	imidazolonepropionase
Chl:1009786	G61E (GGA→GAA)	24.4%	30.1%	31.1%	30.3%	32.8%	29.3%	23.8%	36.6%	26.9%	imidazolonepropionase
Chl:1009787	G61R (GGA→AGA)	22.6%	30.8%	29.7%	30.3%	33.7%	23.4%	28.7%	27.7%	20.0%	imidazolonepropionase
Chl:1009788	P60P (CCG→CCA)	17.8%	23.8%	29.2%	32.4%	32.0%	28.7%	26.6%	27.7%	25.5%	imidazolonepropionase
Chl:1009789	P60Q (CCG→CAG)	17.1%	26.3%	22.6%	31.6%	25.5%	23.2%	16.0%	20.7%	17.5%	imidazolonepropionase
Chl:1009790	P60T (CCG→ACG)	24.0%	27.8%	22.8%	26.0%	30.7%	25.8%	26.0%	23.5%	23.2%	imidazolonepropionase
Chl:1009792	T59K (ACA→AAA)	22.0%	23.9%	22.2%	34.5%	23.2%	19.5%	16.6%		28.8%	imidazolonepropionase
Chl:1009794	V58V (GTC→GTG)	21.1%	32.4%	29.6%	31.4%	32.7%	31.0%	26.4%	31.7%	28.8%	imidazolonepropionase
Chl:1009796	V58F (GTC→TTC)	21.4%	34.4%	29.3%	34.9%	39.5%	27.6%	26.0%	36.4%	27.6%	imidazolonepropionase
Chl:1009797	L57F (TTA→TTC)	28.2%	40.7%	40.1%	40.9%	40.7%	33.6%	24.1%	36.7%	38.5%	imidazolonepropionase
Chl:1009798	L57* (TTA→TGA)	22.0%	31.9%	31.2%	40.4%	33.4%	30.3%	27.1%	25.0%	25.4%	imidazolonepropionase
Chl:1009800	K56N (AAA→AAC)	26.1%	38.2%	37.3%	46.0%	38.7%	36.7%	31.7%	37.6%	30.4%	imidazolonepropionase
Chl:1009801	K56I (AAA→ATA)	24.8%	29.8%	33.8%	41.9%	39.1%	34.9%	25.9%	36.0%	31.6%	imidazolonepropionase
Chl:1009802	K56* (AAA→TAA)	25.6%	38.2%	33.0%	38.8%	32.7%	34.6%	33.4%	38.2%	27.2%	imidazolonepropionase
Chl:1009804	G55V (GGC→GTC)	27.3%	30.2%	30.1%	36.9%	32.5%	33.7%	27.4%	28.8%	25.5%	imidazolonepropionase
Chl:1009810	C53Y (TGT→TAT)	31.1%	41.4%	39.0%	55.8%	45.6%	38.9%	43.4%	49.9%	36.0%	imidazolonepropionase
Chl:1022424	intergenic (+3/ 8)				11.8%						tRNA Leu/tRNA Gly
Chl:1207845	V447G (GTC→GGC)			11.4%							molecular chaperone
Chl:1207853	R450C (CGC→TGC)			13.3%	10.8%			10.3%	18.4%		molecular chaperone
Chl:1207858	*451W (TGA→TGG)				11.3%						molecular chaperone
Chl:1207866	intergenic (+8/ 117)			12.8%	10.4%						molecular chaperone/protein ligase A
Chl:1207890	intergenic (+32/ 93)				10.4%						molecular chaperone/protein ligase A
Chl:1207903	intergenic (+45/ 80)			10.8%							molecular chaperone/protein ligase A
Chl:1282254	V1106G (GTG→GGG)		12.4%								multifunctional autoprocessing toxin RtxA
Chl:1282272	V1112G (GTA→GGA)						12.3%			10.0%	multifunctional autoprocessing toxin RtxA
Chl:1290281	G3782S (GGT→AGT)				10.6%	10.4%					multifunctional autoprocessing toxin RtxA
Chl:1290282	G3782D (GGT→GAT)				10.0%						multifunctional autoprocessing toxin RtxA
Chl:1290284	A3783T (GCG→ACG)				10.0%						multifunctional autoprocessing toxin RtxA
Chl:1295059	A68D (GCT→GAT)	100%									XRE family transcriptional regulator
Chl:1295272	intergenic (+77/ 265)	39.3%	100%			47.5%	100%	42.3%	100%		XRE transcriptional regulator/protein ligase
Chl:1302195	intergenic (+76/ 265)		80.3%	51.5%	49.0%		79.1%		79.1%	55.1%	XRE transcriptional regulator/protein ligase
Chl:1335141	intergenic (488/ 461)								10.0%		MarR regulator/hypothetical protein
Chl:1335146	intergenic (493/ 456)			10.2%							MarR regulator/hypothetical protein
Chl:1361001	intergenic (312/+159)	22.2%	18.5%	15.5%	18.2%	17.3%	16.5%	24.3%	18.8%	17.7%	phage terminase/hypothetical protein
Chl:1361002	intergenic (313/+158)			12.5%			12.4%	13.6%			phage terminase/hypothetical protein
Chl:1361005	intergenic (316/+155)	12.6%		10.7%	16.9%		14.4%	12.8%	13.4%		phage terminase/hypothetical protein
Chl:1361010	intergenic (321/+150)	13.7%	14.6%	12.9%	26.0%	18.3%	16.5%	23.8%	18.8%	15.8%	phage terminase/hypothetical protein
Chl:1361012	intergenic (323/+148)	23.1%	18.1%	20.2%	13.6%	21.1%	21.7%	21.5%	22.6%	19.4%	phage terminase/hypothetical protein
Chl:1361014	intergenic (325/+146)	14.2%	14.8%	13.1%	16.6%	14.0%	13.9%		13.6%		phage terminase/hypothetical protein
Chl:1361016	intergenic (327/+144)	13.3%		13.0%			14.3%		12.5%		phage terminase/hypothetical protein
Chl:1361019	intergenic (330/+141)	12.3%									phage terminase/hypothetical protein
Chl:1361033	intergenic (344/+127)								10.0%		phage terminase/hypothetical protein
Chl:1361047	intergenic (358/+113)	15.6%	12.6%	13.4%	12.4%	10.8%	15.1%	18.7%	18.0%	13.4%	phage terminase/hypothetical protein
Chl:1361054	intergenic (365/+106)	14.3%	14.0%		15.9%	15.5%	20.0%	17.3%	21.5%	14.2%	phage terminase/hypothetical protein
Chl:1361058	intergenic (369/+102)	11.4%			12.3%	10.4%		12.7%	13.2%		phage terminase/hypothetical protein

Chl:1361058	intergenic (369/+102)			12.4%							phage terminase/hypothetical protein
Chl:1361064	intergenic (375/+96)								13.9%		phage terminase/hypothetical protein
Chl:1361068	intergenic (379/+92)	11.4%		10.4%	11.1%						phage terminase/hypothetical protein
Chl:1361086	intergenic (397/+74)	10.5%	11.8%					11.5%			phage terminase/hypothetical protein
Chl:1361090	intergenic (401/+70)	11.0%		11.8%				13.5%	12.3%	11.9%	phage terminase/hypothetical protein
Chl:1361092	intergenic (403/+68)	10.2%									phage terminase/hypothetical protein
Chl:1361101	intergenic (412/+59)	10.2%									phage terminase/hypothetical protein
Chl:1361105	intergenic (416/+55)	11.1%			10.1%			12.1%	13.6%		phage terminase/hypothetical protein
Chl:1361115	intergenic (426/+45)	11.6%			11.8%			11.8%	11.0%		phage terminase/hypothetical protein
Chl:1361144	intergenic (455/+16)	15.0%		14.6%	13.6%		11.3%	15.3%	11.1%		phage terminase/hypothetical protein
Chl:1361157	intergenic (468/+3)	10.2%									phage terminase/hypothetical protein
Chl:1375934	C98F (TGC→TTC)									11.1%	resolvase
Chl:1461020	L234S (TTG→TCG)	12.4%									cytochrome ubiquinol oxidase subunit I
Chl:1461027	Q232* (CAG→TAG)	12.0%	10.8%		12.4%	10.1%	13.7%		10.2%	10.6%	cytochrome ubiquinol oxidase subunit I
Chl:1469052	V65V (GTG→GTT)							11.6%			LysR family transcriptional regulator
Chl:1531058	K140N (AAA→AAC)					10.8%					ABC transporter permease
Chl:1573197	S61F (TCT→TTT)			100%			100%			100%	ABC transporter permease
Chl:1619916	L584P (CTC→CCC)				10.9%						PAS domain S box protein
Chl:1719984	E292G (GAG→GGG)		10.9%	10.4%		10.3%		11.7%			ATPase AAA
Chl:1738516	G189V (GGT→GTT)				18.8%	15.1%		18.3%			PTS fructose transporter subunit IIC
Chl:1738518	A190S (GCG→TCG)				20.4%	16.6%		20.7%			PTS fructose transporter subunit IIC
Chl:1738519	A190V (GCG→GTG)	21.3%	28.8%	22.9%	26.4%	28.4%	24.9%	26.8%	30.7%	26.7%	PTS fructose transporter subunit IIC
Chl:1738520	A190A (GCG→GCT)	16.5%	17.1%	10.6%	24.0%	22.9%	14.5%	22.3%	19.4%	15.4%	PTS fructose transporter subunit IIC
Chl:1738521	I191F (ATT→TTT)	21.9%	25.8%	23.4%	28.9%	30.6%	29.9%	32.7%	37.4%	28.8%	PTS fructose transporter subunit IIC
Chl:1738524	L192F (CTT→TTT)	26.4%	25.5%	19.4%	29.2%	26.7%	30.4%	29.0%	32.6%	31.3%	PTS fructose transporter subunit IIC
Chl:1738526	L192L (CTT→CTC)	23.3%	27.7%	17.6%	31.3%	29.6%	29.2%	31.6%	28.0%	25.7%	PTS fructose transporter subunit IIC
Chl:1738527	G193S (GGT→AGT)	15.8%	15.9%	12.7%	23.9%	17.3%	18.5%	19.1%	26.6%	26.5%	PTS fructose transporter subunit IIC
Chl:1738528	G193D (GGT→GAT)	11.2%	12.5%	15.1%	24.0%	17.8%	20.2%	21.9%	13.9%	22.3%	PTS fructose transporter subunit IIC
Chl:1738529	G193G (GGT→GGG)	29.3%	26.5%	25.0%	35.0%	30.1%	34.8%	33.2%	35.3%	32.5%	PTS fructose transporter subunit IIC
Chl:1738530	G194R (GGT→CGT)	21.4%	30.4%	15.8%	26.1%	26.9%	22.9%	19.1%	29.5%	20.6%	PTS fructose transporter subunit IIC
Chl:1738531	G194D (GGT→GAT)	17.6%	20.3%	14.3%	18.9%	22.6%	21.9%	14.6%	24.4%	16.5%	PTS fructose transporter subunit IIC
Chl:1738532	G194G (GGT→GGG)	32.2%	30.9%	24.2%	32.5%	26.3%	30.2%	32.6%	32.3%	29.7%	PTS fructose transporter subunit IIC
Chl:1738534	M195K (ATG→AAG)	27.2%	27.5%	22.3%	29.5%	25.5%	28.9%	32.2%	36.7%	32.2%	PTS fructose transporter subunit IIC
Chl:1738543	F198Y (TTC→TAC)	33.2%	33.1%	22.7%	34.2%	34.8%	32.2%	27.8%	36.2%	36.9%	PTS fructose transporter subunit IIC
Chl:1738547	D199E (GAT→GAG)	25.7%	27.3%	16.7%	19.9%	24.2%	18.3%	18.6%	27.6%		PTS fructose transporter subunit IIC
Chl:2082608	G71G (GGC→GGA)						13.2%				BamC
Chl:2106203	G83G (GGA→GGG)									12.7%	redox regulated ATPase YchF
Chl:2314325	I84F (ATT→TTT)			10.7%							glutamate synthase large subunit
Chl:2329775	intergenic (66/ 123)			12.6%	14.9%	16.6%		11.7%	14.9%		hypothetical protein/hypothetical protein
Chl:2329802	intergenic (93/ 96)								11.2%		hypothetical protein/hypothetical protein
Chl:2329804	intergenic (95/ 94)	16.3%	11.9%	10.7%	13.1%		12.1%				hypothetical protein/hypothetical protein
Chl:2329815	intergenic (106/ 83)		11.9%				10.7%				hypothetical protein/hypothetical protein
Chl:2440413	intergenic (311/+174)							10.4%			acetolactate synthase /CoA ligase
Chl:2440440	intergenic (338/+147)		10.1%					15.0%			acetolactate synthase /CoA ligase
Chl:2,547,193:1	coding (375/636 nt)					11.8%			43.5%		Sodium type flagellar protein motX
Chl:2564127	D13G (GAT→GGT)						11.7%				aspartate aminotransferase
Chl:2564137	S10G (AGT→GGT)					12.2%		10.0%			aspartate aminotransferase
Chl:2564312	intergenic (148/+250)		15.4%	12.8%	11.9%	14.5%	12.9%	17.6%	14.4%		asp aminotransferase/anthranilate synthase
Chl:2564313	intergenic (149/+249)		11.4%			11.2%		12.4%			asp aminotransferase/anthranilate synthase
Chl:2564315	intergenic (151/+247)							17.1%			asp aminotransferase/anthranilate synthase
Chl:2564316	intergenic (152/+246)		10.8%					16.5%		11.8%	asp aminotransferase/anthranilate synthase
Chl:2564319	intergenic (155/+243)							10.8%			asp aminotransferase/anthranilate synthase
Chl:2564321	intergenic (157/+241)							11.3%			asp aminotransferase/anthranilate synthase
Chl:2564323	intergenic (159/+239)		11.1%					12.1%	10.0%		asp aminotransferase/anthranilate synthase
Chl:2646776	pseudogene (2113/3599 nt)			10.4%							DUF3372 domain containing protein
Chl:2699564	V224V (GTG→GTT)	10.6%					11.7%		14.1%	12.1%	nitrogen regulation protein NR(I)
Chl:2731231	I59F (ATT→TTT)		13.8%								hypothetical protein, VC0143
Chl:2965510	T267S (ACT→AGT)									12.5%	ABC transporter substrate binding protein
Chl:2965511	T267A (ACT→GCT)									15.6%	ABC transporter substrate binding protein
Chl:2965514	F266V (TTC→GTC)									11.2%	ABC transporter substrate binding protein
Chl:2969114	intergenic (49/+22)						13.5%				tRNA His/tRNA Pro
Chl:2969235	intergenic (23/+39)	10.3%									tRNA Pro/tRNA His
Chl:2969248	intergenic (36/+26)				11.6%		12.6%			10.9%	tRNA Pro/tRNA His
Chl:2983998	noncoding (43/76 nt)	45.7%		30.2%					61.6%		tRNA Val
Chll:187313	A443E (GCA→GAA)							10.8%			VWA domain containing protein
Chll:286269	E607G (GAG→GGG)	11.2%	13.4%		16.1%	11.3%					methyl accepting chemotaxis protein
Chll:445274	A54E (GCA→GAA)			13.4%							1 phosphofructokinase
Chll:458584	intergenic (115/ 352)									11.5%	H(+)/Cl( )transporter/GTP binding protein
Chll:458603	intergenic (134/ 333)		11.6%				14.2%			10.9%	H(+)/Cl( )transporter/GTP binding protein
Chll:458604	intergenic (135/ 332)	11.6%					12.4%			11.8%	H(+)/Cl( )transporter/GTP binding protein
Chll:610081	A7S (GCG→TCG)	11.5%									periplasmic nitrate reductase

Supplementary Data 3. Mutations detected in adapted isolates.

chromosome: position	annotation	Day 3			Day 45			Day 90			description
		D3A1	D3A2	D3A3	D45A1	D45A2	D45A3	D90A1	D90A2	D90A3	
Ch I:85696	noncoding (52/77 nt)	20.9%			11.8%		12.8%		28.0%	15.6%	tRNA Met
Ch I:85708	noncoding (64/77 nt)				11.7%					14.5%	tRNA Met
Ch I:309548	noncoding (5/77 nt)								11.5%		tRNA Arg
Ch I:526198	E101G (GAG→GGG)							10.4%			protein translocase subunit SecF
Ch I:563402	E246G (GAG→GGG)		10.4%								Fe(3+) siderophore ABC transporter permease
Ch I:701773	noncoding (14/85 nt)	16.2%									tRNA Tyr
Ch I:796023	D948E (GAT→GAG)							11.3%			Polar transmembrane protein
Ch I:796276	T1033A (ACA→GCA)		10.9%								Polar transmembrane protein
Ch I:796374	T1065T (ACA→ACC)	18.0%									Polar transmembrane protein
Ch I:796416	A1079A (GCC→GCA)				11.7%		11.1%				Polar transmembrane protein
Ch I:796444	L1089L (TTA→CTA)		12.0%								Polar transmembrane protein
Ch I:796460	V1094A (GTC→GCC)		13.7%				11.5%				Polar transmembrane protein
Ch I:796467	E1096E (GAG→GAA)		15.0%	13.6%					14.8%		Polar transmembrane protein
Ch I:796491	E1104E (GAA→GAG)			12.6%							Polar transmembrane protein
Ch I:796553	V1125A (GTA→GCA)			10.8%							Polar transmembrane protein
Ch I:796584	L1135L (CTA→CTG)	13.3%									Polar transmembrane protein
Ch I:796596	P1139P (CCT→CCA)						11.1%	15.2%	14.7%		Polar transmembrane protein
Ch I:796613	S1145F (TCT→TTT)	13.5%						11.2%		14.6%	Polar transmembrane protein
Ch I:796641	P1154P (CCC→CCT)			11.9%				11.1%	13.5%		Polar transmembrane protein
Ch I:796733	L1185P (CTC→CCC)	15.8%									Polar transmembrane protein
Ch I:796829	V1217A (GTC→GCC)										Polar transmembrane protein
Ch I:796836	S1219S (TCT→TCG)						14.5%			11.2%	Polar transmembrane protein
Ch I:796865	T1229S (ACT→AGT)								13.6%		Polar transmembrane protein
Ch I:796890	F1237F (TTC→TTT)			10.7%				11.0%			Polar transmembrane protein
Ch I:796891	P1238T (CCC→ACC)	10.0%		11.5%				10.0%			Polar transmembrane protein
Ch I:811852	A721A (GCT→GCC)			22.4%						13.4%	electron transport complex subunit RsxC
Ch I:811924	A697A (GCG→GCC)					10.3%					electron transport complex subunit RsxC
Ch I:1009789	P60Q (CCG→CAG)									21.1%	imidazolonepropionase
Ch I:1009790	P60T (CCG→ACG)				25.8%						imidazolonepropionase
Ch I:1009792	T59K (ACA→AAA)									19.8%	imidazolonepropionase
Ch I:1295059	A68D (GCT→GAT)	100%		100%						100%	XRE family transcriptional regulator
Ch I:1295272	intergenic (+77/ 265)		100%		100%	100%	41.0%		44.6%	42.3%	XRE transcriptional regulator/protein ligase
Ch I:1302195	intergenic (+76/ 265)		77.2%		80.9%	79.8%		54.3%			XRE transcriptional regulator/protein ligase
Ch I:1335141	intergenic (488/ 461)	12.2%									MarR regulator/hypothetical protein
Ch I:1335146	intergenic (493/ 456)				10.6%						MarR regulator/hypothetical protein
Ch I:1361001	intergenic (312/+159)	27.4%			15.2%	17.0%			18.4%		phage terminase/hypothetical protein
Ch I:1361033	intergenic (344/+127)						10.0%	10.3%			phage terminase/hypothetical protein
Ch I:1361074	intergenic (385/+86)	11.5%									phage terminase/hypothetical protein
Ch I:1738518	A190S (GCG→TCG)				18.2%						PTS fructose transporter subunit IIC
Ch I:1738521	I191F (ATT→TTT)					22.6%			25.6%		PTS fructose transporter subunit IIC
Ch I:1738526	L192L (CTT→CTC)				28.8%	22.2%					PTS fructose transporter subunit IIC
Ch I:1738532	G194G (GGT→GGG)					26.5%				15.3%	PTS fructose transporter subunit IIC
Ch I:1738543	F198Y (TTC→TAC)									24.4%	PTS fructose transporter subunit IIC
Ch I:1738547	D199E (GAT→GAG)		13.0%		15.3%	22.3%			14.5%	12.2%	PTS fructose transporter subunit IIC
Ch I:1951003	I244L (ATC→CTC)			15.4%						10.0%	beta ketoacyl ACP reductase
Ch I:2068416	V261G (GTG→GGG)				100%			100%			σ 54 dependent family transcriptional regulator
Ch I:2068560	A213V (GCG→GTG)					74.8%	100%		100%	100%	σ 54 dependent family transcriptional regulator
Ch I:2329804	intergenic (95/ 94)							17.4%		16.2%	hypothetical protein/hypothetical protein
Ch II:303353	coding (1013/1206 nt)					23.6%					hypothetical protein

Supplementary Data 4. Mutations detected in non-adapted isolates.

chromosome: position	annotation	Day 3			Day 45			Day 90			description
		D3NA1	D3NA2	D3NA3	D45NA1	D45NA2	D45NA3	D90NA1	D90NA2	D90NA3	
Ch I:84732	noncoding (37/76 nt)					14.5%					tRNA-Gly
Ch I:85696	noncoding (52/77 nt)					27.7%		14.2%		24.4%	tRNA-Met
Ch I:309548	noncoding (5/77 nt)							10.3%			tRNA-Arg
Ch I:309612	noncoding (69/77 nt)								15.1%		tRNA-Arg
Ch I:547560	S148P (TCA→CCA)	13.1%									exodeoxyribonuclease VII large subunit
Ch I:575629	Y183S (TAC→TCC)								10.8%		sensor histidine kinase
Ch I:694022	N58K (AAT→AAA)									11.0%	MetQ
Ch I:702475	N78K (AAT→AAA)						10.1%			15.3%	MexH family multidrug efflux transporter
Ch I:796167	D996E (GAT→GAG)							10.7%	19.3%		Polar transmembrane protein
Ch I:796444	L1089L (TTA→CTA)			13.1%	10.2%						Polar transmembrane protein
Ch I:796460	V1094A (GTC→GCC)						11.0%		14.2%		Polar transmembrane protein
Ch I:796462	T1095A (ACG→GCG)		11.1%		12.2%			11.2%			Polar transmembrane protein
Ch I:796467	E1096E (GAG→GAA)								11.2%	15.4%	Polar transmembrane protein
Ch I:796491	E1104E (GAA→GAG)							12.1%	11.7%		Polar transmembrane protein
Ch I:796613	S1145F (TCT→TTT)			13.4%	13.8%	11.5%	12.3%	12.3%			Polar transmembrane protein
Ch I:796641	P1154P (CCC→CCT)						12.5%				Polar transmembrane protein
Ch I:796733	L1185P (CTC→CCC)	15.3%									Polar transmembrane protein
Ch I:796829	V1217A (GTC→GCC)		10.5%	10.8%						10.6%	Polar transmembrane protein
Ch I:796890	F1237F (TTC→TTT)						10.7%				Polar transmembrane protein
Ch I:796891	P1238T (CCC→ACC)			10.5%				12.2%			Polar transmembrane protein
Ch I:811852	A721A (GCT→GCC)		14.1%					11.7%			electron transport complex subunit RsxC
Ch I:811924	A697A (GCG→GCC)							12.1%			electron transport complex subunit RsxC
Ch I:811927	A696A (GCT→GCC)									11.4%	electron transport complex subunit RsxC
Ch I:1009792	T59K (ACA→AAA)							17.7%	28.5%		imidazolonepropionase
Ch I:1009796	V58F (GTC→TTC)		31.3%				30.5%				imidazolonepropionase
Ch I:1009798	L57* (TTA→TGA)				14.4%						imidazolonepropionase
Ch I:1009804	G55V (GGC→GTC)						27.8%				imidazolonepropionase
Ch I:1282272	V1112G (GTA→GGA)	10.4%									multifunctional autoprocessing toxin RtxA
Ch I:1295059	A68D (GCT→GAT)	100%							100%		XRE family transcriptional regulator
Ch I:1295272	intergenic (+77/-265)	43.5%				40.6%	50.0%				XRE transcriptional regulator/protein ligase
Ch I:1302195	intergenic (+76/-265)				58.1%					43.5%	XRE transcriptional regulator/protein ligase
Ch I:1361001	intergenic (-312/+159)			17.9%							phage terminase/hypothetical protein
Ch I:1361047	intergenic (-358/+113)			19.7%					14.6%		phage terminase/hypothetical protein
Ch I:1361127	intergenic (-438/+33)								10.6%		phage terminase/hypothetical protein
Ch I:1719984	E292G (GAG→GGG)			10.4%							ATPase AAA
Ch I:1738518	A190S (GCG→TCG)		18.5%			20.6%	18.2%		18.9%		PTS fructose transporter subunit IIC
Ch I:1738521	I191F (ATT→TTT)			22.3%				25.2%			PTS fructose transporter subunit IIC
Ch I:1738526	L192L (CTT→CTC)			19.4%							PTS fructose transporter subunit IIC
Ch I:1738528	G193D (GGT→GAT)								19.7%		PTS fructose transporter subunit IIC
Ch I:1738531	G194D (GGT→GAT)		17.3%								PTS fructose transporter subunit IIC
Ch I:1738532	G194G (GGT→GGG)		19.4%			22.1%					PTS fructose transporter subunit IIC
Ch I:1738547	D199E (GAT→GAG)				24.4%	12.8%					PTS fructose transporter subunit IIC
Ch I:1951003	I244L (ATC→CTC)				17.2%						beta-ketoacyl-ACP reductase
Ch I:2106203	G83G (GGA→GGG)								10.6%		redox-regulated ATPase YchF
Ch I:2621139	V111V (GTG→GTT)		100%								DNA-binding transcriptional regulator CytR

References

1. Pallen MJ, Wren BW. Bacterial pathogenomics. Nature. 2007;449:835.

2. Jürgens K, and Matz C. Predation as a shaping force for the phenotypic and genotypic composition of planktonic bacteria. Ant Van Leeuwen. 2002;81:413-34.

3. Sherr EB, and Sherr BF. Significance of predation by protists in aquatic microbial food webs. Ant Van Leeuwen. 2002;81:293–308.

4. Matz C, and Kjelleberg S. Off the hook–how bacteria survive protozoan grazing. Trends in Microbiol. 2005;13:302-7.

5. Seiler C, van Velzen E, Neu TR, Gaedke U, Berendonk TU, Weitere M. Grazing resistance of bacterial biofilms: a matter of predators' feeding trait. FEMS Microbiol Ecol. 2017;93.

6. Jeon KW. Bacterial endosymbiosis in amoebae. Trends Cell Biol. 1995;5:137-40.

7. Alsam S, Jeong SR, Sissons J, Dudley R, Kim KS, Khan NA. *Escherichia coli* interactions with *Acanthamoeba*: a symbiosis with environmental and clinical implications. J Med Microbiol. 2006;55:689-94.

8. Erken M, Lutz C, McDougald D. The Rise of pathogens: Predation as a factor driving the evolution of human pathogens in the environment. Microb Ecol. 2013;65:860-8.

9. Sun S, Noorian P, McDougald D. Dual role of mechanisms involved in resistance to predation by protozoa and virulence to humans. Front Microbiol. 2018;9.

10. Gunnar S, Amir S, Hadi A. *Acanthamoeba*-bacteria: A model to study host interaction with human pathogens. Curr Drug Targets. 2011;12:936-41.

11. Faruque SM, Naser IB, Islam MJ, Faruque ASG, Ghosh AN, Nair GB, et al. Seasonal epidemics of cholera inversely correlate with the prevalence of environmental cholera phages. Proc Natl Acad Sci USA. 2005;102:1702–7.

12. Matz C, McDougald D, Moreno AM, Yung PY, Yildiz FH, Kjelleberg S. Biofilm formation and phenotypic variation enhance predation driven persistence of *Vibrio cholerae*. Proc Natl Acad Sci USA. 2005;102:16819-24.

13. Abd H, Saeed A, Weintraub A, Nair GB, Sandström G. *Vibrio cholerae* O1 strains are facultative intracellular bacteria, able to survive and multiply symbiotically inside the aquatic free-living amoeba *Acanthamoeba castellanii*. FEMS Microbiol Ecol. 2007;60:33-9.

14. Noorian P, Hu J, Chen Z, Kjelleberg S, Wilkins MR, Sun S, et al. Pyomelanin produced by *Vibrio cholerae* confers resistance to predation by *Acanthamoeba castellanii*. FEMS Microbiol Ecol. 2017;93.

15. Van der Henst C, Vanhove AS, Drebes Dörr NC, Stutzmann S, Stoudmann C, Clerc S, et al. Molecular insights into *Vibrio cholerae*'s intra-amoebal host-pathogen interactions. Nat Commun. 2018;9:3460.

16. Guerrant RL, Carneiro-Filho BA, Dillingham RA. Cholera, diarrhea, and oral rehydration therapy: triumph and indictment. Clin Infect Dis. 2003;37:398-405.

17. World H, Organization. Cholera. wwwwhoint/mediacentre/factsheets/fs107/en/.

18. Harris JB, LaRocque RC, Qadri F, Ryan ET, Calderwood SB. Cholera. Lancet. 2012;379:2466–76.

19. Weill FX, Domman D, Njamkepo E, Tarr C, Rauzier J, Fawal N, et al. Genomic history of the seventh pandemic of cholera in Africa. Science. 2017;358:785–9.

20. Snow J, Frost W, Richardson B. Snow on cholera. New York: Commonwealth Fund. 1936.

21. Bentivoglio M, Pacini P. Filippo Pacini: a determined observer. Brain Res Bull. 1995;38:161-5.

22. Koch R. An address on cholera and its bacillus. Br Med J. 1884;2:453-9.

23. Colwell RR. Global climate and infectious disease: the cholera paradigm. Science. 1996;274:2025-31.

24. Gardner AD, Venkatraman KV. The antigens of the cholera group of vibrios. J Hyg. 1935;35:262-82.

25. Sack DA, Sack RB, Nair GB, Siddique AK. Cholera. Lancet. 2004;363:223–33.

26. Mutreja A, Kim DW, Thomson NR, Connor TR, Lee JH, Kariuki S, et al. Evidence for several waves of global transmission in the seventh cholera pandemic. Nature. 2011;477:462–5.

27. Faruque SM, Albert MJ, and Mekalanos JJ. Epidemiology, genetics, and ecology of toxigenic *Vibrio cholerae* Microbiol Mol Biol Rev. 1998;62:1301-14.

28. Huq A SR, Nizam A, Longini IM, Nair GB, Ali A, Morris JG, Jr., Khan MN, Siddique AK, Yunus M, Albert MJ, Sack DA, Colwell RR. Critical factors influencing the occurrence of *Vibrio cholerae* in the environment of Bangladesh. Appl Environ Microbiol. 2005;71:4645-54.

29. Faruque SM, Nair GB. *Vibrio cholerae*: Genomics and Molecular Biology. Caister Academic Press. 2008;ISBN 978-1-904455-33-2.

30. Davis B, Waldor M,. Filamentous phages linked to virulence of *Vibrio cholerae*. Curr Opin Microbiol. 2003;6:35–42.

31. Walia K, Ghosh S, Singh H, Nair GB, Ghosh A, et al. Purification and characterization of novel toxin produced by *Vibrio cholerae* O1. Infect Immun. 1999;67:5215–22.

32. Johnson TL, Abendroth J, Hol WG, Sandkvist M. Type II secretion: from structure to function. FEMS Microbiol Lett. 2006;255:175–86.

33. Holmgren J, Lonnroth I, Svennerholm L. Tissue receptor for cholera exotoxin postulated structure from studies with GM1 ganglioside and related glycolipids. Infect Immun. 1973;8:208–14.

34. Torgersen ML, Skretting G., van Deurs B., Sandvig K. Internalization of cholera toxin by different endocytic mechanisms. J Cell Sci. 2001;114:3737–47.

35. Sonawane ND, Zhao D, Zegarra-Moran O, Galietta LJ, Verkman AS. Lectin conjugates as potent non-absorbable CFTR inhibitors for reducing intestinal fluid secretion in cholera. Gastroenterol. 2007;132:1234–44.

36. Sánchez J, & Holmgren, J. Cholera toxin — A foe & a friend. Indian J Med Res. 2011;133:153–63.

37. Kaper JB, Morris J G, Levine M M. Cholera. Clin Microbiol Rev. 1995;8:48–86.

38. Herrington DA, Hall RH, Losonsky G, Mekalanos JJ, Taylor RK, and Levine MM. Toxin, toxin-coregulated pili and ToxR regulon are essential for *Vibrio cholerae* pathogenesis in humans. J Exp Med 1988;168:1487-92.

39. Taylor RK, Miller VL, Furlong DB, and Mekalanos JJ. Use of phoA gene fusions to identify a pilus colonization factor coordinately regulated with cholera toxin. Proc Natl Acad Sci USA. 1987;84:2833-7.

40. Kirn TJ, Lafferty MJ, Sandoe CM, and Taylor RK. Delineation of pilin domains required for bacterial association into microcolonies and intestinal colonization by *Vibrio cholerae*. Mol Microbiol. 2000;35:896-910.

41. Waldor MK, and Mekalanos JJ. Lysogenic conversion by a filamentous phage encoding cholera toxin. Science. 1996;272:1910–4.

42. Trucksis M, Galen JE, Michalski J, Fasano A, and Kaper JB. Accessory cholera enterotoxin (Ace), the third toxin of a *Vibrio cholerae* virulence cassette. Proc Natl Acad Sci USA. 1993;90:5267-71.

43. Fasano A, Baudry B, Pumplin DW, Wasserman SS, Tali BD, Ketley JM, and Kaper JB. *Vibrio cholerae* produces a second enterotoxin, which affects intestinal tight junctions. Proc Natl Acad Sci USA. 1991;88:5442-246.

44. Fullner KJ, and Mekalanos JJ. *In vivo* covalent cross-linking of cellula ractin by the *Vibrio cholerae* RTX toxin. EMBO J. 2000;19:5315-23.

45. Honda T, and Finkelstein RA. . Purification and characterization of ahemolysin produced by *Vibrio cholerae* biotype El Tor: another toxic substance produced by cholera vibrios. Infect Immun. 1979;26:1020-7.

46. Silva AJ, Leitch GJ, Camilli A, and Benitez JA. Contribution of hemagglutinin/protease and motility to the pathogenesis of El Tor biotype cholera. Infect Immun. 2006;74:2072-9.

47. DiRita VJ, Parsot C, Jander G, and Mekalanos JJ. Regulatory cascades controls virulence in *Vibrio cholerae*. Proc Natl Acad Sci USA. 1991;88:5403–7.

48. Kovacikova G, and Skorupski K. A *Vibrio cholerae* LysR homolog, AphB, cooperates with AphA at the tcpPH promoter to activate expression of the ToxR virulence cascade. J Bacteriol. 1999;181:4250-6.

49. Higgins DE, and DiRita VJ. Transcriptional control of toxT, a regulatory gene in the ToxR regulon of *Vibrio cholerae*. Mol Microbiol. 1994;14:17-29.

50. Peterson KM, and Mekalanos JJ. Characterization of the *Vibrio cholerae* ToxR regulon: identification of novel genes involved in intestinal colonization. Infect Immun. 1988;56:2822–9.

51. Miller VL, and Mekalanos JJ. . A novel suicide vector and is use in construction of insertion mutations: osmoregulation of outer membrane proteins and virulence determinants in *Vibrio cholerae* requires toxR. J Bacteriol 1988;170:2575–83.

52. Parsot C, Taxman E, and Mekalanos JJ. ToxR regulates the production of lipoproteins and the expression of serum resistance in *Vibrio cholerae*. Proc Natl Acad Sci USA. 1991;88:1641–5.

53. Jung SA, Hawver LA, Ng WL. Parallel quorum sensing signaling pathways in *Vibrio cholerae*. Curr Genet. 2016;62:255–60.

54. Jung SA, Chapman CA, Ng WL. Quadruple quorum-sensing inputs control *Vibrio cholerae* virulence and maintain system robustness. PLoS Pathog. 2015;11:e1004837.

55. Herzog R, Peschek N, Fröhlich KS, Schumacher K, Papenfort K. Three autoinducer molecules act in concert to control virulence gene expression in *Vibrio cholerae*. Nucleic Acid Res. 2019;47:3171-83.

56. Higgins DA, Pomianek ME, Kraml CM, Taylor RK, Semmelhack MF, Bassler BL. The major *Vibrio cholerae* autoinducer and its role in virulence factor production. Nature. 2007;450:883–6.

57. Watve S, Barrasso K, Jung SA, Davis KJ, Hawver LA, Khataokar A, et al. Parallel quorum-sensing system in *Vibrio cholerae* prevents signal interference inside the host. PLoS Pathogen. 2020;16:e1008313.

58. Wei Y, Ng W-L, Cong J, Bassler BL. Ligand and antagonist driven regulation of the Vibrio cholerae quorum-sensing receptor CqsS. Mol Microbiol 2012;83:1095–108.

59. Lenz D, H, Mok KC, Lilley BN, Kulkarni R V, Wingreen NS, Bassler BL. The small RNA chaperone Hfq and multiple small RNAs control quorum sensing in *Vibrio harveyi* and *Vibrio cholerae*. Cell. 2004;118:69–82.

60. Rutherford ST, Van-Kessel JC, Shao Y, Bassler BL. AphA and LuxR/HapR reciprocally control quorum sensing in vibrios. Genes Dev. 2011;25:397–408.

61. Zhu J, Miller MB, Vance RE, Dziejman M, Bassler BL, Mekalanos JJ. Quorum-sensing regulators control virulence gene expression in *Vibrio cholerae*. Proc Natl Acad Sci USA. 2002;99:3129-34.

62. Hammer BK, and Bassler BL. Quorum sensing controls biofilm formation in *Vibrio cholerae*. Mol Microbiol. 2003;50:101–14.

63. Silva AJ, Pham K, Benitez JA. Haemagglutinin/protease expression and mucin gel penetration in El Tor biotype *Vibrio cholerae*. Microbiol. 2003;149:1883–91.

64. Hengge R. Principles of c-di-GMP signalling in bacteria. Nat Rev Microbiol. 2009;7:263-73.

65. Ryjenkov DA, Tarutina M, Moskvin OV, and Gomelsky M. Cyclic diguanylate is a ubiquitous signaling molecule in bacteria:insights into biochemistry of the GGDEF protein domain. J Bacteriol. 2005;187:1792-8.

66. Schmidt AJ, Ryjenkov DA, and Gomelsky M. Theubiquitous protein domain EAL is a cyclic diguanylate-specificphosphodiesterase: enzymatically active and inactive EAL domains. J Bacteriol. 2005;187:4774-81.

67. Beyhan S, Odell LS, Yildiz FH. Identification and characterization ofcyclic diguanylate signaling systems controlling rugosity in *Vibrio cholerae*. J Bacteriol. 2008;190:7392–405.

68. Tischler AD, Camilli A. Cyclic diguanylate (c-di-GMP) regulates *Vibrio cholerae* biofilm formation. Mol Microbiol. 2004;53:857– 69.

69. Srivastava D, Hsieh ML, Khataokar A, Neiditch MB, Waters CM. Cyclic di-GMP inhibits *Vibrio cholerae* motility by repressing induction of transcription and inducing extracellular polysaccharide production. Mol Microbiol. 2013;90:1262–76.

70. Krasteva PV, Fong JC, Shikuma NJ, Beyhan S, Navarro MV, Yildiz FH, and Sondermann H. . *Vibrio cholerae* VpsT regulates matrix production and motility by directly sensing cyclicdi-GMP. Science. 2010;327:866-8.

71. Lipp EK, Huq A, and Colwell RR. Effects of global climate oninfectious disease: the cholera model. Clin Microbiol Rev. 2002;15:757-70.

72. Faruque SM, Biswas K, Udden SMN, Ahmad QS, Sack DA, and Nair GB. Transmissibility of cholera: In vivo-formed biofilms and their relationship to infectivity and persistence in the environment. Proc Natl Acad Sci USA. 2006;103:6350-5.

73. McDougald D, Rice SA, Barraud N, Steinberg PD, Kjelleberg S. Should we stay or should we go: mechanisms and ecological consequences for biofilm dispersal. Nat Rev Microbiol. 2012;10:39–50.

74. Watnick PI, Fullner KJ, Kolter R. A role for the mannose-sensitive hemagglutinin in biofilm formation by *Vibrio cholerae* El Tor. J Bacteriol. 1999;181:3606–9.

75. Meibom KL, Li XB, Nielsen AT, Wu CY, Roseman S, & Schoolnik GK. The *Vibrio cholerae* chitin utilization program. Proc Natl Acad Sci USA. 2004;101:2524–9.

76. Fong JCN, & Yildiz FH. The rbmBCDEF gene cluster modulates development of rugose colony morphology and biofilm formation in *Vibrio cholerae*. J Bacteriol. 2007;189:2319–30.

77. Seper A, Fengler VHI, Roier S, Wolinski H, Kohlwein SD, Bishop AL, Schild S. Extracellular nucleases and extracellular DNA play important roles in Vibrio cholerae biofilm formation. Mol Microbiol. 2011;82:1015–37.

78. Fong JCN, Syed KA, Klose KE, & Yildiz FH. Role of Vibrio polysaccharide (vps) genes in VPS production, biofilm formation and *Vibrio cholerae* pathogenesis. Microbiol. 2010;156:2757–69.

79. Waters CM, Lu W, Rabinowitz JD, Bassler BL. Quorum sensing controls biofilm formation in *Vibrio cholerae* through modulation of cyclic di-GMP levels and repression of vpsT. J Bacteriol. 2008;190:2527–36.

80. Watnick PI, Lauriano CM, Klose KE, Croal L, and Kolter R. The absence of a flagellum leads to altered colony morphology, biofilmdevelopment and virulence in *Vibrio cholerae* O139. Mol Microbiol. 2001;39:223–35.

81. Yildiz FH, Schoolnik GK. *Vibrio cholerae* O1 El Tor identification of a gene cluster required for the rugose colony type,exopolysaccharide production, chlorine resistance, and biofilm formation. Proc Natl Acad Sci USA. 1999;96:4028-33.

82. Tamplin ML, Gauzens AL, Huq A, Sack DA, and Colwell RR. Attachment of *Vibrio cholerae* serogroup 01 to zooplankton andphytoplankton of Bangladesh waters. Appl Environ Microbiol. 1990;56:1977-80.

83. Huq A, Small EB, West PA, Huq MI, Rahman R, Colwell RR. Ecological relationship between *Vibrio cholerae* and planktonic crustacean copepods. Appl Environ Microbiol. 1983;45:275-83.

84. Meibom KL, Blokesch M, Dolganov NA, Wu CY, Schoolnik GK. Chitin induces natural competence in *Vibrio cholerae.* Science. 2005;310:1824–7.

85. Turner JW, Malayil L, Guadagnoli D, Cole D, & Lipp EK. Detection of *Vibrio parahaemolyticus, Vibrio vulnificus* and *Vibrio cholerae* with respect to seasonal fluctuations in temperature and plankton abundance. Environ Microbiol. 2014;16:1019–28.

86. Chaiyanan S, Huq A, Maugel T, and Colwell RR. Viability ofthe nonculturable *Vibrio cholerae* O1 and O139. Syst Appl Microbiol. 2001;24:331-41.

87. Bari SM, Roky MK, Mohiuddin M, Kamruzzaman M, Mekalanos JJ, Faruque SM. Quorum-sensing autoinducers resuscitate dormant Vibrio cholerae in environmental water samples. Proc Natl Acad Sci USA. 2013;110:9926–31.

88. Tamayo R, Patimalla B, Camilli A. Growth in a biofilm induces a hyperinfectious phenotype in *Vibrio cholerae*. Infect Immun. 2010;78:3560-9.

89. Colwell RR, Huq A, Islam MS, Aziz KM, Yunus M, Khan NH, Mahmud A, Sack RB, Nair GB, Chakraborty J, Sack DA, RussekCohen E. Reduction of cholera in Bangladeshi villages by simple filtration. Proc Natl Acad Sci USA. 2003;100:1051-5.

90. Bilecen K, Fong JC, Cheng A, Jones CJ, Zamorano-Sanchez D, Yildiz FH. Polymyxin B Resistance and biofilm formation in *Vibrio cholerae* is controlled by the response regulator CarR. Infect Immun 2015;83:1199-209.

91. Zhu J, and Mekalanos JJ. Quorum sensing-dependent biofilms enhance colonization in *Vibrio cholerae*. Dev Cell. 2003;5:647–56.

92. Heidelberg JF, Eisen JA, Nelson WC, Clayton RA, Gwinn ML, Dodson RJ, et al. DNA sequence of both chromosomes of the cholera pathogen *Vibrio cholerae*. Nature. 2000;406:477–83.

93. Hassan F, Kamruzzaman M, Mekalanos JJ, Faruque SM. Satellite phage TLCphi enables toxigenic conversion by CTX phage through dif site alteration. Nature. 2010;467:982–5.

94. Karaolis DK, Johnson JA, Bailey CC, Boedeker EC, Kaper JB, Reeves PR. A *Vibrio cholerae* pathogenicity island associated with epidemic and pandemic strains. . Proc Natl Acad Sci USA. 1998;95:3134-9.

95. Waldor MK, Tschäpe H, Mekalanos JJ. A new type of conjugative transposon encodes resistance to sulfamethoxazole, trimethoprim, and streptomycin in *Vibrio cholerae* O139. J Bacteriol. 1996;178:4157–65.

96. Dziejman M, Balon E, Boyd D, Fraser CM, Heidelberg JF, Mekalanos JJ. Comparative genomic analysis o f *Vibrio cholerae*: genes that correlate with cholera endemic and pandemic disease. Proc Natl Acad Sci USA. 2002;99:1556-61.

97. Li M, Shimada T, Morris JG Jr, Sulakvelidze A, Sozhamannan S. Evidence for the emergence of non-O1 and non-O139 *Vibrio cholerae* strains with pathogenic potential by exhange of O-antigen biosynthesis regions. Infect Immun. 2002;70:2441-53.

98. Parry JD. Protozoan Grazing in Freshwater Biofilms. Adv Appl Microbiol. 2004;54:167-96.

99. Sherr EB, and Sherr BF. Bacterivory and herbivory: key roles of phagotrophic protists in pelagic food webs. Microb Ecol. 1994;28:223-35.

100. Patterson DJ, and Burford MA. Guide to protozoa of marine aquaculture ponds: Csiro Publishing Victoria.; 2001.

101. Weisman RA. Differentiation in *Acanthamoeba castellanii*. Annu Rev Microbiol. 1976;30:189-219.

102. Butler H, and Rogerson A. Consumption rates of six species of marine benthic naked amoebae (*Gymnamoeba*) from sediments in the Clyde Sea area. J Mar Biol Assoc UK. 1997;77:898-997.

103. Hilbi H, Weber SS, Raga, C, Nyfeler Y, and Urwyler S. . Environmental predators as models for bacterial pathogenesis. Environ Microbiol. 2007;9:563-75.

104. Pernthaler J, Sattler B, Simek K, Szhwarzenbacher A, and Psenner R. Top-down effects on the size-biomass distribution of a freshwater bacterioplankton community Aquat Microb Ecol. 1996;10:255-63.

105. Sherr BF, Sherr EB and Berman T. Grazing, growth, and ammonium excretion rates of a heterotrophic microflagellate fed with four species of bacteria. Appl Environ Microbiol. 1983;45:1196-201.

106. Hahn MW, and Höfle MG. Grazing of protozoa and its effect on populations of aquatic bacteria. FEMS Microbiol Ecol. 2001;35:113-21.

107. Finlay BJ. Protozoa. Encyclopedia of Biodiversity, Academic Press. 2001;4:901-15.

108. Sherr BF, Sherr EB, and Berman T. Decomposition of organic detritus: A selective role for microflagellate protozoa. Limnol and Ocean. 1982;27:765-9.

109. Thingstad TF, and Lignell R. Theoretical models for the control of bacterial growth rate, abundance, diversity and carbon demand. Aquat Microb Ecol. 1997;13:19-27.

110. Pace ML, and Cole JJ. Comparative and experimental approaches to top-down and bottom-up regulation of bacteria. Microb Ecol. 1994;28:181-93.

111. Fenchel T. Ecology of heterotrophic microflagellates. IV. Quantitative occurrence and importance as bacterial consumers. Mar Ecol Prog 1982;9:35–42.

112. Kathol M, Norf H, Arndt H, Weitere M. Effects of temperature increase on the grazing of planktonic bacteria by biofilm-dwelling consumers. Aquat Microb Ecol. 2009; 55:65–79.

113. Tsyganov AN, Nijs I, Beyens L. Does climate warming stimulate or inhibit soil protist communities? A test on testate amoebae in high-arctic tundra with free-air temperature increase. Protist. 2011;162:237-48.

114. Hoekman D. Turning up the heat: Temperature influences the relative importance of top-down and bottom-up effects. Ecology. 2010;91:2819-25.

115. Pernthaler J. Predation on prokaryotes in the water column and its ecological implications. Nat Rev Microbiol. 2005;3:537-46.

116. González JM, Sherr EB. & Sherr BF. Size selective grazing on bacteria by natural assemblages of estuarine flagellates and ciliates. Appl Environ Microbiol. 1990;56:583–9.

117. Hahn MW, and Höfle MG. Grazing pressure by a bacterivorous flagellate reverses the relative abundance of *Comamonas acidovorans* PX54 and *Vibrio* Strain CB5 in chemostat cocultures. Appl Environ Microbiol. 1998;64:1910-8.

118. Corno G, and Jürgens K. Direct and indirect effects of protist predation on population size structure of a bacterial strain with high phenotypic plasticity. Appl Environ Microbiol. 2006;72:78-86.

119. Shikano S, Luckinbill LS. and Kurihara Y. Changes of traits in a bacterial population associated with protozoal predation. Microb Ecol. 1990;20:75–84.

120. Matz C, and Jurgens K. High motility reduces grazing mortality of planktonic bacteria. Appl Environ Microbiol. 2005;71:921–9.

121. Wildschutte H, Wolfe DM, Tamewitz A, and Lawrence JG. Protozoan predation, diversifying selection, and the evolution of antigenic diversity in *Salmonella*. Proc Natl Acad Sci USA. 2004;101:10644-9.

122. March C, Cano V, Moranta D, Llobet E, Pérez-Gutiérrez C, Tomás JM, Suárez T, Garmendia J & Bengoechea JA. Role of bacterial surface structures on the interaction of *Klebsiella pneumoniae* with phagocytes. PLoS One. 2013;8:e56847.

123. Matz C, Bergfeld, T, Rice SA, and Kjelleberg S. Microcolonies, quorum sensing and cytotoxicity determine the survival of *Pseudomonas aeruginosa* biofilms exposed to protozoan grazing. Environ Microbiol. 2004;6:218–26.

124. Hao X, Lüthje F, Rønn R, German NA, Li X, Huang F, Kisaka J, Huffman D, Alwathnani HA, & Zhu YG. A role for copper in protozoan grazing–two billion years selecting for bacterial copper resistance. Mol Microbiol. 2016;102:628-41.

125. Matz C, Moreno AM, Alhede M, Manefield M, Hauser AR, Givskov M, and Kjelleberg S. *Pseudomonas aeruginosa* uses type III secretion system to kill biofilm-associated amoebae. ISME J. 2008;2:843-52.

126. Matz C, Nouri B, McCarter L, Martinez-Urtaza J. Acquired Type III Secretion System Determines Environmental Fitness of Epidemic *Vibrio parahaemolyticus* in the Interaction with Bacterivorous Protists. PLoS One. 2011;5:e20275.

127. MacIntyre DL, Miyata ST, Kitaoka M, Pukatzki S. The *Vibrio cholerae* type VI secretion system displays antimicrobial properties. . Proc Natl Acad Sci USA. 2010;107:19520–4.

128. Matz C, Deines P, Boenigk J, Arndt H, Eberl L, Kjelleberg S, & Jürgens K. Impact of violacein-producing bacteria on survival and feeding of bacterivorous nanoflagellates. Environ Microbiol. 2004;70:1593-9.

129. Lainhart W, Stolfa G, & Koudelka GB. Shiga toxin as a bacterial defense against a eukaryotic predator, *Tetrahymena thermophila*. J Bacteriol. 2009;191:5116-22.

130. Swart AL, Harrison CF, Eichinger L, Steinert M, Hilbi H. *Acanthamoeba* and *Dictyostelium* as cellular models for *Legionella* Infection. Front Cell Infect Microbiol. 2018;8.

131. Espinoza-Vergara G, Noorian P, Silva-Valenzuela CA, Raymond BBA, Allen C, Hoque MM, et al. *Vibrio cholerae* residing in food vacuoles expelled by protozoa are more infectious in vivo. Nat Microbiol. 2019.

132. Rowbotham TJ. Isolation of *Legionella pneumophila* from clinical specimens via amoebae, and the interaction of those and other isolates with amoebae. J Clin Pathol. 1983;36:978-86.

133. Scola BL, Raoult D. Survival of *Coxiella burnetii* within free-living amoeba *Acanthamoeba castellanii*. Clin Microbiol Infect. 2001;7:75-9.

134. Greub G, Raoult D. Microorganisms Resistant to Free-Living Amoebae. Clin Microbiol Rev. 2004;17:413-33.

135. Bozue JA, Johnson W. Interaction of *Legionella pneumophila* with *Acanthamoeba castellanii*: uptake by coiling phagocytosis and inhibition of phagosome-lysosome fusion. Infect Immun. 1996;64:668-73.

136. Rowbotham TJ. Preliminary report on the pathogenicity of *Legionella pneumophila* for freshwater and soil amoebae. J Clin Pathol. 1980;33:1179-83.

137. Chen J, de Felipe KS, Clarke M, Lu H, Anderson OR, Segal G, et al. Effectors that promote nonlytic release from protozoa. Science. 2004;303:1358-61.

138. Michel R, Burghardt H, & Bergmann H. *Acanthamoeba*, naturally intracellularly infected with Pseudomonas aeruginosa, after their isolation from a microbiologically contaminated drinking water system in a hospital. Zentralbl Hyg Umweltmed. 1995;196:532–44.

139. Amann R, Springer N, Schönhuber W, Ludwig W, Schmid EN, Müller KD, et al. Obligate intracellular bacterial parasites of *Acanthamoebae* related to *Chlamydia* spp. Appl Environ Microbiol. 1997;63:115-21.

140. Pushkareva VI, Ermolaeva SA. *Listeria monocytogenes* virulence factor Listeriolysin O favors bacterial growth in co-culture with the ciliate *Tetrahymena pyriformis*, causes protozoan encystment and promotes bacterial survival inside cysts. BMC Microbiol. 2010;10:26.

141. Thom S, Warhurst D, Drasar BS. . Association of *Vibrio cholerae* with fresh water amoebae. J Med Microbiol. 1992;36:303-6.

142. Abd H, Weintraub A, Sandström G. Intracellular survival and replication of *Vibrio cholerae* O139 in aquatic free-living amoebae. Environ Microbiol. 2005;7:1003-8.

143. Shanan S, Abd H, Hedenström I, Saeed A, Sandström G. Detection of *Vibrio cholerae* and *Acanthamoeba* species from same natural water samples collected from different cholera endemic areas in Sudan. BMC Research Notes. 2011;4:109.

144. Adékambi T, Ben Salah S, Khlif M, Raoult D, Drancourt M. Survival of Environmental *Mycobacteria* in *Acanthamoeba polyphaga*. Appl Environ Microbiol. 2006;72:5974-81.

145. Landers P, Kerr KG, Rowbotham TJ, Tipper JL, Keig PM, Ingham E, & Denton MS. Survival and growth of Burkholderia cepacia within the free-living amoeba *Acanthamoeba polyphaga*. Eur J Clin Microbiol Infect Dis. 2000;19:121–3.

146. Winiecka-Krusnell J, Wreiber K, von Euler A, Engstrand L, & Linder E. Free-living amoebae promote growth and survival of Helicobacter pylori. Scand J Infect Dis. 2002;34:253–6.

147. Axelsson-Olsson D, Waldenström J, Broman T, Olsen B, Holmberg M. Protozoan *Acanthamoeba polyphaga* as a potential reservoir for *Campylobacter jejuni*. Appl Environ Microbiol. 2005;71:987-92.

148. Hudson LD, Hankins JW, & Battaglia M. Coliforms in a water distribution system: a remedial approach. J Am Water Works Assoc. 1983;75:564-8.

149. Barker J, Brown MRW. Trojan Horses of the microbial world: protozoa and the survival of bacterial pathogens in the environment. Microbiol. 1994;140:1253-9.

150. Cavalier-Smith T. The phagotrophic origin of eukaryotes and phylogenetic classification of Protozoa. Int J Syst Evol Microbiol. 2002;52:297-354.

151. Strassmann JE, Shu L. Ancient bacteria–amoeba relationships and pathogenic animal bacteria. PLoS Biol. 2017;15:e2002460.

152. Levin B. The evolution and maintenance of virulence in microparasites. Emerg Infect Dis. 1996;2:93–102.

153. Cirillo JD, Cirillo SLG, Yan L, Bermudez LE, Falkow S, Tompkins LS. Intracellular growth in *Acanthamoeba castellanii* affects monocyte entry mechanisms and enhances virulence of *Legionella pneumophila*. Infect Immun. 1999;67:4427-34.

154. Tomov AT, Tsvetkova ED, Tomova IA, Michailova LI, Kassovski VK. Persistence and multiplication of obligate anaerobe bacteria in amoebae under aerobic conditions. Anaerobe. 1999;5:19-23.

155. Adiba S, Nizak C, van Baalen M, Denamur E, Depaulis F. From grazing resistance to pathogenesis: The coincidental evolution of virulence Factors. PLoS One. 2010;5:e11882.

156. Taylor-Mulneix DL, Hamidou Soumana I, Linz B, Harvill ET. Evolution of *Bordetellae* from environmental microbes to human respiratory pathogens: amoebae as a missing link. Front Cell Infect Microbiol. 2017;7.

157. Cirillo JD, Falkow S, Tompkins LS, Bermudez LE. Interaction of *Mycobacterium avium* with environmental amoebae enhances virulence. Infect Immun. 1997;65:3759-67.

158. Liu J, Dong Y, Wang N, Li S, Yang Y, Wang Y, et al. *Tetrahymena thermophila* predation enhances environmental adaptation of the carp pathogenic strain *Aeromonas hydrophila* NJ-35. Front Cell Infect Microbiol. 2018;8.

159. Mikonranta L, Friman V-P, Laakso J. Life history trade-offs and relaxed selection can decrease bacterial virulence in environmental reservoirs. PLoS One. 2012;7:e43801.

160. Siddiqui R, Khan NA. *Acanthamoeba* is an evolutionary ancestor of macrophages: A myth or reality? Exp Parasitol. 2012;130:95-7.

161. Harb OS, Gao L-Y, Kwaik YA. From protozoa to mammalian cells: a new paradigm in the life cycle of intracellular bacterial pathogens. Environ Microbiol. 2000;2:251-65.

162. Molmeret M, Horn M, Wagner M, Santic M, Abu Kwaik Y. Amoebae as training grounds for intracellular bacterial pathogens. Appl Environ Microbiol. 2005;71:20-8.

163. Gomez-Valero L, Rusniok C, Cazalet C, Buchrieser C. Comparative and functional genomics of *Legionella* identified eukaryotic like proteins as pey players in host–pathogen interactions. Front Microbiol. 2011;2.

164. Price C, Abu Kwaik Y. Amoebae and mammals deliver protein-rich atkins diet meals to Legionella cells. Microbe Magazine. 2012.

165. Worden AZ, Seidel M, Smriga S, Wick A, Malfatti F, Bartlett D, et al. Trophic regulation of *Vibrio cholerae* in coastal marine waters. Environ Microbiol. 2006;8:21-9.

166. Erken M, Weitere M, Kjelleberg S, McDougald D. In situ grazing resistance of *Vibrio cholerae* in the marine environment. FEMS Microbiol Ecol. 2011;76:504-12.

167. Vaitkevicius K, Lindmark B, Ou G, Song T, Toma C, Iwanaga M, et al. A *Vibrio cholerae* protease needed for killing of *Caenorhabditis elegans* has a role in protection from natural predator grazing. Proc Natl Acad Sci USA. 2006;103:9280-5.

168. Pukatzki S, Ma AT, Sturtevant D, Krastins B, Sarracino D, Nelson WC, et al. Identification of a conserved bacterial protein secretion system in *Vibrio cholerae* using the *Dictyostelium* host model system. Proc Natl Acad Sci USA. 2006;103:1528-33.

169. Brüssow H. Bacteria between protists and phages: from antipredation strategies to the evolution of pathogenicity. Mol Microbiol. 2007;65:583-9.

170. Cirillo JD, Falkow S, Tompkins LS. Growth of *Legionella pneumophila* in *Acanthamoeba castellanii* enhances invasion. Infect Immun. 1994;62:3254-61.

171. Rasmussen MA, Carlson SA, Franklin SK, McCuddin ZP, Wu MT, Sharma VK. Exposure to rumen protozoa leads to enhancement of pathogenicity of and invasion by multiple-antibiotic-resistant *Salmonella enterica* bearing SGI1. Infect Immun. 2005;73:4668-75.

172. Azumah BK, Addo PG, Dodoo A, Awandare G, Mosi L, Boakye DA, et al. Experimental demonstration of the possible role of *Acanthamoeba polyphaga* in the infection and disease progression in Buruli Ulcer (BU) using ICR mice. PLoS One. 2017;12:e0172843.

173. Jansen G, Crummenerl LL, Gilbert F, Mohr T, Pfefferkorn R, Thänert R, et al. Evolutionary transition from pathogenicity to commensalism: global regulator mutations mediate fitness gains through virulence attenuation. Mol Biol Evol. 2015;32:2883-96.

174. Zhang J, Ketola T, Örmälä-Odegrip A-M, Mappes J, Laakso J. Coincidental Loss of Bacterial Virulence in Multi-Enemy Microbial Communities. PLoS One. 2014;9:e111871.

175. Ensminger AW, Yassin Y, Miron A, Isberg RR. Experimental evolution of *Legionella pneumophila* in mouse macrophages leads to strains with altered determinants of environmental survival. PLoS Pathog. 2012;8:e1002731.

176. Espinoza-Vergara G, Hoque MM, McDougald D, Noorian P. The Impact of Protozoan Predation on the Pathogenicity of *Vibrio cholerae*. Front Microbiol. 2020;11.

177. Faruque SM, Naser IB, Islam MJ, Faruque ASG, Ghosh AN, Nair GB, et al. Seasonal epidemics of cholera inversely correlate with the prevalence of environmental cholera phages. Proc Natl Acad Sci USA. 2005;102:1702-7.

178. Van der Henst C, Scrignari T, Maclachlan C, Blokesch M. An intracellular replication niche for *Vibrio cholerae* in the amoeba *Acanthamoeba castellanii*. ISME J. 2016;10:897-910.

179. Vaitkevicius K, Lindmark B, Ou G, Song T, Toma C, Iwanaga M, et al. A *Vibrio cholerae* protease needed for killing of *Caenorhabditis elegans* has a role in protection from natural predator grazing. Proc Natl Acad Sci USA. 2006;103:9280-5.

180. Noorian P, Hu J, Chen Z, Kjelleberg S, Wilkins MR, Sun S, et al. Pyomelanin produced by *Vibrio cholerae* confers resistance to predation by *Acanthamoeba castellanii*. FEMS Microbiol Ecol. 2017;93.

181. Matz C, McDougald D, Moreno AM, Yung PY, Yildiz FH, Kjelleberg S. Biofilm formation and phenotypic variation enhance predation-driven persistence of *Vibrio cholerae*. Proc Natl Acad Sci USA. 2005;102:16819-24.

182. Matz C, Jürgens K. High motility reduces grazing mortality of planktonic bacteria. Appl Environ Microbiol. 2005;71:921-9.

183. Gonzalez JM, Sherr, E., and Sherr, B. F. Differential feeding by marine flagellates on growing versus starving, and on motile versus nonmotile, bacterial prey. Marine Ecol Prog Series. 1993:257-67.

184. Matz C, Boenigk, J., Arndt, H., and Jürgens, K. Role of bacterial phenotypic traits in selective feeding of the heterotrophic nanoflagellate Spumella sp. Aquat Microb Ecol. 2002; 27:137–48.

185. Seiler C, van Velzen E, Neu TR, Gaedke U, Berendonk TU, Weitere M. Grazing resistance of bacterial biofilms: a matter of predators feeding trait. FEMS Microbiol Ecol. 2017;93.

186. Paludan-Müller C, Weichart D, McDougald D, Kjelleberg S. Analysis of starvation conditions that allow for prolonged culturability of *Vibrio vulnificus* at low temperature. Microbiol. 1996;142:1675-84.

187. Neidhardt FC, Bloch PL, Smith DF. Culture medium for enterobacteria. J Bacteriol. 1974;119:736-47.

188. O'Toole GA, Pratt LA, Watnick PI, Newman DK, Weaver VB, Kolter R. Genetic approaches to study of biofilms. Methods Enzymol. 1999;310:91-109.

189. Petersen LM, Tisa LS. Molecular Characterization of Protease Activity in *Serratia* sp. Strain SCBI and Its Importance in Cytotoxicity and Virulence. J Bacteriol. 2014;196:3923-36.

190. Gardel CL, Mekalanos JJ. Alterations in *Vibrio cholerae* motility phenotypes correlate with changes in virulence factor expression. Infect Immun. 1996;64:2246-55.

191. Horton RM, Hunt HD, Ho SN, Pullen JK, Pease LR. Engineering hybrid genes without the use of restriction enzymes: gene splicing by overlap extension. Gene. 1989;77:61-8.

192. Meibom KL, Blokesch M, Dolganov NA, Wu CY, Schoolnik GK. Chitin induces natural competence in *Vibrio cholerae*. Science. 2005;310:1824-7.

193. Silva ODS, Blokesch M. Genetic manipulation of *Vibrio cholerae* by combining natural transformation with FLP recombination. Plasmid. 2010;64:186-95.

194. Gibson DG, Young L, Chuang RY, Venter JC, Hutchison CA, 3rd, Smith HO. Enzymatic assembly of DNA molecules up to several hundred kilobases. Nat Methods. 2009;6:343-5.

195. Lambertsen L, Sternberg C, Molin S. Mini-Tn7 transposons for site-specific tagging of bacteria with fluorescent proteins. Environmental Microbiology. 2004;6:726-32.

196. Mitchell KC, Withey JH. *Danio rerio* as a native host model for understanding pathophysiology of *Vibrio cholerae*. Methods Mol Biol. 2018;1839:97-102.

197. Cheng T, Kam JY, Johansen MD, Oehlers SH. High content analysis of granuloma histology and neutrophilic inflammation in adult zebrafish infected with *Mycobacterium marinum*. Micron. 2020;129:102782.

198. Schindelin J, Arganda-Carreras I, Frise E, Kaynig V, Longair M, Pietzsch T, et al. Fiji: an open-source platform for biological-image analysis. Nat Methods. 2012;9:676-82.

199. Vaudaux P, Waldvogel FA. Gentamicin antibacterial activity in the presence of human polymorphonuclear leukocytes. Antimicrob Agents Chemother. 1979;16:743-9.

200. Klose KE, Mekalanos JJ. Distinct roles of an alternative sigma factor during both free-swimming and colonizing phases of the *Vibrio cholerae* pathogenic cycle. Mol Microbio. 1998;28:501-20.

201. Syed KA, Beyhan S, Correa N, Queen J, Liu J, Peng F, et al. The *Vibrio cholerae* Flagellar Regulatory Hierarchy Controls Expression of Virulence Factors. J Bacteriol. 2009;191:6555-70.

202. Manneh-Roussel J, Haycocks JRJ, Magán A, Perez-Soto N, Voelz K, Camilli A, et al. cAMP receptor protein controls *Vibrio cholerae* gene expression in response to host colonization. mBio. 2018;9:e00966-18.

203. Runft DL, Mitchell KC, Abuaita BH, Allen JP, Bajer S, Ginsburg K, et al. Zebrafish as a natural host model for *Vibrio cholerae* colonization and transmission. Appl Environ Microbiol. 2014;80:1710-7.

204. Logan SL, Thomas J, Yan J, Baker RP, Shields DS, Xavier JB, et al. The *Vibrio cholerae* type VI secretion system can modulate host intestinal mechanics to displace gut bacterial symbionts. Proc Natl Acad Sci USA. 2018;115.

205. Hayashi F, Smith KD, Ozinsky A, Hawn TR, Yi EC, Goodlett DR, et al. The innate immune response to bacterial flagellin is mediated by Toll-like receptor 5. Nature. 2001;410:1099-103.

206. Lovewell RR, Collins RM, Acker JL, O'Toole GA, Wargo MJ, Berwin B. Step-Wise Loss of Bacterial Flagellar Torsion Confers Progressive Phagocytic Evasion. PLoS Pathog. 2011;7:e1002253.

207. Francke C, Groot Kormelink T, Hagemeijer Y, Overmars L, Sluijter V, Moezelaar R, et al. Comparative analyses imply that the enigmatic sigma factor 54 is a central controller of the bacterial exterior. BMC Genomics. 2011;12:385.

208. Bush M, Dixon R. The role of bacterial enhancer binding proteins as specialized activators of σ54-dependent transcription. Microbiol Mol Biol Rev. 2012;76:497-529.

209. Srivastava D, Hsieh M-L, Khataokar A, Neiditch MB, Waters CM. Cyclic di-GMP inhibits *Vibrio cholerae* motility by repressing induction of transcription and inducing extracellular polysaccharide production. Mol Microbiol. 2013;90:1262-76.

210. Watnick PI, Lauriano CM, Klose KE, Croal L, Kolter R. The absence of a flagellum leads to altered colony morphology, biofilm development and virulence in *Vibrio cholerae* O139. Mol Microbiol. 2001;39:223-35.

211. Tsou AM, Zhu J. Quorum sensing negatively regulates hemolysin transcriptionally and post translationally in *Vibrio cholerae*. Infect Immun. 2010;78:461-7.

212. Zhu J, Miller MB, Vance RE, Dziejman M, Bassler BL, Mekalanos JJ. Quorum-sensing regulators control virulence gene expression in *Vibrio cholerae*. Proc Natl Acad Sci U S A. 2002;99:3129-34.

213. Liu Z, Miyashiro T, Tsou A, Hsiao A, Goulian M, Zhu J. Mucosal penetration primes *Vibrio cholerae* for host colonization by repressing quorum sensing. Proc Natl Acad Sci U S A. 2008;105:9769.

214. Halpern M, Izhaki I. Fish as Hosts of *Vibrio cholerae*. Front Microbiol. 2017;8:282.

215. Hossain ZZ, Farhana I, Tulsiani SM, Begum A, Jensen PKM. Transmission and toxigenic potential of *Vibrio cholerae* in Hilsha fish (Tenualosa ilisha) for human consumption in Bangladesh. Front Microbiol. 2018;9:222.

216. Hounmanou YMG, Mdegela RH, Dougnon TV, Madsen H, Withey JH, Olsen JE, et al. Tilapia (*Oreochromis niloticus*) as a putative reservoir host for survival and transmission of *Vibrio cholerae* O1 biotype El Tor in the aquatic environment. Front Microbiol. 2019;10:1215.

217. Legros D. Global cholera epidemiology: opportunities to reduce the burden of cholera by 2030. J Infect Dis. 2018;218:S137-S40.

218. Clemens JD, Nair GB, Ahmed T, Qadri F, Holmgren J. Cholera. The Lancet. 2017;390:1539-49.

219. Cassat JE, Skaar EP. Iron in infection and immunity. Cell Host Microbe. 2013;13:509-19.

220. Payne SM, Mey AR, Wyckoff EE. Vibrio iron transport: evolutionary adaptation to life in multiple environments. Microbiol Mol Biol Rev. 2016;80:69-90.

221. Imlay JA. Cellular defenses against superoxide and hydrogen peroxide. Annu Rev Biochem. 2008;77:755-76.

222. Fenton HJH. Oxidation of tartaric acid in presence of iron. J of the Chem Soc Transact. 1894;65:899-910.

223. Mey AR, Wyckoff EE, Kanukurthy V, Fisher CR, Payne SM. Iron and fur regulation in *Vibrio cholerae* and the role of fur in virulence. Infect Immun. 2005;73:8167-78.

224. Troxell B, Hassan HM. Transcriptional regulation by Ferric Uptake Regulator (Fur) in pathogenic bacteria. Front Cell Infect Microbiol. 2013;3:59.

225. Niederhoffer EC, Naranjo CM, Bradley KL, Fee JA. Control of Escherichia coli superoxide dismutase (sodA and sodB) genes by the ferric uptake regulation (fur) locus. J Bacteriol. 1990;172:1930-8.

226. Horsburgh MJ, Ingham E, Foster SJ. In *Staphylococcus aureus*, fur is an interactive regulator with PerR, contributes to virulence, and is necessary for oxidative stress resistance through positive regulation of catalase and iron homeostasis. J Bacteriol. 2001;183:468-75.

227. Wang H, Chen S, Zhang J, Rothenbacher FP, Jiang T, Kan B, et al. Catalases promote resistance of oxidative stress in *Vibrio cholerae*. PLoS One. 2013;7:e53383.

228. Heidelberg JF, Eisen JA, Nelson WC, Clayton RA, Gwinn ML, Dodson RJ, et al. DNA sequence of both chromosomes of the cholera pathogen *Vibrio cholerae*. Nature. 2000;406:477-83.

229. Cosson P, Soldati T. Eat, kill or die: when amoeba meets bacteria. Curr Opin Microbiol. 2008;11:271-6.

230. Pukatzki S, Ma AT, Revel AT, Sturtevant D, Mekalanos JJ. Type VI secretion system translocates a phage tail spike-like protein into target cells where it cross-links actin. Proc Natl Acad Sci USA. 2007;104:15508-13.

231. Miyata ST, Kitaoka M, Brooks TM, McAuley SB, Pukatzki S. *Vibrio cholerae* requires the type VI secretion system virulence factor VasX to kill *Dictyostelium discoideum*. Infect Immun. 2011;79:2941-9.

232. Crisan CV, Hammer BK. The *Vibrio cholerae* type VI secretion system: toxins, regulators and consequences. Environ Microbiol. 2020;22:4112-22.

233. Dong TG, Ho BT, Yoder-Himes DR, Mekalanos JJ. Identification of T6SS-dependent effector and immunity proteins by Tn-seq in *Vibrio cholerae*. Proc Natl Acad Sci USA. 2013;110:2623.

234. Hersch SJ, Manera K, Dong TG. Defending against the Type Six Secretion System: beyond Immunity Genes. Cell Rep. 2020;33:108259.

235. Hersch SJ, Watanabe N, Stietz MS, Manera K, Kamal F, Burkinshaw B, et al. Envelope stress responses defend against type six secretion system attacks independently of immunity proteins. Nat Microbiol. 2020;5:706-14.

236. Dong TG, Dong S, Catalano C, Moore R, Liang X, Mekalanos JJ. Generation of reactive oxygen species by lethal attacks from competing microbes. Proc Natl Acad Sci USA. 2015;112:2181-6.

237. Kamal F, Liang X, Manera K, Pei T-T, Kim H, Lam LG, et al. Differential cellular response to translocated toxic effectors and physical penetration by the type VI secretion system. Cell Reports. 2020;31:107766.

238. Wong MJQ, Liang X, Smart M, Tang L, Moore R, Ingalls B, et al. Microbial herd protection mediated by antagonistic interaction in polymicrobial communities. App Environ Microbiol. 2016;82:6881-8.

239. Babraham. Bioinformatics Trim Galore. https://www.bioinformatics.babraham.ac.uk/projects/trim_galore/ Accessed on 12 Nov 2019.

240. Andrews S. FastQC: A quality control tool for high throughput sequence data. http://www.bioinformatics.babraham.ac.uk/projects/fastqc/ 2010.

241. Liao Y, Smyth GK, Shi W. The Subread aligner: fast, accurate and scalable read mapping by seed-and-vote. Nucleic Acids Res. 2013;41.

242. Liao Y, Smyth GK, Shi W. featureCounts: an efficient general purpose program for assigning sequence reads to genomic features. Bioinformatics. 2013;30:923-30.

243. Love MI, Huber W, Anders S. Moderated estimation of fold change and dispersion for RNA-seq data with DESeq2. Genome Biology. 2014;15:550.

244. Lin SM, Du P, Huber W, Kibbe WA. Model-based variance-stabilizing transformation for Illumina microarray data. Nucleic Acids Res. 2008;36:e11-e.

245. Wilkinson L. ggplot2: Elegant graphics for data analysis by WICKHAM, H. Biometrics. 2011;67:678-9.

246. Iwase T, Tajima A, Sugimoto S, Okuda K-i, Hironaka I, Kamata Y, et al. A simple assay for measuring catalase activity: a visual approach. Sci Rep. 2013;3:3081-.

247. González-Escalona N, Fey A, Höfle MG, Espejo RT, C AG. Quantitative reverse transcription polymerase chain reaction analysis of *Vibrio cholerae* cells entering the viable but non-culturable state and starvation in response to cold shock. Environ Microbiol. 2006;8:658-66.

248. Dongre M, Singh B, Aung KM, Larsson P, Miftakhova R, Persson K, et al. Flagella-mediated secretion of a novel *Vibrio cholerae* cytotoxin affecting both vertebrate and invertebrate hosts. Com Biol. 2018;1:59.

249. Rivera-Chávez F, Mekalanos JJ. Cholera toxin promotes pathogen acquisition of host-derived nutrients. Nature. 2019;572:244-8.

250. Dubrac S, Touati D. Fur positive regulation of iron superoxide dismutase in *Escherichia coli*: functional analysis of the sodB promoter. J Bacteriol. 2000;182:3802-8.

251. Fernandez NL, Waters CM, Kivisaar M. Cyclic di-GMP increases catalase production and hydrogen peroxide tolerance in *Vibrio cholerae*. App Environ Microbiol. 2019;85:e01043-19.

252. Bourdon E, Loreau N, Lagrost L, Blache D. Differential effects of cysteine and methionine residues in the antioxidant activity of human serum albumin. Free Radic Res. 2005;39:15-20.

253. Nobechi K. Contributions to the knowledge of *Vibrio cholerae*. Fermentation of carbohydrates and polyatomic alcohols by *Vibrio cholerae*. J Bacteriol. 1925;10:197-215.

254. Hawver LA, Giulietti JM, Baleja JD, Ng W-L, Bassler B. Quorum sensing coordinates cooperative expression of pyruvate metabolism genes to maintain a sustainable environment for population stability. mBio. 2016;7:e01863-16.

255. Miyata ST, Unterweger D, Rudko SP, Pukatzki S. Dual expression profile of type VI secretion system immunity genes protects pandemic *Vibrio cholerae*. PLoS Pathog. 2013;9.

256. Kitaoka M, Miyata ST, Brooks TM, Unterweger D, Pukatzki S. VasH is a transcriptional regulator of the type VI secretion system functional in endemic and pandemic *Vibrio cholerae*. J Bacteriol. 2011;193:6471-82.

257. Dong TG, Mekalanos JJ. Characterization of the RpoN regulon reveals differential regulation of T6SS and new flagellar operons in *Vibrio cholerae* O37 strain V52. Nucleic Acids Res. 2012;40:7766-75.

258. Mavian C, Paisie TK, Alam MT, Browne C, Beau De Rochars VM, Nembrini S, et al. Toxigenic *Vibrio cholerae* evolution and establishment of reservoirs in aquatic ecosystems. Proc Natl Acad Sci USA. 2020;117:7897-904.

259. Faruque SM, Mekalanos JJ. Phage-bacterial interactions in the evolution of toxigenic *Vibrio cholerae*. Virulence. 2012;3:556-65.

260. Faruque SM, Mekalanos JJ. Pathogenicity islands and phages in *Vibrio cholerae* evolution. Trends Microbiol. 2003;11:505-10.

261. Arenas M, Araujo NM, Branco C, Castelhano N, Castro-Nallar E, Pérez-Losada M. Mutation and recombination in pathogen evolution: Relevance, methods and controversies. Infect Gen Evol. 2018;63:295-306.

262. Bjedov I, Tenaillon O, Gérard B, Souza V, Denamur E, Radman M, et al. Stress-induced mutagenesis in bacteria. Science. 2003;300:1404-9.

263. Colwell RR, Huq A. Environmental reservoir of *Vibrio cholerae*. The causative agent of cholera. Ann N Y Acad Sci. 1994;740:44-54.

264. Lodish H, Berk A, Zipursky SL, Matsudaira P, Baltimore D, Darnell J. Molecular Cell Biology. 4th edition.: New York: W. H. Freeman; 2000. ; 2000.

265. Old D, Mortlock RP. The metabolism of D-arabinose by *Salmonella typhimurium*. J Gen Microbiol. 1977;101:341-4.

266. Frost SDW, Dumaurier M-J, Wain-Hobson S, Brown AJL. Genetic drift and within-host metapopulation dynamics of HIV-1 infection. Proc Natl Acad Sci USA. 2001;98:6975-80.

267. Foll M, Poh Y-P, Renzette N, Ferrer-Admetlla A, Bank C, Shim H, et al. Influenza virus drug resistance: A time-sampled population genetics perspective. PLoS Gen. 2014;10:e1004185.

268. Ghosh A, N S, Saha S. Survey of drug resistance associated gene mutations in *Mycobacterium tuberculosis*, ESKAPE and other bacterial species. Sci Rep. 2020;10:8957.

269. Philippe N, Pelosi L, Lenski RE, Schneider D. Evolution of penicillin-binding protein 2 concentration and cell shape during a long-term experiment with Escherichia coli. J Bacteriol. 2009;191:909-21.

270. Sokurenko EV, Hasty DL, Dykhuizen DE. Pathoadaptive mutations: gene loss and variation in bacterial pathogens. Trends Microbiol. 1999;7:191-5.

271. McDonald MJ. Microbial Experimental Evolution – a proving ground for evolutionary theory and a tool for discovery. EMBO reports. 2019;20:e46992.

272. Lenski RE. Experimental evolution and the dynamics of adaptation and genome evolution in microbial populations. ISME J. 2017;11:2181-94.

273. Blount ZD, Barrick JE, Davidson CJ, Lenski RE. Genomic analysis of a key innovation in an experimental *Escherichia coli* population. Nature. 2012;489:513-8.

274. Poltak SR, Cooper VS. Ecological succession in long-term experimentally evolved biofilms produces synergistic communities. ISME J. 2011;5:369-78.

275. Ensminger AW, Yassin Y, Miron A, Isberg RR. Experimental evolution of *Legionella pneumophila* in mouse macrophages leads to strains with altered determinants of environmental survival. PLoS Pathogens. 2012;8:e1002731.

276. Friman VP, Buckling A. Phages can constrain protist predation-driven attenuation of *Pseudomonas aeruginosa* virulence in multienemy communities. ISME J. 2014;8:1820-30.

277. Zhang J, Ketola T, Örmälä-Odegrip AM, Mappes J, Laakso J. Coincidental loss of bacterial virulence in multi-enemy microbial communities. PLoS One. 2014;9.

278. Deatherage DE, Barrick, J.E. Identification of mutations in laboratory-evolved microbes from next-generation sequencing data using breseq. Methods Mol Biol. 2014:165-88.

279. Bankevich A, Nurk S, Antipov D, Gurevich AA, Dvorkin M, Kulikov AS, et al. SPAdes: a new genome assembly algorithm and its applications to single-cell sequencing. J Comput Biol. 2012;19:455-77.

280. Medrano RF, de Oliveira CA. Guidelines for the tetra-primer ARMS-PCR technique development. Mol Biotechnol. 2014;56:599-608.

281. Hanson PI, Whiteheart SW. AAA+ proteins: have engine, will work. Nat Rev Mol Cell Biol. 2005;6:519-29.

282. Klose KE, Mekalanos JJ. Distinct roles of an alternative sigma factor during both free-swimming and colonizing phases of the *Vibrio cholerae* pathogenic cycle. Molecular Microbiology. 1998;28:501-20.

283. Sinha-Ray S, Ali A. Mutation in flrA and mshA genes of *Vibrio cholerae* inversely involved in vps-independent biofilm driving bacterium toward nutrients in lake wSater. Front Microbiol. 2017;8.

284. Jain R, Kazmierczak BI. A conservative amino acid mutation in the master regulator FleQ renders *Pseudomonas aeruginosa* aflagellate. PLoS One. 2014;9:e97439.

285. Chekabab SM, Daigle F, Charette SJ, Dozois CM, Harel J. Shiga toxins decrease enterohaemorrhagic *Escherichia coli* survival within *Acanthamoeba castellanii*. FEMS Microbiol Let. 2013;344:86-93.

286. Jousset A, Rochat L, Scheu S, Bonkowski M, Keel C. Predator-prey chemical warfare determines the expression of biocontrol genes by rhizosphere-associated *Pseudomonas fluorescens*. App Environ Microbiol. 2010;76:5263-8.

287. Wenger JW, Piotrowski J, Nagarajan S, Chiotti K, Sherlock G, Rosenzweig F. Hunger artists: Yeast adapted to carbon limitation show trade-offs under carbon sufficiency. PLoS Gen. 2011;7:e1002202.

288. Barea F, Bonatto D. Relationships among carbohydrate intermediate metabolites and DNA damage and repair in yeast from a systems biology perspective. Mutat Res. 2008;642:43-56.

289. Morin M, Enjalbert B, Ropers D, Girbal L, Cocaign-Bousquet M, Ellermeier CD. Genomewide stabilization of mRNA during a Feast-to-Famine growth transition in *Escherichia coli*. mSphere. 2020;5:e00276-20.

290. Wrande M, Roth JR, Hughes D. Accumulation of mutants in "aging" bacterial colonies is due to growth under selection, not stress-induced mutagenesis. Proc Natl Acad Sci USA. 2008;105:11863-8.

291. McKenzie GJ, Harris RS, Lee PL, Rosenberg SM. The SOS response regulates adaptive mutation. Proc Natl Acad Sci USA. 2000;97:6646.

292. Rasmussen MA, Carlson SA, Franklin SK, McCuddin ZP, Wu MT, Sharma VK. Exposure to rumen protozoa leads to enhancement of pathogenicity of and invasion by multiple-antibiotic-resistant *Salmonella enterica* bearing SGI1. Infect Immun. 2005;73:4668-75.

293. Hossain ZZ, Farhana I, Tulsiani SM, Begum A, Jensen PKM. Transmission and toxigenic potential of *Vibrio cholerae* in Hilsha fish (*Tenualosa ilisha*) for human consumption in Bangladesh. Front Microbiol. 2018;9.

294. Hoque MM, Naser IB, Bari SMN, Zhu J, Mekalanos JJ, Faruque SM. Quorum regulated resistance of *Vibrio cholerae* against environmental bacteriophages. Sci Rep. 2016;6:37956.

295. Faruque SM, Naser IB, Islam MJ, Faruque ASG, Ghosh AN, Nair GB, et al. Seasonal epidemics of cholera inversely correlate with the prevalence of environmental cholera phages. Proc Natl Acad Sci USA. 2005;102:1702-7.

296. Bjorbækmo MFM, Evenstad A, Røsæg LL, Krabberød AK, Logares R. The planktonic protist interactome: where do we stand after a century of research? ISME J. 2020;14:544-59.

297. Tsou AM, Zhu J. Quorum sensing negatively regulates hemolysin transcriptionally and posttranslationally in *Vibrio cholerae*. Infect Immun. 2010;78:461.

298. Collins HL, Kaufmann SH, Schaible UE. Iron chelation via deferoxamine exacerbates experimental salmonellosis via inhibition of the nicotinamide adenine dinucleotide phosphate oxidase-dependent respiratory burst. J Immunol. 2002;168:3458-63.

299. Price C, Abu Kwaik Y. Amoebae and mammals deliver protein-rich Atkins diet meals to *Legionella* cells. Microbe. 2012;7:506–13.

300. Nydahl A, Panigrahi S, Wikner J. Increased microbial activity in a warmer and wetter climate enhances the risk of coastal hypoxia. FEMS Microbiol Ecol. 2013;85:338-47.

301. Richardson AJ. In hot water: zooplankton and climate change. J Marine Sci. 2008;65:279-95.

302. Trombetta T, Vidussi F, Mas S, Parin D, Simier M, Mostajir B. Water temperature drives phytoplankton blooms in coastal waters. PLoS One. 2019;14:e0214933.

303. Gittings JA, Raitsos DE, Krokos G, Hoteit I. Impacts of warming on phytoplankton abundance and phenology in a typical tropical marine ecosystem. Sci Rep. 2018;8:2240.

304. Vezzulli L, Grande C, Reid PC, Hélaouët P, Edwards M, Höfle MG, et al. Climate influence on *Vibrio* and associated human diseases during the past half-century in the coastal North Atlantic. Proc Natl Acad Sci USA. 2016;113:E5062.

305. Vezzulli L, Brettar I, Pezzati E, Reid PC, Colwell RR, Höfle MG, et al. Long-term effects of ocean warming on the prokaryotic community: evidence from the vibrios. ISME J. 2012;6:21-30.

306. Stauder M, Vezzulli L, Pezzati E, Repetto B, Pruzzo C. Temperature affects *Vibrio cholerae* O1 El Tor persistence in the aquatic environment via an enhanced expression of GbpA and MSHA adhesins. Environ Microbiol Rep. 2010;2:140-4.

307. Yildiz FH, Schoolnik GK. Role of rpoS in stress survival and virulence of *Vibrio cholerae*. J Bacteriol. 1998;180:773-84.

308. Datsenko KA, Wanner BL. One-step inactivation of chromosomal genes in *Escherichia coli* K-12 using PCR products. Proc Natl Acad Sci USA. 2000;97:6640.

309. Lambertsen L, Sternberg C, Molin S. Mini-Tn7 transposons for site-specific tagging of bacteria with fluorescent proteins. Environ Microbiol. 2004;6:726-32.